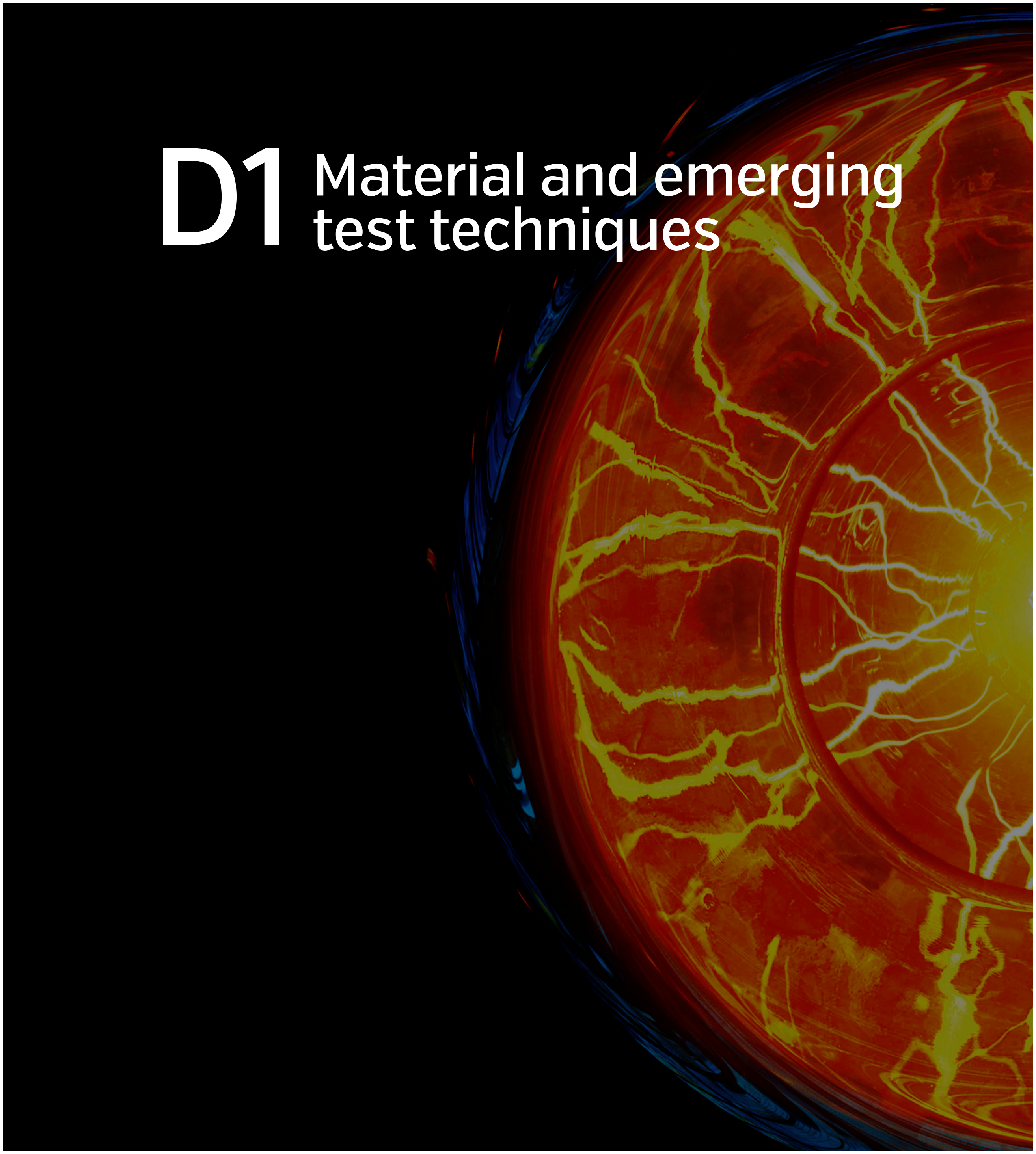

Basic principles and practical methods to measure the AC and DC resistance of conductors of power cables

cigre
TECHNICAL BROCHURES
March 2023 - Reference 894

TECHNICAL BROCHURE

Basic principles and practical methods to measure the AC and DC resistance of conductors of power cables

WG D1.54

Members

B. DARDEL, **Convenor**	CH
C. J. LIU	US
P. DE BRUYNE	CH
A. FUSTIER	FR
S. GROßMANN	DE
R. PLATH	DE
T. AARIANS	NL
I. BOEV	CA
C. MICHELSEN	DK

R. SUCHANTKE	DE
D. WILLÉN	DK
Z. LI	CA
E. BEAUGUITTE	FR
M. SJÖBERG	SE
L. MUNTEANU	US
G. SCHRÖDER	DE
T. ISRAEL	DE

cigre

ISBN : 978-2-85873-599-0

Executive Summary

Transmission systems, such as high voltage overhead lines and cables, are an integral part of the power grid. Due to large currents and their electrical resistance, the inner or main conductor of such a cable or transmission line is responsible for most of its electrical losses, as evidenced by its heat dissipation. This brochure deals with the accurate resistance measurement of power cable conductors, typically used in AC and DC transmission systems.

Conductors for insulated cables are classified according to their size defined by their DC electrical resistance in IEC 60228. Nevertheless, most of the power lines are used in AC mode, where for large conductors for cables and overhead lines, skin effect may lead to important load capacity reductions. These are dependent on the conductor design, thus the qualification of AC conductor resistance becomes a critical aspect of cable design. Though the subject has been studied theoretically in detail, and different methods for measurement of AC resistance have been proposed in CIGRÉ TB272 by SC B1 [1], no specific measurement setup or method is presently prescribed in the IEC standards for conductor resistance measurements, even for DC.

First, in chapter 1, this brochure gives a general introduction to the topic by discussing the theoretical background of AC loss mechanisms and describing critical influences in the electrical measurement of complex conductors. In chapter 2 state of the art measurement practices are shown, both for DC and AC measurements. Additionally, best practices of connection systems and temperature measurement and stabilization are discussed. Also, the results of the round robin test performed during this research, both of reference conductors and different power cable conductors, are presented. The focus of this document lies in chapter 3. It is based on accumulated knowledge from the literature and research conducted by the group. In this chapter, the reader can find the proposed recommendations for accurate measurement of AC and DC resistances, using the electrical method. It details the requirements of the environment and equipment, the performance check of the measurement system, the preparation of the conductor sample and the complete measurement setup. Moreover, the measurement procedure is described and a new metric is proposed, which shall be used as a future performance rating value, namely the R_s value.

From the analyses and investigations performed, it can be concluded that DC and especially AC resistance measurement is a difficult task, if the desired accuracy is high. Many influencing factors need to be considered, to be able to accurately rate a complex conductor design, such as a Milliken conductor. This is especially true, when using the electrical measurement method, as proposed in the brochure. This method is easier to apply but needs to be handled with great care. Calorimetric measurements were not considered due to its high temporal and logistical demands and inherent drawbacks of the method itself. Introduction of a new performance metric stresses the importance of performing a measurement to reliably assess the conductor performance.

This brochure establishes well defined setups and allows users to perform accurate measurement on their conductor(s) under test, accounting for influences of different conductor designs choices. The R_s performance value allows a trustworthy comparison of conductors across different laboratories.

Table of Contents

List of figures

List of Tables

1. Introduction

1.1 General

The main component of power cables and overhead lines is the inner conductor itself that contributes in a large portion to the cost and the weight of the product. Its design is then of great importance in the optimization process. The power transmission capacity of the line is directly linked to its resistance. It is thus critical to define adequate procedures to measure this property.

The intention of this brochure is to give an overview of possible measurement setups, identify critical parameters and give recommendations on operational aspects and result interpretation of AC (alternating current) and DC (direct current) resistance measurements of the inner conductor of a power cable solely. Additional losses due to sheath design or laying conditions are not in scope of this brochure (for example three phase losses of submarine cables). For calculating these additional losses, the reader is referred to the relevant standards such as IEC (International Electrotechnical Commission) 60287.

1.1.1 Motivation

Power cable transport capacity is limited by the maximum service temperature of materials used in their design. It is strongly related to electrical losses that are directly converted into heat. The largest contribution originates usually from the ohmic losses due to electrical resistance of the conductor. Characterization of this resistance is therefore of utmost importance. This is reflected in IEC 60228, where the conductor sizes are defined in terms of the DC resistance of the conductor.

In AC mode, other phenomena such as skin effect, modifies the distribution of current in the conductor and hence leads to increased losses. Conductor design becomes critical for large cross-sections where these effects are important – the AC resistance at 50 Hz is for example 60 % higher than in DC for 2000 mm² solid copper conductor. Reduction of the AC resistance and hence of the associated losses can, for example, be obtained using insulated wires.

Characterization of the AC electrical resistance of large conductor is then required for design and qualification purposes.

Based on theoretical considerations and available literature, this work intends to give an overview of the state-of-the-art in AC conductor measurements, comparing existing measurement techniques developed in different labs worldwide through a round robin test on well-defined conductors that can be easily modelled as well as on real conductors used in cables.

The ultimate objective is to define a test procedure including suitable equipment for the measurement of AC and DC resistance, identify and evaluate the factors of influence and determine the precision and reliability of the proposed test set-up. Today, many different measurement setups are still used, leading to ambiguous results even for identical conductor designs [2, p. 147].

1.1.2 Standardization

IEC 60228 defines conductors of insulated cables. Besides some mechanical consideration on wire diameters intended to reflect the flexibility of the conductor, requirements for DC resistance of conductors using copper, aluminum or metallic coated wires are given. The effect of temperature is also considered and correction factors are provided. Other parameters that might strongly affect AC resistance such as for example non-metallic coating, detailed conductor design (number and diameter of wires, assembly configuration, compaction) are not mentioned.

Although measurement of the DC resistance is briefly discussed in this standard, no procedure is defined by the IEC. Measurements are then performed using specific equipment developed by the industry and based on empirical interpretations and best practices.

IEC 60287-1-1 gives calculation formulas (based on approximation) for the skin effect factor ($y_s = R_{AC}/R_{DC}$) as well as experimental values of correction coefficient k_s to be considered for evaluating the AC resistance of different conductor designs.

Besides giving some basic background of modeling, interpretation and derived values of the skin effect factor for the AC resistance of large conductors, CIGRÉ (Conseil International des Grands

Réseaux Électriques) TB (Technical Brochure) 272 [1] presents 3 electrical and 1 calorimetric method of AC measurements but no standard or specific implementation has emerged from this study.

Note that the calorimetric method is not considered here because of the following inconveniences:

- It is not practical and more difficult to put in place.
- The uncertainty of the measurement is considered to be higher than with electrical methods.
- The longitudinal flux at both ends of the sample is difficult to master.
- There is a need for a thermal model to relate the measured parameters to the losses and hence to the resistance.

This method has nevertheless the advantage that it is not perturbated by environment (electrical pollution), and the setup can be used for any cable design and needs no special consideration for more complex measurement configurations (3 phases, …).

1.2 Theoretical Background

The purpose of this chapter is to introduce the reader to basic concepts of AC loss mechanisms. In the following, physical phenomena, which cause additional losses in conductors, are described and some important references are given. The theoretical investigations on AC losses started at the end of the 19th century [2, p. 35].

1.2.1 Particularities of AC

Alternating currents, unlike direct currents, do not flow uniformly through a straight conductor due to the skin effect and possibly also proximity effect in case multiple conductors are present. Both phenomena are caused by the changing electromagnetic field at AC. The effects arise due to a limited penetration of the electromagnetic field, which is initially present outside of the conductor, into the inside of the conductor. The penetration of the electromagnetic field into the conductor is limited in speed and depth, and causes heat losses. Hence, at larger frequencies or larger conductor dimensions it is harder for the electromagnetic field to penetrate into the whole conductor cross section. That is the reason the current density is larger at the surface of the conductor than on the inside and varies in phase in the cross section. Skin effect describes this phenomenon for a single isolated conductor, whereas proximity effect describes this phenomenon for multiple conductors in interaction. [2, p. 40]

Stranded conductors show a slight decrease in AC resistance due to the spirality effect. This is caused by the wires being helically twisted and spaced from each other, which slightly changes the direction and intensity of the magnetic field in the other strands. This decrease is negligible for typical conductor sizes and at power frequency [3].

1.2.2 Theory of Skin Effect

Figure 1-1 shows the current density in the cross section of a single solid cylindrical conductor at different frequencies, due to skin effect.

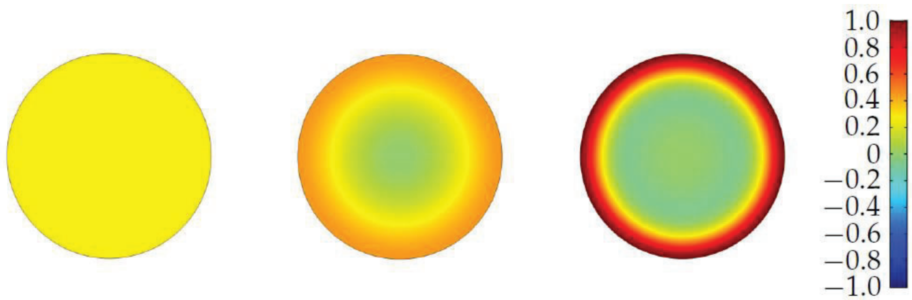

Figure 1-1: Normalized in-plane current density in a circular conductor cross section; from DC (left) to increasing frequencies (to the right) [2, p. 42]

The current penetration depth into the conductor varies with the inverse of square root of the applied frequency [4]. Skin depth δ is the depth at which the current density at AC is equal to the current density at DC [5]. Skin depth decreases rapidly as frequency increases, as shown here for copper and aluminum in Figure 1-2.

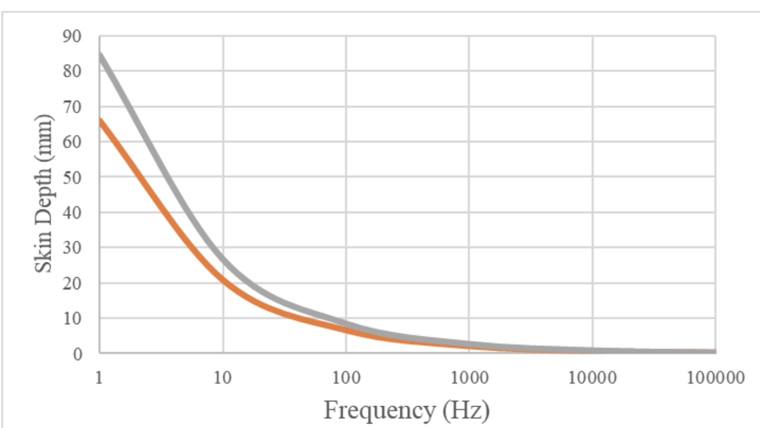

Figure 1-2: Skin depth for aluminum (gray) and copper (orange) at different frequencies

Figure 1-3 shows the AC to DC resistance ratio for solid cylindrical conductors with increasing cross sections at 50 Hz and 60 Hz and different materials.

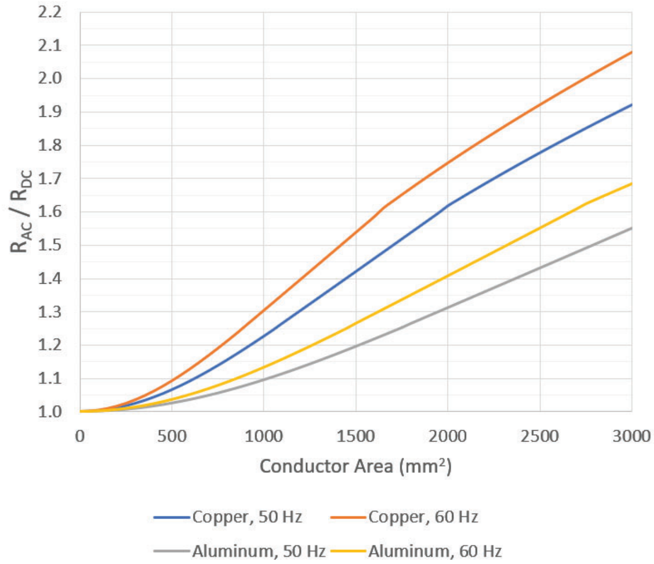

Figure 1-3: Resistance ratio for different cross-sectional sizes of a cylindrical copper conductor

1.2.3 Theory of Proximity Effect

The proximity effect describes the interaction of at least two conductors. As conductors for wire-based energy transmission act as a guideway for the electromagnetic field traveling along the conductor, a second conductor in close proximity to the first conductor will distort the electromagnetic field. Figure 1-4 shows the current distribution in case of two closely spaced conductors in return circuit (opposite current flows in both conductors) and go circuit (parallel connection, meaning current flows in the same direction in both conductors).

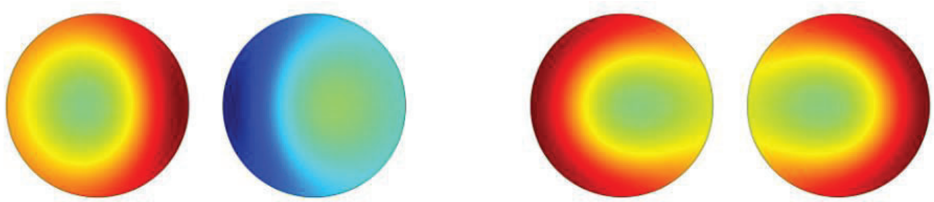

Figure 1-4: Normalized in-plane current density of two circular conductors (proximity effect); *left*: in return circuit; *right*: in go-circuit (parallel); same scale as in Figure 1-1 [2, p. 43]

1.2.4 Review of Analytical Formulas

Since the discovery of the skin effect in the 1880s, multiple analytical formulas have been developed for the AC resistance of conductors with *simple* geometries. In comparison to approximations, analytical formulas give the AC resistance without a restriction to a certain range of the involved geometric or electrical parameters. A comprehensive collection of analytical formulas can be found in [2, p. 51]. In the following, the two most important analytical formulas for this study are given.

1.2.4.1 Solid Cylindrical Conductor

The AC resistance, formula taken from [1, p. 6], of a solid cylindrical conductor is

$$R_{\mathrm{AC}} = R_{\mathrm{DC}}(1 + y_s)\,, \tag{1}$$

where

$$y_s(x) = \frac{x}{2}\left(\frac{\mathrm{ber}_0(x)\mathrm{bei}_0{}'(x) - \mathrm{bei}_0(x)\mathrm{ber}_0{}'(x)}{\mathrm{ber}_0{}'(x)^2 + \mathrm{bei}_0{}'(x)^2}\right) - 1 \tag{2}$$

$$x = \sqrt{\frac{\omega\mu}{\pi R_{\mathrm{DC}}}}$$

$$\omega = 2\pi f \ .$$

R_{DC} is the DC resistance per unit length, ber_0, bei_0, ber_0', bei_0' are the Kelvin functions (real and imaginary part of the Bessel function of the first kind J and order 0) and their derivatives. f is the frequency and μ is the magnetic permeability ($\mu = \mu_0\mu_r$).

1.2.4.2 Hollow Cylindrical (Tubular) Conductor

For a hollow conductor, the following formula from [6] applies

$$R_{\mathrm{AC}} = \mathrm{Re}\left\{\frac{\bar{k}}{2\pi\sigma r_e}\frac{\mathrm{J}_1(\bar{k}_i)\mathrm{Y}_0(\bar{k}_e) - \mathrm{Y}_1(\bar{k}_i)\mathrm{J}_0(\bar{k}_e)}{\mathrm{J}_1(\bar{k}_i)\mathrm{Y}_1(\bar{k}_e) - \mathrm{Y}_1(\bar{k}_i)\mathrm{J}_1(\bar{k}_e)}\right\}, \quad (3)$$

where

$$\bar{k} = k\mathrm{e}^{-j\frac{\pi}{4}} = \sqrt{\omega\mu\sigma}\,\mathrm{e}^{-j\frac{\pi}{4}}$$

$$\bar{k}_e = \bar{k}r_2$$

$$\bar{k}_i = \bar{k}r_1$$

Re takes the real part of the argument, j is the imaginary number, J and Y are the Bessel functions of the first and second kind and σ is the electrical conductivity, r_1 is the inner radius of the tube and r_2 the outer radius. Figure 1-5 shows the effect of geometric variations of a tubular conductor on AC resistance.

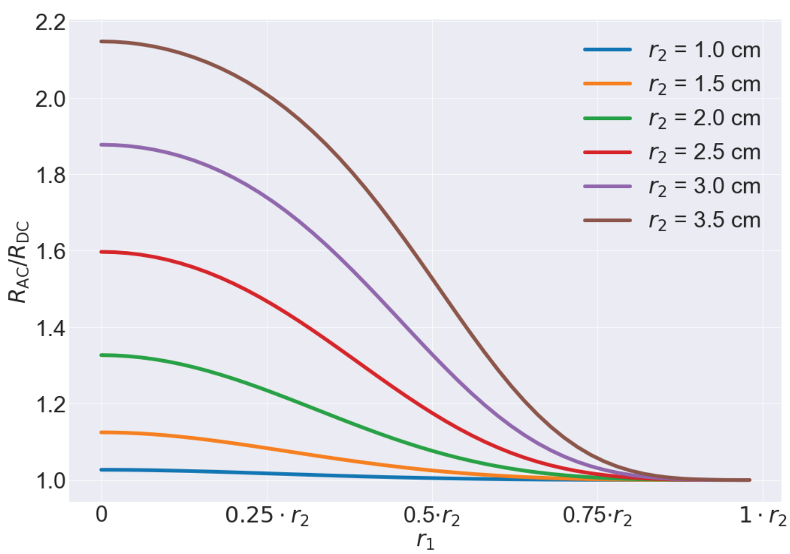

Figure 1-5: Resistance ratio depending on the size of inner radius r_1 and outer radius r_2 at 50 Hz for a copper tube

1.2.5 Principle of Similitude

In 1918 Herbert B. Dwight introduced the *Principle of Similitude* in [7]. It states that a certain conductor shape or arrangement has a fixed $R_{\mathrm{AC}}/R_{\mathrm{DC}}$ ratio for a certain $f\ /\ R_{\mathrm{DC}}$ ratio. For example: a cylindrical conductor with a cross section of 3000 mm² will have the same resistance ratio as a cylindrical conductor of 10 mm² at the same $f\ /\ R_{\mathrm{DC}}$ ratio. As the DC resistance of the small conductor is much larger than that of the 3000 mm² conductor, the applied frequency to reach this resistance ratio must be much larger. Additional examples including multiple conductors are given in [2, p. 65] for example. A factor, namely the *Principle of Similitude parameter* p in $\sqrt{\mathrm{m}/(\Omega\mathrm{s})}$, can be introduced:

$$p = \sqrt{\frac{f}{R_{\mathrm{DC}}}} \cdot 1 \times 10^{-3} \, . \quad (4)$$

Using the root operator on the f / R_{DC} term, will make the following curves for solid circular conductors become straight lines at larger p values. The curves shown in Figure 1-6 are valid for every conductor of the same proportionate shape (solid cylindrical conductors and tubular conductors with these radii ratios).

Also shown on top of the plot in gray is a solid cylindrical copper conductor and its behavior at different temperatures. As the temperature increases, the conductivity decreases and hence the DC resistance increases. This is equal to moving along the horizontal axis to the left.

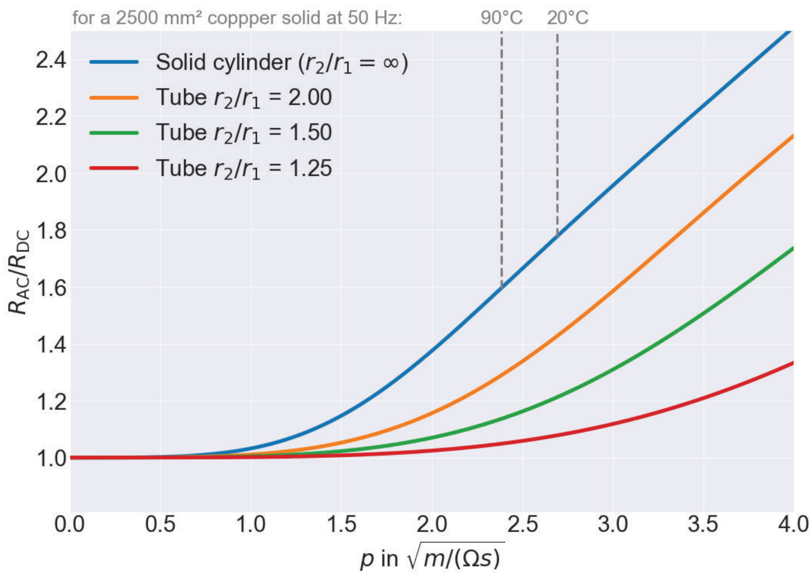

Figure 1-6: *Principle of Similitude* for different conductor shapes; on top in gray is an example for a solid cylindrical copper conductor at 50 Hz having different temperatures and therefore different *p* values

For conductors where all geometric dimensions are exactly known (including contacts between conductors, which can influence the current density distribution) authors should rather plot the resistance ratio over p instead of f for better comparability. One can then directly use these curves to determine the resistance ratio of this shape at every frequency and DC resistance or temperature desired. Nevertheless, this is typically only possible for very simple shapes and conductor arrangements, which can also be quickly calculated by numerical methods. In stranded or Milliken[1] conductors for example, the important influence of the inter-wire resistances cannot be known exactly in advance and hence the plot cannot be generalized.

The rate of increase in the resistance ratio over p differs for different cross-sectional shapes. This can be seen more clearly in Figure 3.12 of [2, p. 65]. This however is in contradiction with the use of a k_s factor as described in CIGRÉ TB 272 [1] and in IEC 60287-1-1 which is assuming a design independent shape of the curve. The k_s factor was derived on the assumptions that a Milliken conductor behaves like a solid conductor as parameter x in equation (2) also uses the *Principle of Similitude*. Compared to a solid conductor, which behaves according to the first order Bessel function, multiple parallel conductors (as the single strands in a Milliken conductor) will follow the trend of higher order Bessel functions [8]. Moreover, other parameters like wire diameters, stranding pitch, contact resistance between wires, etc., will break the similitude considered here and make the use of a fixed k_s value only valid in a limited range of geometries.

1.2.6 Temperature Scaling

Temperature Scaling was introduced in [2, p. 24]. The variation of resistivity of the conductor material with temperature is described, as defined in IEC 60228, by its resistance-temperature coefficient α_T.

The resistance of the conductor is then calculated as

[1] Named after the inventor Humphreys Milliken ("Electrical Cable." Patent: 1,904,162 (USA). 1933.).

$$R(T_0) = T_{\mathrm{SF}} \cdot R(T) \quad , \tag{5}$$

where

$$T_{\mathrm{SF}} = \frac{1 + \alpha_{\mathrm{T}}(T_0 - 20°C)}{1 + \alpha_{\mathrm{T}}(T - 20°C)} . \tag{6}$$

T is the temperature at which the resistance measurement was performed at (e.g., 23 °C or 89 °C) and T_0 is the temperature at which the measurement value is desired to be evaluated at (usually 20 °C or 90 °C). Considering the *Principle of Similitude* above, it becomes clear that the same conductor will show a different resistance ratio at different temperatures, because its conductivity changes with temperature and with the conductivity the AC losses are influenced. Hence, measurement curves plotted over f must be scaled accordingly, if the measurement was not performed at the desired temperature of evaluation, which is typically 20 °C or 90 °C. The curve must be stretched or compressed along the frequency axis depending on whether scaling the measurement values from higher to lower temperatures or the other way around. It is important to note that it is not sufficient to move or shift the complete curve only (offset), as this would keep the resistance ratio unchanged between different temperatures. For appropriate scaling one needs to multiply the resistances at measured temperature $R(T)$ and the frequencies $f(T)$ belonging to these resistances with the dimensionless factor T_{SF} to obtain the desired resistance over frequency curve at the reference temperature T_0. The frequency can be scaled accordingly:

$$f(T_0) = T_{\mathrm{SF}} \cdot f(T) \quad . \tag{7}$$

Note that in formula (5) and (7), f and R can be single values or vectors in case measurements were performed at multiple frequencies. An example of the routine which needs to be performed can be found in section 1.3.8.

Figure 1-7 shows that the original curves, obtained at T, perfectly coincide with the analytical (reference) solution for T = 20 °C when scaled using this method. In Figure 1-7, T is either -50 °C or 90 °C and T_0 is 20 °C. The temperature coefficient is that of copper.

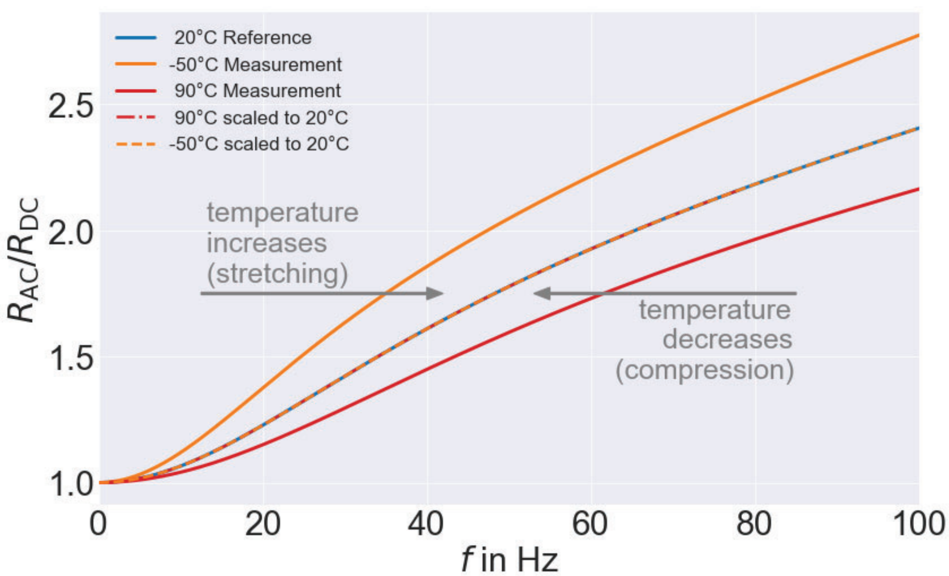

Figure 1-7: Example of *Temperature Scaling* shown on a 2500 mm² copper solid; the analytical curves for -50 °C, 20 °C and 90 °C are shown (solid lines); additionally, the -50 °C and 90 °C curves were scaled to 20 °C with the *Temperature Scaling* technique to show that the scaled curves coincide with the analytical solution at 20 °C

For complex conductors, it cannot be guaranteed that conductor properties affecting skin effect and hence AC resistance remain unchanged at different temperatures (e.g. strand insulation, thermal induced stress leading to geometric changes, …). Ideally, a measurement should be performed at the desired temperature directly (typically 20 °C or 90 °C). *Temperature Scaling* should only be used to correct small deviations (e.g., ±5 °C).

The procedure of *Temperature Scaling* is shown in detail in section 1.3.8 and 3.1.2.

1.2.7 Important Literature

This chapter lists some additional important references concerning AC losses and their measurements, which were not referenced elsewhere in the text directly. Other publications referenced in the text directly, can be found at the end of this brochure in chapter 4.

John R. Carson. “LIV.Wave propagation over parallel wires: The proximity effect.” In: Philosophical Magazine Series 6 41.244 (1921), pp. 607–633. doi: 10.1080/14786442108636251.

M. Däumling, S. Krüger Olsen, C. Traeholt, Dag Willén, and A. Kühle. “Ac loss in superconducting power cables.” In: Studies of High Temperature Superconductors. Vol. 33. 2000, p. 73.

P. Dolez, M. Aubin, W. Zhu, and J. Cave. “A comparison between ac losses obtained by the null calorimetric and a standard electrical method.” In: Superconductor Science and Technology 11.12 (1998), pp. 1386–1390. doi: 10.1088/0953-2048/11/12/006.

A. Ducluzaux. “Extra losses caused in high current conductors by skin and proximity effects.” In: Schneider Electric Cahier Techniques no. 83 (1983). url: https://www.ops-ecat.schneider-electric.com/cut.CatalogueRetrieverServlet/CatalogueRetrieverServlet?fct=get_element&env=publish&scp_id=Z000&el_typ=rendition&cat_id=DesignerV4&maj_v=2&min_v=14&nod_id=0000000008&doc_id=H383536&frm=pdf&usg=&dwnl=true (visited on 09/20/2017).

J. A. Ferreira. “Analytical computation of AC resistance of round and rectangular litz wire windings.” In: Electric Power Applications, IEE Proceedings B 139.1 (1992), pp. 21–25.

Peter Graneau. Underground power transmission: The science, technology, and economics of high voltage cables. A Wiley-Interscience publication. New York NY u.a.: Wiley, 1979. isbn: 0-471-05757-6.

Oliver Heaviside. “Transmission of Energy into a Conducting Core.” In: The Electrician (1884), p. 133.

Oliver Heaviside. “Electrical Papers - Vol. 2.” In: (1894). url: https://archive.org/details/electricalpapers02heavrich (visited on 09/20/2017).

Dominik F. P. Joachim. “Stromverdrängungseffekte bei Millikenleitern.” PhD thesis. Duisburg: Universität Duisburg, 1998.

David W. Knight. “Practical continuous functions for the internal impedance of solid cylindrical conductors.” In: ResearchGate (2016). doi: 10.13140/RG.2.1.3865.1284. url: http://g3ynh.info/zdocs/comps/Zint.pdf (visited on 11/16/2017).

James Clerk Maxwell. A treatise on electricity and magnetism - Vol. 2: 1st edition. 1873. url: https://archive.org/stream/electricandmagne02maxwrich#page/n7/mode/2up (visited on 04/22/2016).

Humphreys Milliken. “Electrical Cable.” Patent: 1,904,162 (USA). 1933.

Humphreys Milliken. “Electrical Power Cable.” Patent: 2,187,213 (USA). 1940.

Paul J. Nahin. Oliver Heaviside: The life, work, and times of an electrical genius of the Victorian age. Baltimore, Md. and London: Johns Hopkins University Press, 2002. isbn: 0801869099.

John Henry Poynting. “On the Transfer of Energy in the Electromagnetic Field.” In: Philosophical Transactions of the Royal Society of London 175 (1884), pp. 343–361. doi: 10.1098/rstl.1884.0016.

Robert H. Romer. “What do “voltmeters” measure? Faraday’s law in a multiply connected region.” In: American Journal of Physics 50.12 (1982), pp. 1089–1093. doi: 10.1119/1.12923.

P. Silvester. “AC Resistance and Reactance of Isolated Rectangular Conductors.” In: IEEE Transactions on Power Apparatus and Systems PAS-86.6 (1967), pp. 770–774. doi: 10.1109/TPAS.1967.291888.

JohnWilliam (Baron Rayleigh) Strutt, ed. Scientific Papers. Vol. II. London: C.J. Clay and Sons, 1891. url: https://ia801409.us.archive.org/20/items/cu31924005544139/cu31924005544139.pdf (visited on 09/20/2017).

Charles R. Sullivan and Richard Y. Zhang. “Analytical model for effects of twisting on litz-wire losses.” In: 2014 IEEE 15th Workshop on Control and Modeling for Power Electronics (COMPEL). 2014, pp. 1–10.

Ido Yavetz. From obscurity to enigma: The work of Oliver Heaviside, 1872-1889. Reprint of the 1995 ed. Modern Birkhäuser Classics. Basel: Birkhäuser, 2011. isbn: 9783034801775.

Richard Y. Zhang, Jacob K. White, John G. Kassakian, and Charles R. Sullivan. “Realistic litz wire characterization using fast numerical simulations.” In: Twenty-Ninth Annual IEEE Applied Power Electronics Conference and Exposition (APEC), 2014. Ed. by Haidong Yu. IEEE, 2014, pp. 738–745. isbn: 978-1-4799-2325-0.

1.3 Influences in the Electrical Measurement Method of Conductors

1.3.1 Particularities of Electrical Measurements at AC

The electrical measurement method uses electrical signals, namely the measured voltage drop $\underline{u}_{\mathrm{meas}}$ and the total conductor current $\underline{I}$, to determine the AC resistance R_{meas} of a conductor section. Underlined symbols indicate complex values, arrows indicate vector quantities. Different methods to obtain these signals are available and further described in section 2. Typically, a current path and a voltage measurement loop are present in the setup.[2] The closed current path delivers the test current to the conductor under test (CUT). The voltage loop is composed by both voltage lead wires, which are attached to the CUT directly at locations a and b, the CUT itself and the inner measurement resistance of the measurement system R_{im} (see Figure 1-8).

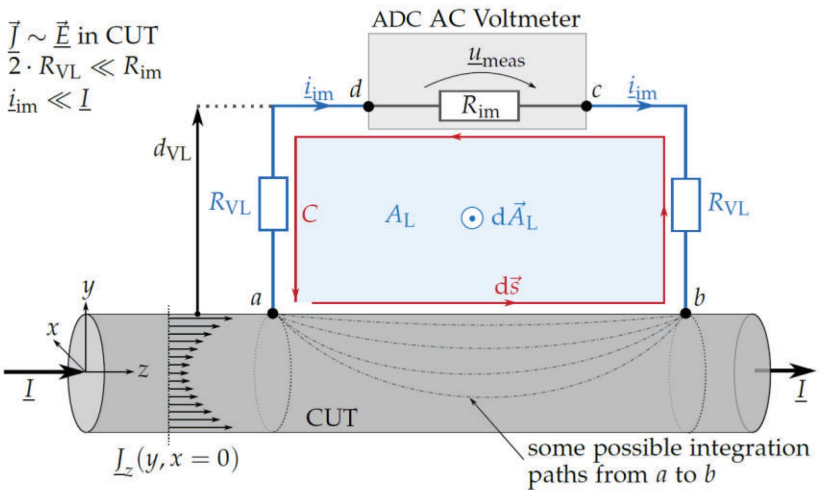

Figure 1-8: Measurement setup on a cylindrical solid CUT highlighting the voltage leads (blue lines) and voltage loop (blue area) [2, p. 75]

It is important to note that at AC, the measured AC resistance can depend on the arrangement of the voltage loop as it can be influenced by complex magnetic fields penetrating the voltage loop. The measured resistance is composed of:

$$R_{\mathrm{meas}} = \frac{1}{l_{\mathrm{meas}}} \mathrm{Re}\left(\frac{\int_a^b \underline{\vec{E}} \cdot \mathrm{d}\vec{s} + \mathrm{d}/\mathrm{d}t \iint_{A_{\mathrm{L}}} \underline{\vec{B}} \cdot \mathrm{d}\vec{A_{\mathrm{L}}}}{\underline{I}} \right). \qquad (8)\ [2,\ \mathrm{p.}\ 76]$$

In the formula above l_{meas} is the length between voltage tap-offs a and b. $\underline{\vec{B}}$ is the complex flux density vector, $\underline{\vec{E}}$ is the complex electric field vector, $\mathrm{d}\vec{s}$ is the vector boundary element of the voltage loop and $\mathrm{d}\vec{A_{\mathrm{L}}}$ is the vector area element of the voltage loop. The resistance of the CUT is connected to the losses by:

$$P_{\mathrm{meas}} = \underline{I}^2 \cdot R_{\mathrm{meas}} \quad . \qquad (9)$$

Due to this simple connection the term *losses* and *resistance* can both be used equally to describe a conductor's performance. From that observation arises the differentiation between the *true* losses of the CUT—also called Joule, resistive or ohmic losses—which directly lead to heating of the conductor and *measured* losses, also called *apparent* losses. The goal of a measurement is that the *measured* resistance is as close as possible to the unknown *true* resistance. It is also important to acknowledge that the supplied power to a conductor can differ from the *true* losses in the conductor. The reason for that are losses in adjacent conductors due to eddy-currents in these parts. This is further elaborated in [9] for the measurement of superconducting tapes and in report [10].

---

[2] This excludes the use of bridge-measurement techniques.

In the following chapters, first the influences of the setup on the *true* losses are analyzed (e.g., additional proximity effect losses, …) and then the influence of the setup on the *measured* losses are analyzed (e.g., position of voltage loops, …).

1.3.2 Influence of Nearby Conductors on *True* Losses of the CUT (Losses due to Proximity Effect)

In a real measurement setup, the current path will form a closed loop in connection with the power source. Hence, in a 2D section of the setup, one will find the CUT and a return conductor placed at a certain distance d to the CUT. Figure 1-9 shows different setups analyzed in the following, which are frequently found in the literature. In the simulation results shown in Figure 1-10 and Figure 1-11 the CUT is a 2500 mm² solid cylindrical copper conductor. This conductor size and geometry was chosen, as it shows the worst case for the influence of nearby conductors, while still assuming a realistic cross-sectional size.

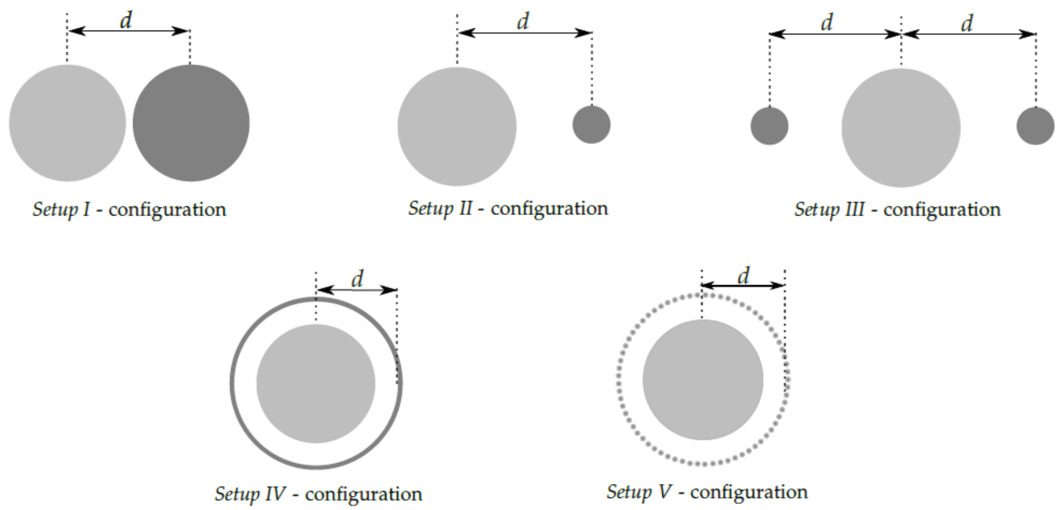

Figure 1-9: Different measurement setups with CUT (light gray) and return conductor (dark gray) in cross sectional view; d is the distance between CUT and return conductor (edited from [2, p. 93])

1.3.2.1 Influence of Different Return Conductor Setups

Numeric simulations in [2] have shown that typical setups presented in literature do not experience significant (> 0.1 %) proximity effect losses due to the position of return conductor(s) or other metallic components. These results of different configurations are shown in the following.

Setup I uses the same conductor as a return, *Setup II* uses a smaller solid cylindrical copper conductor with a cross section of 240 mm² as a return and *Setup III* uses two 240 mm² solid copper conductors as the return conductors and located in the same plane as the CUT.

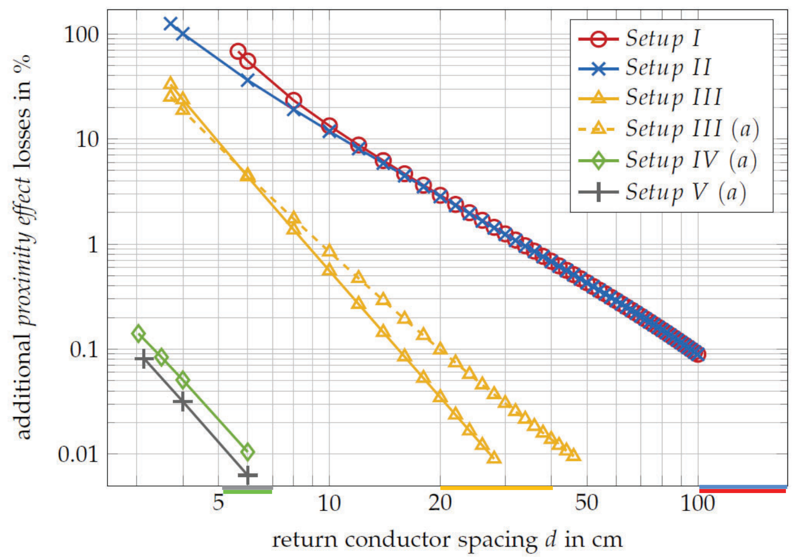

Figure 1-10: Additional losses in the CUT due to proximity effect for different return conductor setups and spacings (edited from [2, p. 94]); the colored lines on the horizontal axis indicate typical d ranges found in the literature

Asymmetric (denoted as (a) in the plots) relates to one return conductor being placed at d+3 cm and inbalanced return conductor current (one with 0.45 and the other with 0.55 times the total test current). In these setups parameter d indicates the centre-to-centre distance between both conductors. *Setup IV* has a solid tubular aluminum conductor as a coaxial current return path with a cross section of 600 mm² and *Setup V* has a copper wire screen as a coaxial current return path with an overall cross section of 257 mm² for 69 wires. In both setups, d denotes the distance from the center of the CUT to inner side of the metallic screen. In *Setup IV* and *V*, asymmetry is obtained by shifting the CUT 2 mm from the geometric center of the return conductor. This is an estimate of the maximum allowed eccentricity of the insulation for large cables according to IEC 62067.

1.3.2.2 Influence of Conducting Material in the Surrounding

The presence of magnetic or metallic materials is the surroundings of the measurement set-up can influence the *true* resistance of the conductor through proximity effects and hysteretic losses.

Figure 1-11 shows additional *true* losses in a single cylindrical 2500 mm² copper CUT placed above a conductive surface. It shows up the differences depending on the grounding condition of this piece of conducting material and the influence of different materials used. For iron a predefined Soft-Iron material from COMSOL Multiphysics including its non-linear behavior was used with a magnetic permeability μ_r of 100 and a measurement current of a couple of amperes in the CUT.

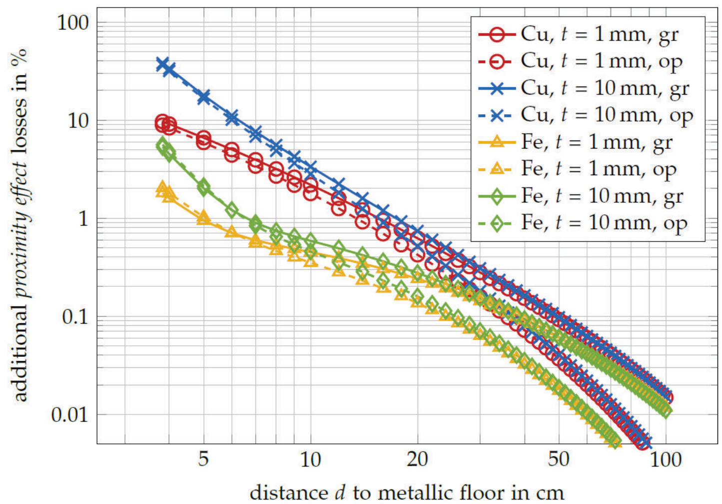

Figure 1-11: Additional losses in the CUT due to proximity effect because of different metallic ground plates and spacings d [2, p. 95]; "gr" = grounded, "op" = open/floating

In order to reduce the proximity effect, the metallic materials must be as thin as possible (to reduce eddy currents) and as far as possible from the measurement set-up. Only the latter can usually be influenced by the user. Proximity effect decreases with increasing distance between adjacent conductors as seen in the figures above.

Magnetic material losses are proportional to the magnetic field they "see". Magnetic materials in the vicinity of the measurement set-up must be avoided.

In theory, using a perfectly concentric coaxial set-up (opposing currents in inner conductor and screen) will cancel the magnetic field outside the set-up and so the effects of metallic and magnetic materials external to the setup. However, deviations from concentricity in realistic setups or gaps in the screen as in copper wire screens, can lead to magnetic field leakage outside of the coaxial arrangements and then again, the CUT can be influenced by other conductors or conductive parts outside of the coaxial arrangement.

1.3.3 Influence of Nearby Conductors on *Measured* Conductor Losses

Measured or *apparent* losses can differ from the *true* losses of the conductor if complex magnetic fields are captured in the measurement loop [2]. From equation (8) it can be seen that the *measured* AC resistance also depends on the magnetic field penetrating the voltage loop. If the magnetic field $\underline{B}$ in the loop is purely real (also called in-phase) to the test current $\underline{I}$ (the test current is always purely real by definition as it is the reference), its derivative makes the induced voltage purely imaginary. Therefore, it will only influence the reactance but not the resistance, for which the real part of the voltage measurement is considered. If outer magnetic fields are complex (also having an imaginary or out-of-phase component), its derivative will have an in-phase component, resulting in an in-phase/resistive voltage drop and hence influence the *measured* resistance.

Complex magnetic fields outside of a conductors arise whenever non-rotationally symmetric current densities are present. Hence at AC, purely real magnetic fields are only present under special circumstances, where the current density is perfectly rotationally symmetric: outside of an isolated[3] cylindrical conductor (either solid or hollow) or in any perfectly concentric combination of these two cylindrical conductor types (for example in a coaxial cable). Plots of the imaginary magnetic field component are shown for simple arrangements in [2, p. 78] and some more realistic arrangements, where the real and imaginary part of the magnetic field is plotted are shown in Figure 1-12.

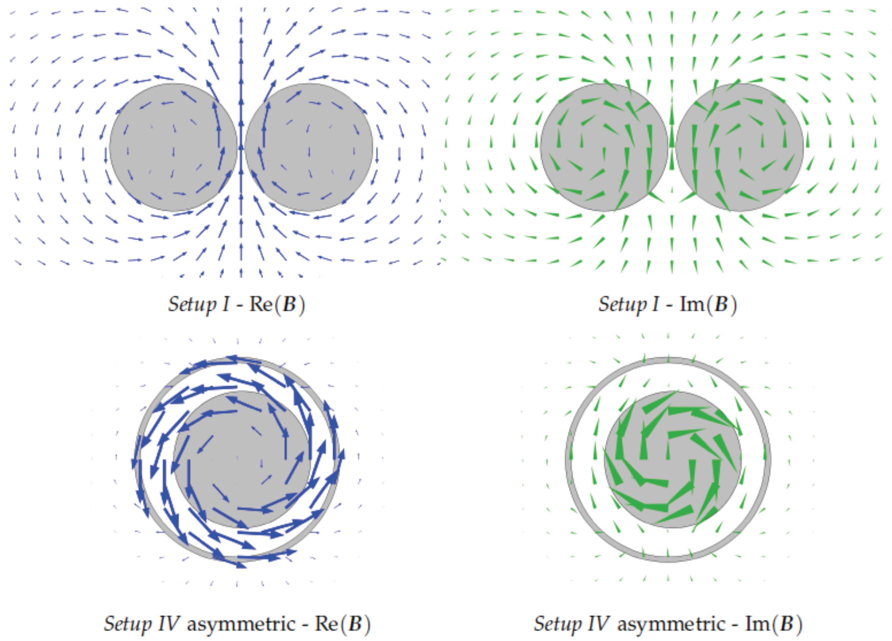

Figure 1-12: Real (blue arrows) and imaginary (green cones) for *Setup I* and *Setup IV* from [2, p. 97]

At AC, when significant AC losses are present in the setup and result in complex outer magnetic fields, the *measured* resistance can depend on the position of the voltage measurement loop. The main goal is to find a configuration/position that leads to the *measured* resistance being as close as possible to the *true* resistance of the CUT. Different configurations are discussed later in section 3.4.

1.3.4 Influence of Current Contact System

Especially when measuring short conductor samples of a couple of meters length, the current path connection on both end of the specimen can greatly influence the measurement [11].

End-effects must also be taken into consideration. For example, the field generated by the connections between the conductor under test and the return conductor is not negligible near the connection points. Therefore, the conductor/set-up dimensions must be much larger than the voltage drop measurement set-up.

The following subsections show some basic investigations on current homogenization in different conductor types. The main goal in any case is to establish a representative current density distribution in the CUT and especially in short samples and not include end-effects from the terminals in the measurement.

1.3.4.1 Solid Conductors

The importance of the need for a steady current distribution in the measurement of voltage drop is demonstrated in a simple experiment, where a current is injected in a tubular conductor through

[3] Meaning that there is no other conductor nearby.

either two single connection points or in a symmetrical way by multiple contact points [12]. The current distribution is not equivalent over the whole cross-section.

The voltage drop is then measured at different radial angles from the injection plane. For distributed injection, the voltage drop measurement is relatively independent of the radial angle of application of the voltage taps (See fig Figure 1-13). For single injection points, the non-symmetrical current distribution is clearly demonstrated. Thus, a steady current distribution over the conductor cross-section is necessary to achieve precise and reproducible measurements. This demonstrates the need for symmetrical connections and/or large distance between the injection points and voltage taps application.

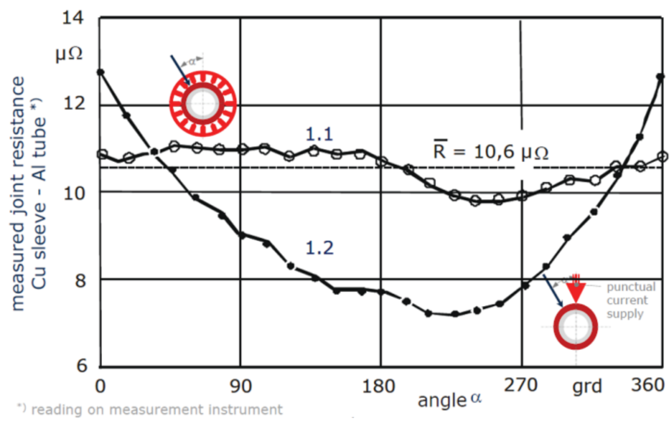

Figure 1-13: Voltage drop measured at different radial angles for 2 different current injection configurations [33]

Preliminary FEA studies in [13] have shown that in a frequency range from 0-300 Hz the current distribution becomes nearly the same (deviation <1 %) as for a homogeneous current injection after approximately 15 cm from the punctiform injection for a 2500 mm² copper solid (see Figure 1-14) and the copper tube used in the round robin test.

Another finite element analysis on a thin plate with current injection through a single contact point in

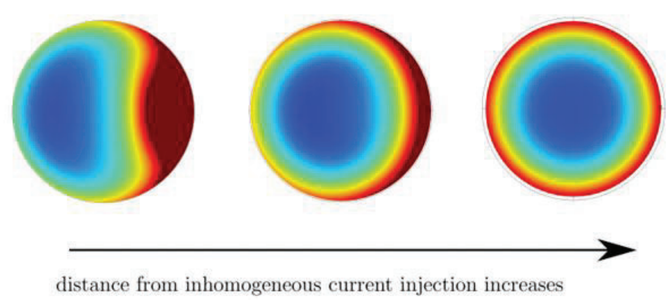

Figure 1-14: FEA analysis current density of punctiform current injection into a solid conductor (edited from [13])

the corner show that a uniform current distribution of $(I_{\max} - I_{\min})/I_{\min}$ = 0.01 % is reached after approximately 3 times the width of the plate. This is in line with the previous value obtained for round conductors.

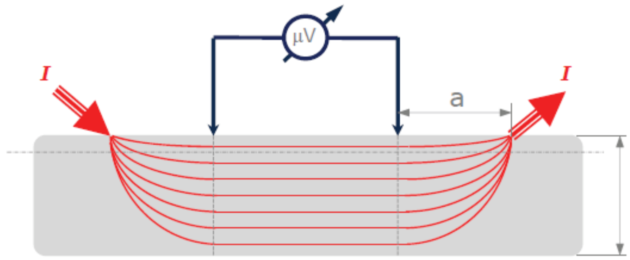

Figure 1-15: Sketch of current distribution for punctiform injection [12]

1.3.4.2 Stranded Conductors

In stranded conductors, the problematic of steady current distribution over the cross-section of the conductor is reinforced by the non-uniform contact resistances between the wires. For example, even in case of a symmetrical current injection at the conductor's surface (as in Figure 1-13) the injected current may not reach all strands in the cross section due to contact resistances between the single wires and hence would deliver a misleading resistance measurement. This is particularly true for aluminum conductors where an insulating oxide layer (Al_2O_3) quickly forms on the wire surface and for water-blocked conductor where interstitial material is present. The contacts are then random and not well established and their statistical distribution and possible modification with temperature, bending, etc. may strongly influence the AC electrical behavior of the conductor.

The homogenization of the current through the cross-section will need a longer distance from the current injection point. This is shown in measurements on aluminum conductors using clamps (jaws) placed at different distances from voltage measurement knives (see Figure 1-16). The cable is placed in the system, DC resistance is measured and the cable is removed. This operation is repeated 10 times using identical cable and parameters, and the standard deviation of the results is calculated. The deviations obtained are far above the typical resolution of the system (measured for example with a copper rod) and reflect the effect of the changing current distribution whose homogeneity improves with longer distance between current injection and voltage measurement.

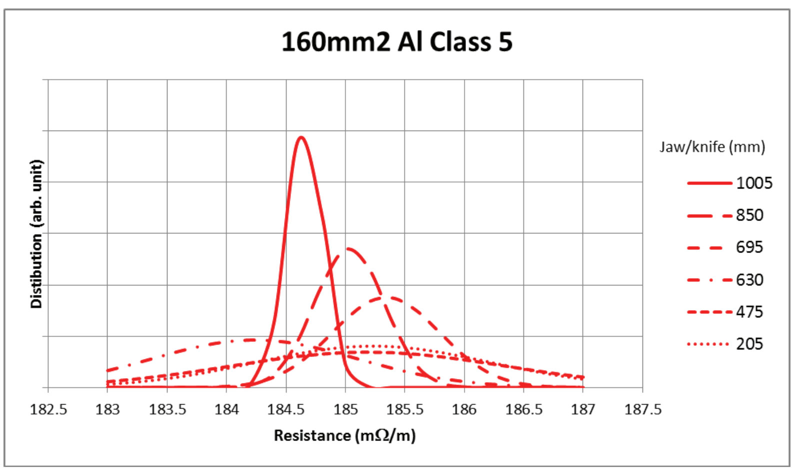

Figure 1-16: Reproducibility of the measurement of the DC resistance of a 160 mm² class 5 aluminum conductor for different distances between the current injection point (jaw) and the voltage tap (knife)

In addition, mechanical constraints on the conductor may also modify inter-wire contacts, affecting distribution of eddy currents and hence AC resistance value. This means that measurements in the lab may not always faithfully reflect the real value of a conductor during service.

- Increasing the constraints by longitudinal tension of the conductor have been shown to improve the repartition of the current through the cross-section and hence the precision of the measurement for DC resistance [14]. Applied to AC, this will usually increase the AC value by reducing inter-wire contact resistance and hence increasing skin effect.

- Torsion/detorsion (twist) will have similar impact as tension, although the behavior is more difficult to interpret and reproducibility is worse.
- For insulated cables, mechanical constraints on the conductor due to insulations system may also affect the measurement. Moreover, they may relax with time/temperature (frozen constraints due to the manufacturing process). Cable metallic screen can also impact these constraints. Preconditioning of the sample in a way these constraints are fully relaxed (thermal cycles until the measured value is stable) is of interest.

One can then expect different behavior depending on the material and conductor design:

- For copper, the inter-wire resistance is generally low and a behavior close to solid conductor can be expected.
- For aluminum, the presence of an insulating oxide layer at the surface of each wire usually leads to larger inter-wire resistance, depending on the degree of oxidation of the wires. But this is also influenced by geometrical aspects such as wire sizes, cabling length, compaction degree of conductor and wire deformation, non-uniformities due to the manufacturing process, as well as twist and tension of the conductor during the measurement. The distance from the injection point to get a steady current distribution will then strongly increase as compared to solid conductor.
- Conductor watertightness systems may lead to similar behavior (for example by the use of insulating tapes between each layer of wires).
- Milliken conductors, where the sectors, as well as the central core, are usually insulated, show similar problematic current distribution through the cross-section
- In the case of insulated wires (enameled wires), current cannot at all flow between the wires and the distribution must be steady from the connection point, which renders the preparation of the injection system essential.

From these comments it appears that the connection system for the current injection is critical. Steady current distribution is essential for proper measurement. Welding all the wires together over a defined length or use a butt-to-butt connection, for example by welding a solid conductor directly on the end of the conductor to be measured, are the best suited solutions. Repeatability of the welding process must however be demonstrated.

Welding of the conductor terminals itself will provide the best solution as this guarantees that all wires have a low resistive contact to the current injection. However, the length of the weld needs to be sufficiently large for the current to not have a preferable path between injection point and single strands. To reduce the necessary distance of the weld or short circuit of all the single wires, the current should still be injected into the solid section as homogeneous as possible (compare symmetrical injection into a solid in Figure 1-13).

For example, in the case of a weld over the conductor, the contacting system is preferably a ring connected over a short distance at cable end (see Figure 1-17) or has a connection to the complete surface at the end.

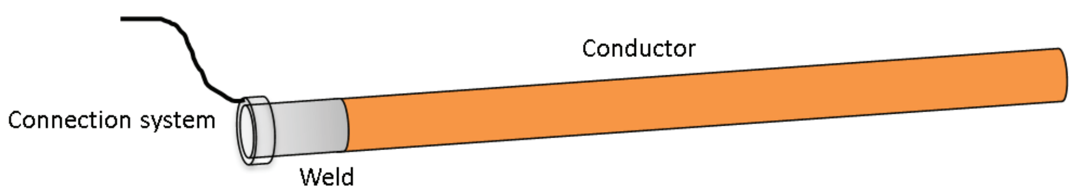

Figure 1-17: CUT with welded terminal and a ring connection to the solid section (lower resistance than the weld itself)

1.3.4.3 Conclusion

Distributing the test current into the whole available conductor cross section, in other words all wires, can be challenging. Especially when the single strands are insulated from one another as with aluminum wires or enameled copper wires, a simple current connection at the surface of the conductor is not sufficient. However, it is necessary for the current to be able to use the whole available cross section, as this influences its resistance. Section 2.5.3 presents different contact systems that are available and can be used.

From the theoretical standpoint a low resistance short circuit of all strands is required at both terminals of the conductor. In reference [11] numerical simulations on a real Milliken conductor cross section connected to lumped circuit elements were conducted. It was found that the main factors influencing the current distribution in the CUT are the type and length of the short circuit of all wires (for example being a solid weld at both terminals of the conductor) and the conductor length between both terminals. In other words, the ratio of resistances of the contact system to the wires to the resistances of the wires over the sample length.

If the length of the CUT is a couple of meters and the length of the low resistance short circuit between all wires (being a weld in this investigation) is approx. 1 cm, the conductor will have a representative current density distribution. This is under the assumption, that the connection of the current path to the weld is also as homogenous as possible and not a point contact on one side of the weld's surface for example. The best a current contact system can do is allow the CUT itself (the impedance of different strands) to determine the distribution of the current density by providing a low resistance homogeneous current injection. In other words, the current contact system should influence the preferred current paths into the strands as little as possible. The representative current distribution, influenced by the exact design and unknown to the user, can then build up in the CUT between both terminals.

The results of this study and also other investigations went into the recommendations put forward later in chapter 3. As with the other influences mentioned in chapter 1.3, following the recommendations presented later will allow an accurate AC resistance measurement.

1.3.5 Influence of Type and Positioning of Voltage Tap-Offs

If all wires have a low resistance connection on both sides of the conductors, as described in the previous subsection, it does not play a role which strands the voltage tap-offs touch (are connected to). Usually, the voltage tap-offs will be connected to the surface of the CUT. In a stranded conductor or Milliken conductor this means the outermost layer of wires has direct contact with the voltage tap-offs. When considering a Milliken conductor with enameled wires (inter-wire resistance is much larger than the resistance along a strand):

- At DC the voltage drop over the measurement length will vary for different layers (as the lengths of wires in different layers may vary). However, according to its resistance also the current in and hence the voltage drop over a strand will vary. Effectively the voltage drop will be the same, independent of which wire is connected to the voltage tap-offs. It is a simple parallel connection of resistances, with the same voltage at both ends due to the short circuit.
- At AC the voltage drop over the measurement length will also vary for different layers (as the lengths of wires in different layers may vary and as strands in different geometric positions will have different impedances at AC). For example, due to skin effect, current flows preferably at the surface of the conductor (if its stranded or solid) and hence bears more current. However, by considering the connection of the voltage tap-offs to different strands (e.g. at the surface or center of the conductor), one will also affect the formed voltage loop $\mathrm{d}\vec{A}_{\mathrm{L}}$. At AC, complex magnetic fields also exist inside conductors (see Figure 1-12) and will then influence the *measured* voltage drop. It can be shown that the voltage drop will be independent of the connected strands, as long as the above-mentioned condition holds. This is demonstrated for a solid conductor in [2, p. 79], as one could also ask what is the path to be taken for the line integral $\int_a^b \underline{\vec{E}} \cdot \mathrm{d}\vec{s}$ of formula (8) in a conductor of a non-zero thickness.

Following the argument above, it is not important, if both voltage tap-offs a and b even touch the same wire or different wires in the outer layer. Again, this only applies when all the wires have a low resistance short circuit at both ends. In practice, usually a circumferential connection is made by a thin[4] wire, touching all strands in the outermost layers.

---

[4] In case of a Milliken conductor, the wire should also be thin to not allow current to jump from one segment surface wire to others (short circuit them). However, if different segments in a Milliken

The voltage drop is proportional the distance between voltage taps. This means that a precise positioning of the taps directly affects the accuracy of the results. Hence, the uncertainty in length measurement (distance between the voltage tap-offs) should be as low as technically possible. This uncertainty or error in length measurement needs to be contributed to the overall measurement error at the end.

For example, to keep this contribution low in the uncertainty budget one could go for an ambitious value of 0.01 %, meaning 0.1 mm on a 1-meter distance between taps, or 1 mm on 10 m. To achieve this, precautions must be taken in the installation of the taps and in the distance measurement. A good practice is to fix the voltage tap-offs on a ruler and measure their distance either mechanically with adapted equipment, or electrically using a calibrated rod placed on the measurement system. In the case the measurement is performed on a bended sample, length measurement should be done on the neutral line (center axis) of the bend.

A general recommendation for the voltage tap-offs is:

- thin conductive wire, to allow accurate length measurement;
- good connection to at least 1 wire of the conductor (alternatively one can make contact to multiple wires on the surface of the conductor by a circumferential connection);
- only little conductive material should be close to the conductor to not introduce additional stray fields and *true* or *apparent* losses.

1.3.6 Influence of Mechanical Stress

The mechanical conditioning of the conductor/cable (history, tension/twist, pressure of insulation system, etc.) can have an influence on cable properties and hence on the AC resistance measurement results.

Basically, the conductor mechanical stress should be representative of the field conditions.

For bare conductors, to get comparable results, it is recommended to use the same procedure for measurements on different samples. However, AC resistance being strongly influenced by inter-wire contacts that directly affect the skin effect, following considerations should apply:

- There should be no twisting of the conductor as compared to its final configuration after field installation. Orientation of the cable ends with regards to each other must then be recorded before cutting the samples and controlled before starting the measurement.
- Tensioning of the conductor should be limited to its straightening to bring it in the position adapted to the measuring equipment.

1.3.7 Influence of Temperature

Temperature is a critical parameter and will affect different aspects of the measurement as described here. Temperature may be considered as an external factor (ambient) or as a consequence of the measurement itself: e.g., change in temperature due to large test currents and Joule heating of the CUT. As shown before, the AC and DC resistances are directly affected by temperature; temperature stability and tracking are therefore of great importance.

The influence of temperature on the resistivity of the material can be taken from the IEC 60228 standard to correct the measured DC value to 20 °C, or by the T_{SF} factor described above in section 1.2.6. There it is also shown that the AC to DC resistance ratio at a certain frequency changes with temperature. With rising temperature, the AC to DC resistance ratio is expected to decrease [15].

The order of magnitude for copper and aluminum is approx. 0.4 %/°C. This highlights the fact that mastering the temperature homogeneity is a key factor for accuracy. This may be quite challenging when the CUT is long.

For the measurement, the mean value of the sections between the voltage taps should be considered as representative.

---

conductor are built identically, there should also be no voltage difference between the surface wires of different segments at a certain axis position and therefore no current flowing over the voltage tap-off wire between different strands of the conductor.

A stable environment (dedicated room without sunlight, direct conditioning air flow, etc.) is of importance. Once the CUT is installed on the system, a period of 12 h of stabilization (depending on conductor size/system configuration) might be necessary to have an evenly distributed temperature. For measurement at non-ambient temperatures, special care must be taken on temperature stability during the whole measurement.

End-effects such as heating at the current injection contact points or thermal dissipation along the cable axis and at the terminals must be avoided as much as possible. If this is not the case, a suitable distance between the current injection point and voltage taps must be considered. Temperature control along the complete cable is necessary to guarantee temperature stability in the measurement section between the voltage tap-offs.

The use of one (or more, depending on the conductor length) thermometers placed in direct contact with the conductor is necessary to get a correct estimate of the temperature and assess possible deviations over the length that are necessary for accuracy evaluation.

1.3.7.1 Temperature Induced Mechanical Effects

Effect of thermal expansion is usually relatively low as typical thermal expansion coefficients of aluminum and copper are respectively $24 \cdot 10^{-6}$ K^{-1} and $17 \cdot 10^{-6}$ K^{-1}, meaning a length variation of less than 0.2 % between 20 °C and 90 °C. The length chosen for evaluation, is the length at 20 °C. Depending on required accuracy, these may however also be considered, as well as the relative expansion of the voltage taps support if relevant.

1.3.7.2 Influence of Thermal EMFs

Thermal voltages generated at the contacting areas of electrical voltage probes can be in the range of several mV. However, these DC voltages do not affect the AC measurements as these uni-directional voltages are averaged out by the changing electromagnetic fields at AC. To prevent their influence on DC resistance measurements, a bipolar DC resistance measurement should be conducted in any case. This means reversing the DC test current direction and measure the voltage drop in the opposite direction. The mean value of both measurements is then taken as the real DC value.

1.3.8 Influence of Choice of Measurement Frequency

Ideally the measurement frequency f does not coincide with the local power grid frequency (50 Hz or 60 Hz) to avoid perturbations due to external electromagnetic fields (interferences). In Figure 1-18, the left curve shows the non-linearity of the resistance with frequency, while the right graph demonstrates the sensitivity of the measurement to external perturbations (the closer to the power frequency, the larger the uncertainty). Measurements were performed on a segmented (Milliken) cable conductor using the setup with symmetric return current leads in the horizontal plane and a single voltage loop 3 mm above the surface of the conductor.

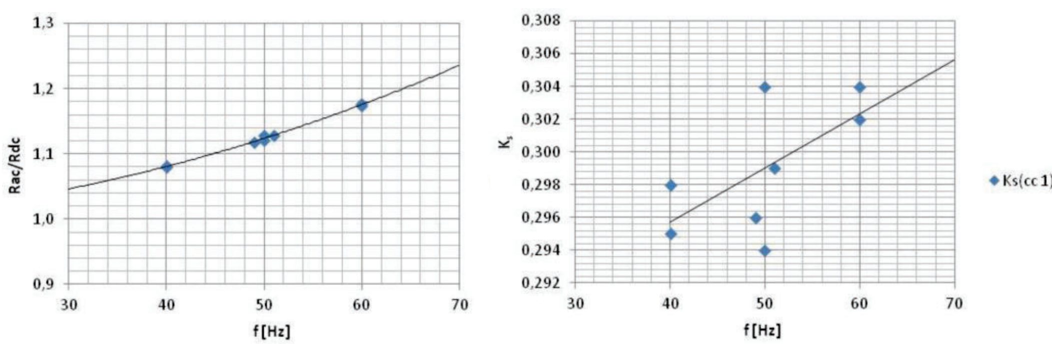

Figure 1-18: Typical resistance over frequency curve (left); influence of interferences close to grid frequency 50 Hz (right)

This effect can then be mitigated by interpolating two or more measurements taken symmetrically around the power frequency and distant by 1 Hz to 5 Hz. Linear interpolation is considered reasonable for small distances on the frequency axis. Using larger measurement currents to increase voltage drop may also help to mitigate this effect.

The ideal case and considered as best practice—if the measurement system allows—is to tune the measurement frequency to the measurement temperature directly, as shown in [2, p. 127] (also refer to section 1.2.6). This pre-scaling has the advantage that only one AC measurement is required, if $T \neq T_0$. The necessary measurement frequency is then not directly at 50 Hz or 60 Hz but close enough and can easily be corrected to the right frequency $f(T_0)$ (e.g. 50 Hz or 60 Hz) and temperature T_0 (e.g. 20 °C or 90 °C).

For example, if the lab and hence copper CUT temperature T is stable at 24 °C, T_{SF} according to formula (6) is approximately 0.98, if the desired temperature for evaluation $T_0 = 20\,°\mathrm{C}$. Using formula (7) one can obtain the measurement frequency at this temperature $f(T)$, which is:

$$\frac{f(T_0)}{T_{\mathrm{SF}}} = f(T) = \frac{50\ \mathrm{Hz}}{0.98} = 51.02\ \mathrm{Hz} \quad . \tag{10}$$

Hence, measuring the CUT at 24 °C and at 51.02 Hz, one gets the same value as with a measurement performed directly at 50.00 Hz and at 20 °C, by only having to perform one measurement.

If scaling is performed afterwards, multiple measurements close above and below 50 Hz need to be performed (see Figure 1-18), so that one can stretch or squeeze the interpolated curve (compare Figure 1-7). In any case the deviation to the desired temperature should not exceed ±5 °C ($|T - T_0| < 5\,°\mathrm{C}$) as the *Principle of Similitude* should not be applied over large frequency ranges for complex conductors (see section 1.2.5).

2. State of the Art Measurement Methods

This chapter presents the state of the art methods concerning different aspects of the AC and DC resistance measurement as the history of such measurements is quite long and rich.

2.1 Measurement of Temperature

Resistance accuracy is directly related to temperature by the thermal coefficient of the resistivity, which for copper and aluminum, is close to 0.4 %/°C.

Depending on required accuracy of the AC resistance measurement, temperature needs to be controlled carefully.

In any case, the error linked to the evaluation of real temperature of the measurement must be considered in the accuracy calculation of the AC resistance measurement. The resistance measurement will be influenced by the distribution of the temperature of the conductor between the voltage taps. The mean temperature of this portion of the cable can be considered as representative of the temperature of the measurement. However, ideally the temperature must be constant between the voltage tap-offs. For a reasonably stable temperature, a single measuring point in the middle of this portion may be considered as sufficient owing to the good thermal conductivity of the metallic materials usually used (copper or aluminum).

However, sufficient stability along the length must be guaranteed.

At room temperature without heating, a stabilization time of about 12 h (depending on conductor cross section and system configuration) in a temperature stable environment is generally sufficient. Care must however be taken to make sure the measurement current does not affect the temperature distribution.

At high temperature, using non-uniform heating (circulating current, localized heaters, etc.) temperature distribution over the conductor length must be controlled. The use of multiple thermometers along the length is recommended.

2.1.1 Thermometers (Thermal Sensors) and Sensor Positioning

Thermometers are preferably placed in direct contact with the metallic conductor (possibly using temperature conducting paste) to avoid large discrepancies between thermometer reading and real conductor temperature.

The number of sensors will depend on:

- The measurement temperature: more sensors are needed at high temperature to check the stability of the system.
- The tested length: sensors are needed to check the gradient over the length.
- The measuring current: high currents may lead to conductor/connector heating.

Typically, for short measurement lengths (e.g., 1 m length between voltage taps) at room temperature: 3 sensors are sufficient, to also be able to check for temperature distribution along the sample (see Figure 3-1 in section 3.1.1).

For large systems at room temperature: At least 1 sensor at the center between the voltage tap-offs and 1 sensor at each voltage tap-off. In addition to those, for measurements at high temperature or for large current, where a gradient due to connector heating may be expected: 1 additional sensor on each side close to the current injection systems is recommended (see Figure 3-2 in section 3.1.1).

The temperature difference and stability over time must be measured and should not be more than:

- ±0.5 °C over the measured length and measurement time for room temperature measurements (up to 40 °C).
- ±2.5 °C over the measured length and measurement time for measurements at high temperatures (above 40 °C).

In any case, the uncertainty on temperature must be considered in the uncertainty budget. The mean value of the sensors placed between and at the voltage taps must be taken as the effective measurement temperature.

More details and specific recommendations can be found in section 3.1.1.

2.1.2 Temperature Measurement by DC Resistance Measurement

When the DC linear resistance of the conductor is known, DC measurement can be used to measure the mean temperature of the conductor.

This might be useful for on-site measurement, when physical access to the conductor for sensor insertion is not possible. As well, when joule heating is used and different temperatures between the center and the surface of the conductor appear during the measurement phase, DC resistance might be relevant. The DC resistance can be directly scaled in temperature using T_{SF} correction factor (see section 1.2.6).

It must however be noted that the temperature must be stable enough so that there is no change during the time of switching form DC to AC measurement or because of the losses due to the measuring current. A good practice is to make a second DC measurement after the AC measurement, check that the difference is reasonable, and use the mean value obtained from both DC measurement as the effective temperature during the AC measurement.

2.1.3 Temperature Stabilization

Stability of the temperature during the measurement is of utmost importance to get reliable and reproducible results. Temperature must be stabilized within the required range (determined by required accuracy of the AC measurement) during at least 10 minutes before starting the measurement. External influences like air conditioning flow or sunshine on the CUT must be avoided. More details and specific recommendations can be found in section 3.1.1.

2.2 DC Resistance Measurement

2.2.1 References to DC Measurements

The amount of literature relating to DC and AC loss measurements is large. The following is a narrow selection that serves to illustrate the variety of methods available and to motivate the selection of a direct electrical measurement.

Reference [16] recommends that DC and AC properties are measured in an immediate sequence to avoid large temperature differences or differences in temperature distributions over the CUT. References [17] and [18] emphasize the importance of even contact resistances for the current injection, in order to not disturb the DC resistance result. References [17] and [19] define how the CUT temperature must stabilize, and the good practice of avoiding drift in the DC measuring location.

Special considerations need to be made, if the conductor is composed of multiple conductive or magnetic materials, when scaling measured results from the measurement temperature to the reference temperatures of 20 °C or 90 °C [19].

2.2.2 Special Considerations of DC Resistance Measurements

Thermal voltages generated at the contacting areas of electrical voltage probes can be in the range of several mV. Contact areas and temperature sensors need to be covered to give true and stable signals, and thermal offset voltage eliminated by the change of measurement current polarity or by taking the slope of the voltage-current curve for multiple DC current amplitudes, i.e., use the relationship $R = \mathrm{d}U/\mathrm{d}I$ instead of $R = U/I$. This is also briefly discussed in section 1.3.7.2 and in the following section.

2.2.3 Equipment and Test Methods

The metrology consists basically in applying Ohm's law by "injecting" a current I and measuring the voltage drop U on a defined length of the CUT: $U = R \cdot I$.

The equipment needs to be designed for responding to the various real constraints and the overall accuracy results from the combination of all uncertainties (also see section 3.6).

The DC resistance of a conductor with a uniform cross-section is given by Pouillet's Law

$$R_{\mathrm{DC}} = \rho \frac{l}{A} \quad , \qquad (11)$$

where ρ is the material resistivity and A the cross section of the CUT. The first constraint is the measurement length l which must be determined with high precision. For linear resistance, the standards fix it to at least 1 meter (IEC 60228). In most of the cases, 1 meter is used.

Practically, with a mechanically stable equipment, it is possible to minimize the corresponding uncertainty by calibrating the length with a traceable certified standard rod, generally in Manganin (which resistivity is almost not affected by temperature, hence reducing a possible uncertainty factor) or copper.

The resistance of large samples can be as low as some μΩ per meter. The measured voltage may be in the range of some hundreds of μV, depending on the test current and gets perturbed by residual voltages U_{res} like thermal voltages and offset voltages of the measuring electronics. It is mandatory to eliminate those residual voltages which are independent of the current flow. That means that DC linear resistances cannot be measured with a single DC current.

A first possibility is to reverse the current. A first measurement gives $U_+ = R \cdot I_+ + U_{\mathrm{res}}$ and the next one $U_- = R \cdot I_- + U_{\mathrm{res}}$. Adding the two $U_+ + U_- = 2U_{\mathrm{res}}$ and U_{res} can be deducted from U_+ to give the result U.

In a second method, the current is reversed recurrently with a duty cycle of 50 % at a low frequency (e.g., 0.5 Hz). The electronics takes the average voltage which corresponds to U.

In a third method, the current is pulsed at low frequency. Both voltages are measured with track and hold (U_+ during the current pulse and U_{res} during the current less phase) and subtracted. An additional advantage of the method is the significant reduction of the duty cycle thus of the average current through the CUT, which then reduces its self-warming.

In a fourth method, a low frequency, say 1 Hz to 5 Hz, AC current is injected in the conductor. Thanks to synchronous rectifiers, current and voltage are measured and the real part of their quotient provides the DC resistance. When measuring on the line, where parasitic currents flow through the manufacturing machinery and the ground, it is the only reliable method for power conductors [18]. Note that for very large conductors the AC resistance at a couple of Hz (1-5 Hz) could already be larger than the claimed DC error and hence should be calculated in advance.

The chosen value of the current is a trade-off between resolution of the voltage measurement and self-warming of the CUT.

The measurement reproducibility may depend on the value of the clamping force and the mechanical longitudinal (axial) tension on the CUT, in particular when characterizing large aluminum conductors.

Furthermore, large conductors may receive additional means to improve their operation and reduce the skin effect at AC, like water blocking tapes or even insulated wires, which are detrimental for the resistance measurement with radial injection of the current, since they dramatically increase the local inter-wires resistance and mitigate the homogenization of the current density. There is presently no alternative but removing those additional layers at each sample end before starting the test, or by using adapted axial connections (for example by welding the extremities [2, p. 110]). See for further details sections 1.3.4 and 2.5.3.

Summarizing, a performing equipment for measuring DC linear resistance may integrate:

- A precision micro-ohmmeter with appropriate mean to eliminate of thermal emf;
- A length correction to the standard 1-meter reference;
- A temperature measurement of the CUT;
- Adapted and reproducible current injecting system and
- An arrangement able to adjust the mechanical tension of the CUT.

2.2.4 Conclusion

DC resistance measurement can be a complex task. The test engineer must consider various influences and possible perturbations. For AC measurement, besides further specific concerns given in Chapter 3, the same considerations apply.

2.3 AC Resistance Measurement

2.3.1 References to AC Resistance Measurements

References [16] and [20] describe a concentric measurement circuit with the conductor inserted into a solid copper end-tube creating a circular-symmetric self-field around the ends of the CUT. The cable screens are used as the return conductor. The current amplitude was determined using a special coaxial shunt with a low phase-angle error and a concentric T-connector for the current that avoids stray fields. The sampling rate is minimized by acquiring "a factor of 2" data points (e.g., 1024 or 2048) over a prime number of cycles (e.g., 7 or 11), followed by FFT analysis. The article gives a good example of an uncertainty analysis, referring to the Guide to the Expression of Uncertainty in Measurement (GUM) [21]. This analysis leads to an expected accuracy in the ratio $R_{\mathrm{AC}}/R_{\mathrm{DC}}$ of 0.1 - 0.5 % in controlled solid samples and 2 - 3 % in large, stranded conductors.

A simplified approach, where the concentric return conductor is approximated by two symmetric return conductors, one on each side of the CUT and in the same plane as the CUT, is described in references [22] and [23]. The magnetic field from the return conductors then cancels out at the centerline of the CUT, and the field is small if the distance to the two return leads is much larger than the radius of the CUT. The approach is used for bare cable conductors without a return screen. In the latter reference, the approach is shown to give the same losses as in a simultaneous calorimetric measurement.

Reference [24] contrasts the advantages and disadvantages with coaxial, asymmetric and symmetric return leads. When a solid concentric return lead (tube) is used, the CUT must be well centered in the tube to avoid large induced losses in the tube and displacement of the current distribution in the CUT. When twin symmetric leads are used, the distance must be significantly larger than the diameter of the CUT, particularly for high frequencies, and lossy conductive or magnetic objects must be kept sufficiently far away from the test circuit.

The distance of the voltage lead to the conductor surface is varied from 0.5 mm to 15 mm in references [25] and [22]. For the cylindrical conductors, there is no dependence on the measured AC resistance from the loop-size of the voltage leads, unlike the situation with non-cylindrical flat conductors which require a larger loop size [26]. Reference [27] elaborates on that a smaller loop size gives a smaller influence from external disturbances, however [22] shows that a small loop size (voltage lead near the conductor surface) is more sensitive to asymmetry in the current return leads. Consequently, a small voltage measurement loop is less sensitive to external disturbance but does not capture the full conductor loss in the case of any asymmetries. Reference [20] describes a double counter-twisted voltage loop which reduces the influence of external fields. This may be suitable when measurements are carried out at grid frequency.

Reference [28] emphasizes that when measuring the AC resistance of a long cable sample placed in a loop, it is important to reduce the inductive signal by routing a voltage lead along the length of the cable instead of connecting directly to the two ends. The accuracy is then similar to using the screen as a return path for the test current, which eliminates external fields but limits the maximum testing current due to the small cross section.

Measurements on full drums of cable are presented in [29] using low currents of several amperes and the stranded wire screen as a return conductor to avoid proximity effects between the turns on the drum. The measurements correspond well to straight sample measurements for frequencies below 100 Hz. At higher frequencies, the curvature of the conductor and any possible non-concentricity of the screen increases the *measured* AC resistance. It is commented that solid thick screens show higher *measured* losses.

In [27] and [2] measurements using the average (AVG) of multiple loops distributed around the CUT have been verified to give accurate results for multiple return conductor configuration, including using the cable sheath as the return.

2.3.1.1 Comparison between Electrical and Calorimetric Measurement

An overview of electric and calorimetric methods in quite general terms is given in [1]. Another more detailed comparison of both methods is given in [2, p. 10].

A detailed comparison of electrical and calorimetric methods is also described in [30]. The calorimetric method uses the temperature profile or the boil-off rate of a known liquid to determine the power dissipation at different current amplitudes. Calorimetric methods were for some time believed to be necessary to determine three-phase losses in non-linear cable conductors (steel armor, superconductors). The electrical measurement using lock-in amplifiers and phase-accurate current signal was described as faster and having higher resolution over a wider range of currents and losses, but with the drawback of being sensitive to external disturbances. Proposed remedies are to measure at a frequency different from the mains (i.e., 50 Hz or 60 Hz), and to pay attention to the geometries of the current circuit and voltage pick-up loops. Some electrical methods also use a resonant circuit to minimize the input power at high currents or variable compensation coils to minimize the inductive pick-up in the *measured* voltage signal. The two methods gave substantially the same result, after proper considerations [31].

An improved sensitivity of a calorimetric AC measurement is described in [31]. The high accuracy was reached by oscillating between AC and DC until a zero-temperature variation was reach. The well-defined DC dissipation is then equal to the AC dissipation.

2.3.2 Special Considerations of AC Resistance Measurements

Two popular measurement options are available for the electrical measurement of the voltages representing the current and the voltage drop along the CUT: 1) high-speed acquisition of single time-resolved samples followed by data treatment; 2) instantaneous data treatment by a lock-in amplifier.

The manual of a common lock-in amplifier [32] states that a lock-in amplifier measures the single Fourier sine component at the reference frequency. This is therefore equivalent to extracting the fundamental Fourier component of time-resolved data. Reference [32] also cautions against the use of Fourier transforms for non-linear signals. The harmonic content of the measurement signal should be below 1 % according to CIGRÉ TB 287.[5]

Reference [27] provides an equation for the total voltage drop along the CUT, ΔU_1, in perfect circular-symmetric conditions, when a second "short-circuit" is close enough to cause additional induced losses:

$$\Delta U_1 = (R_{1\mathrm{AC}} + j\omega L_{1\mathrm{IAC}}) \cdot I_1 + \left(j\omega L_{1\mathrm{EAC}} + \frac{\omega^2 M_{12}^2}{R_{2\mathrm{AC}} + j\omega L_{2\mathrm{IAC}} + j\omega L_{2\mathrm{EAC}}} \right) \cdot I_1 \, , \tag{12}$$

where $R_{1\mathrm{AC}}$ is the AC resistance of the CUT, $R_{2\mathrm{AC}}$ is the AC resistance of a near-by lossy short circuit, and the M_{12} is the mutual inductance between the two circuits. The second term in the second parenthesis relates to the losses in the second circuit. The subscripts, "IAC" and "EAC" define inductances due to fields internal to the conductor and external to the conductor, respectively. This formula is a lumped circuit model equivalent of formula (8), but only applicable for this special case of two parallel conductors. The difficulty in both approaches, whether using a lumped circuit model (equation (12)) or an electromagnetic field model (equation (8)) is that the lumped circuit parameters and fields are not known exactly.

Reference [33] explains how this kind of external losses are driven by an imaginary part of the complex external field (in a perfect sinusoidal approximation) and how also a non-uniform current distribution in the conductor results in an imaginary component in the external magnetic field, i.e., a component that is, at least locally, out of phase with the total of the current running through the CUT. The consequence of this with regards to the preferred geometry of the voltage measurement loop is two-fold:

1) If the current distribution in the CUT is not rotationally symmetric, the voltage loop needs to be sufficiently large to capture enough of the imaginary magnetic field components.
2) If there are large parasitic losses generated by the CUT, the voltage loop needs to be sufficiently small as to not capture too much of these external parasitic losses.

This explains very clearly the earlier findings in references [34], [25], [22] and similar work as [2] regarding the appropriate size and location of the voltage loop. A helical voltage loop, presented in [9] for example, is put forward later in the recommendation section. The correct use of the helical loop allows accurate estimation of the true losses of the CUT.

[5] This concerns signal quality after appropriate filtering techniques (see section 2.5.1).

2.3.3 Conclusion

Many different setups and equipment have been used for the AC resistance determination of simple and complex conductors. Generally, the accuracy of the equipment is sufficient to perform accurate measurements if handled and applied properly. Electric methods offer some inherent advantages over the calorimetric approach. The biggest influence on the electric measurement is the positioning of the voltage loops relative to the conductor and return current path. Many variations exist and were tested. Section 3.4.6 presents the favorable setups to perform accurate AC resistance measurements, which are based upon cumulated knowledge, investigations and literature surveys.

2.4 Definition of the Conductor Under Test (CUT)

IEC 60228, describes standard conductor designs (solid and stranded) and prescribes maximal DC resistance values, is solely limited to bare conductors. The prescriptions are however also generally used when the measurement is performed on complete cables, or full lengths placed on drums.

Though this may be less of a problem for DC measurements, specific issues related to conductor geometry and setup configuration may induce large differences in the conductor's AC behavior (see section 1.3). It has for example been mentioned that mechanical constraints due to the presence of an insulation/screen system may affect inter-wire contact resistance and hence current distribution in AC mode.

It is then of utmost importance to understand the purpose of the measurement to choose the right test configuration.

Different definitions of what the CUT is exactly may apply and are subsequently described.

2.4.1 Bare Conductor (Inner Conductor Only)

Bare conductor measurements may not be fully representative of the behavior of the conductor in the field as mechanical constraints due to insulation, screen, cable installation (bend, tension…) may affect inter-wire contacts or screen influence and hence AC resistance.

Measurement on bare conductor is then important for conductor design consideration and standardization, when the conductor has a simple shape (e.g., solid, tube etc.) or will only be used at DC. It also allows the manufacturer to qualify its products before using it to produce the complete cable.

Stranded conductors must be manipulated with precaution as twisting (or more usually the natural tendency to untwisting due to existing torsions in the conductor) will affect the inter-wire contacts and hence the measured value. Orientation of the cable ends with regards to each other must then recorded before cutting the samples and controlled before starting the measurement.

2.4.2 Insulated Conductor (Inner Conductor & Insulation)

Measurements on insulated conductor present both the disadvantages of not representing the final behavior of the installed cable (as the screen and sheath are missing), and not representing fully the conductor design (as it will be mechanically influenced by the presence of the insulation).

Moreover, the inconvenience of conductor untwisting may not be completely avoided by the presence of the insulation system, or even sometimes made worse depending on the production process.

In addition, the identification of the real position of the conductor as compared to the insulation (centering) may be difficult and lead to some measurement errors.

Relaxation of the insulation material is of importance and care must be taken in the conditioning of the sample.

2.4.3 Complete Cable (Inner Conductor & Insulation & Metallic Screen & Sheath)

Measurements on complete cable presents different advantages such as

- It is representative of the final configuration (not considering laying constraints such as bend, tensions, …).
- It is less sensitive to untwisting, as more stable.
- The metallic screen can be used as coaxial configuration of the return current path.

Nevertheless, some other constraints appear as

- The conductor can be qualified only after manufacture of the full cable.
- The relaxation of constraints to obtain a stabilized configuration representative of final field performance may necessitate thermal cycling of the cable.
- The losses due to the presence of the metallic screen (eddy currents) must be considered.
- The positioning of the voltage taps and pick-up loop may be more difficult.

As for insulated conductor, the insulation/screen/sheath system may affect the AC resistance behavior and care must be taken in the conditioning of the sample and the determination of the position of the conductor. The eccentricity of the conductor and the metallic screen, that is usually in this case taken as the return conductor, may lead to measurement uncertainty or errors. Though this configuration is probably the closest to the final use, measurement difficulty will arise in the placement of the voltage loop if one wants to avoid including screen losses in the measurement.

2.4.4 Complete Cable Length on Drum

Although measurements on drums might look like a good alternative for routine test, the proximity effect due to the presence of the drum (if metallic) and of the juxtaposed coils, as well as the relatively low bending radius of the conductor and sheath and its effect on geometrical (roundness) and mechanical properties of the cable will affect the measurement in an unpredictable manner.

Moreover, in this case, the voltage loop extends over the screen and additional losses in the screen will also be caught, which are increased by proximity effect between different turns of the cable on the drum also. This is also true if considering coaxial current flow as bending and stretching of a solid sheath can destroy coaxial current flow [35].

This leads to measurement uncertainties that are not adequate in the frame of this study. Accurate AC resistance measurement of drummed cables is not recommended.

2.5 Equipment and Test Methods

More details on the equipment listed below can be found in the relevant literature.

2.5.1 Test Current Generation / Power Source

The power source can be a:

- Current Generator, ideally frequency-variable or a
- Transformer: heating transformers (usually used in calorimetric measurements).

In order to avoid issues with harmonic currents, the generator must be able to supply a sine wave of desired frequency (±0.1 Hz) with a harmonic content lower than 1 %. Alternatively, appropriate filtering techniques, such as the Discrete Fourier Transform (DFT) should be used on the measured signals, to accurately evaluate the in- and output-signals at the relevant frequency only. In other words, the harmonic content of the signal used for evaluation is important, not of the input signal.

2.5.2 Current Measurement & Voltage Measurement

Different suitable state of the art equipment may be used to obtain the relevant electrical signals in the DC and AC measurement of large conductors. Typical current measurement devices are:

- Shunt Resistances,
- Rogowski Coils and
- Current Transformers.

The transfer characteristic of these current measuring device, ratio, and phase angle shall be identified. This knowledge shall be used for correction or uncertainty evaluation. To measure the voltage drop over the CUT between the voltage tap-offs, following equipment was widely used in literature:

- Lock-In Amplifiers,
- Digitizers and Synchronous Sampling (ADC Voltmeters),
- AC measurement bridges and
- potentiometers.

Typical combinations of devices and further descriptions can be found in [2, p. 8] and in Figure 2-1. Depending on the measurement current, the measured voltages can be in the range of µV, when measuring large conductors. Also at AC, the phase (between voltage and current) measurement must be very accurate, because the inductive part of the measured voltage is usually much larger than the resistive voltage drop. This depends on the chosen pick-up loop. Hence, accuracy in phase measurement directly affects accuracy in resistance measurement. The error of the equipment used for current and voltage measurement needs to be considered in the final error calculation.

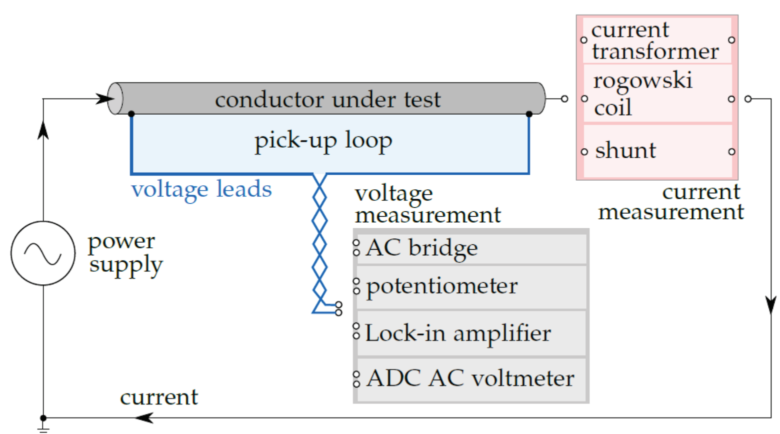

Figure 2-1: Typical equipment for current and voltage measurement in the test circuit [2, p. 9]

2.5.3 Available Connectors for Current Injection

Though the choice of the proper solution depends on cable materials and design parameters, the following list gives examples of such systems and their usual applicability. It must be noted that it is always a compromise between efficiency and cost/preparation time/adaptability to measuring equipment.

The examples given here are not exhaustive but give an overview of current practices. In any case the goal of a connection system is to form a low resistance short circuit of all wires at both ends of the cable as described in detail in section 1.3.4.

2.5.3.1 Radial Connections

Radial connections are generally easy to put in place. Their limitation is given by their ability to allow current flow in the central layer, reaching a sufficient homogeneity of the current for the required measurement accuracy.

- Pressure Clamp (Figure 2-2): connects the current injection system to outer surface of the cable (preferably on a long distance – 2 times the cable diameter and over the whole perimeter – clamp adapted to the conductor size). Pressure is applied through tightening of screws. The system is adapted for solid conductors as well as for bare copper stranded conductors and small stranded aluminum conductors. If the number of wires is higher, each wire should be individually cleaned below the clamp.

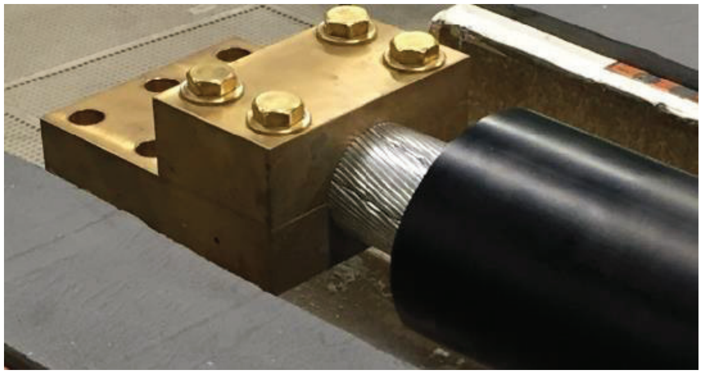

Figure 2-2: Short cable clamp

- Clamp with contact screws (Figure 2-3): connects the current injection system to outer surface of the cable (preferably on a long distance – 2 times the cable diameter). Pressure is applied through tightening of screws that deform and penetrate in the conductor, allowing for an improvement of the inter-wire contact. The system is adapted for solid conductors as well as for bare copper stranded conductors and medium size stranded aluminum conductors.

Figure 2-3: Clamp with contact screws

- Jaw (Figure 2-4): like clamps, jaws allow compressing and deforming the conductor to improve inter-wire contacts. High pressure is applied via mechanical screw or hydraulic cylinder. Note however that the reproducibility of mechanical screws is relatively low (±30 %) as it depends on the lubrification of the screw (not reproducible, variable in time). Adapted jaw design is necessary to apply large pressures; the contact surface is generally smaller for jaws than for clamps. This solution improves the contact to internal wires and allows to measure larger aluminum cross section of class 2 conductors. For class 5 and 6, attention must be paid not to cut the wires and specific jaw designs may be of interest. The system is adapted for solid conductors as well as for bare copper stranded conductors and medium size stranded aluminum conductors.

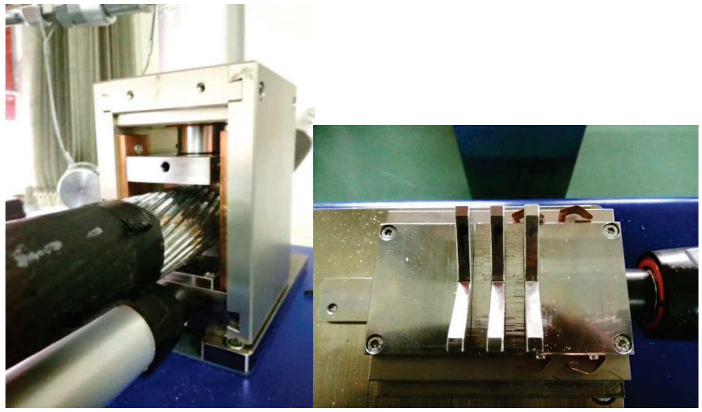

Figure 2-4: Cable teeth jaw with hydraulic cylinder

- Crimped Ferrule (Figure 2-5): A crimped ferule can be placed around the conductor. The axial forced will improve inter-wire contacts, however, unlike the clamp with contact screws, wire deformation will barely allow breaking the oxide layer on aluminum wires. The system is adapted for solid conductors as well as for bare copper stranded conductors and small stranded aluminum conductors.

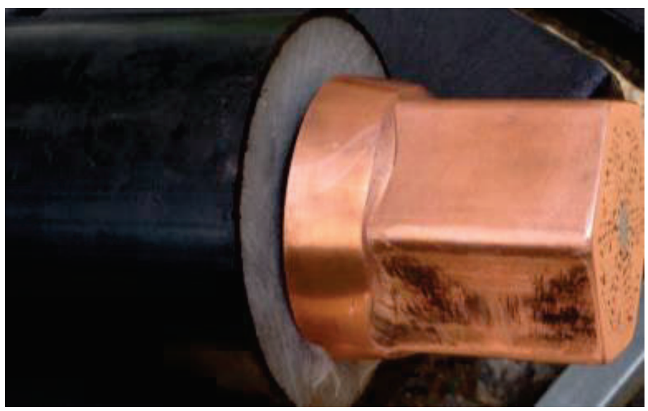

Figure 2-5: Crimped ferrule

2.5.3.2 Axial Connections

Axial connection will improve the connection and solve most of the issues linked with current distribution. This technology usually requires a more complicated contact system to insure homogeneity of the contact to all wires.

The use of this type of connection is compulsory when insulation is present between wires, for example in the case of enameled Milliken conductors and some watertight conductors, unless the single wires are individually cleaned.

- Welding (Figure 2-6): All the wires are welded together at both ends of the sample to a connection rod. From the theoretical standpoint this is the most reliable method to provide a low resistance short circuit of all wires in the cross section of a defined distance, even though practically challenging for larger conductors.

Figure 2-6: Weld of a solid rod at the end of a stranded cable

- Metallic cold spray (Figure 2-7): Cold spray deposition of metallic particles at the cable end will give a uniform contact to each wire and proper design of connection to this layer might result in a quite homogeneous current distribution. This technology requires dedicated equipment for spray application. It is relatively new and characterization is in progress. This type of connection is well adapted for any conductor.

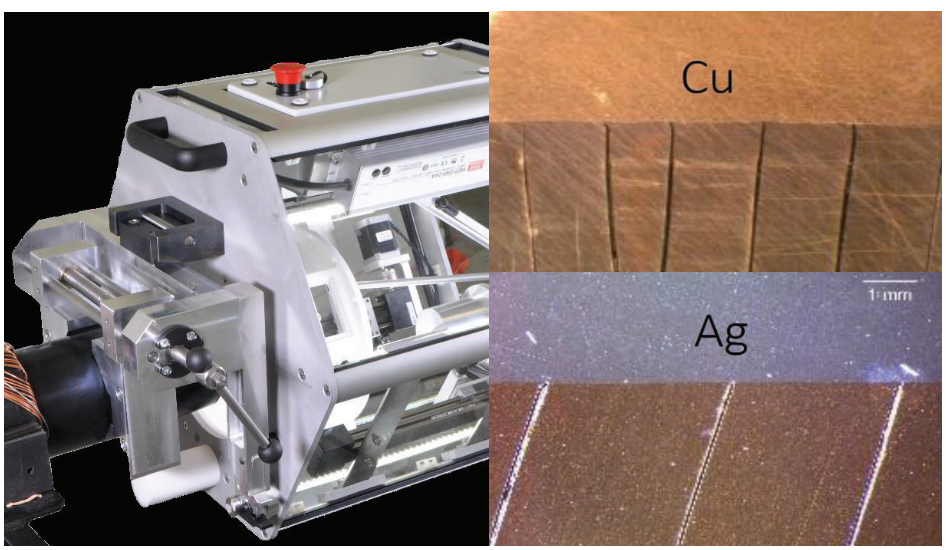

Figure 2-7: Metallic cold spray

- Conical connector (Figure 2-8): Connection is done by drilling a conical hole in the end of the conductor and inserting a conical connector that is ideally in direct contact with each wire. However, practically a step drill design is generally chosen to allow the connector to be screwed in to the created void and so improve the contact to the wires. However, homogeneous contact to each wire might not be complete. This type of connection is well adapted to aluminum, watertight and Milliken conductors. Presently, no experience with enameled wires is available.

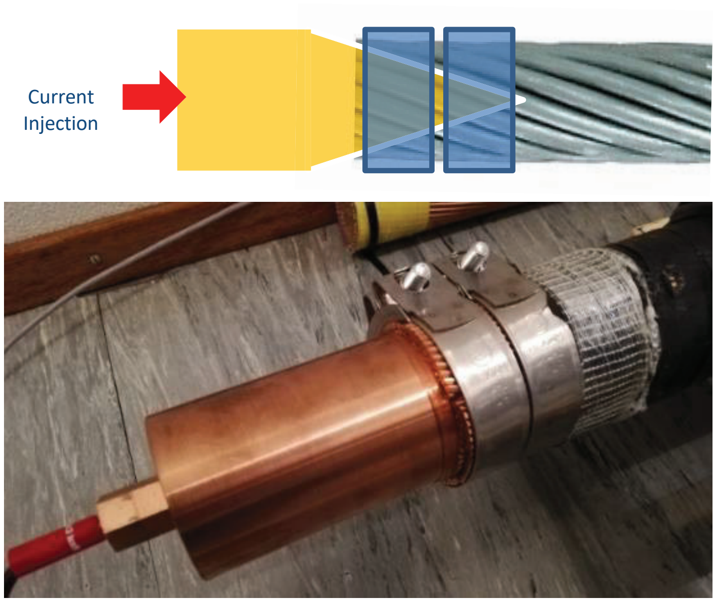

Figure 2-8: Conical connector

- Contact balls (Figure 2-9): The connector is installed directly on the conductor end. The cable is sawn off straight, and the cable insulation is removed. The pressure-stable contact system clamps centrically onto the conductor. Contact balls are poured into the connector. Tightening the pressure screw presses the balls against the front face of the conductor ends. A built-in spring mechanism compensates for settling losses. This ensures that contact forces and low transmission resistances are maintained at different temperatures.

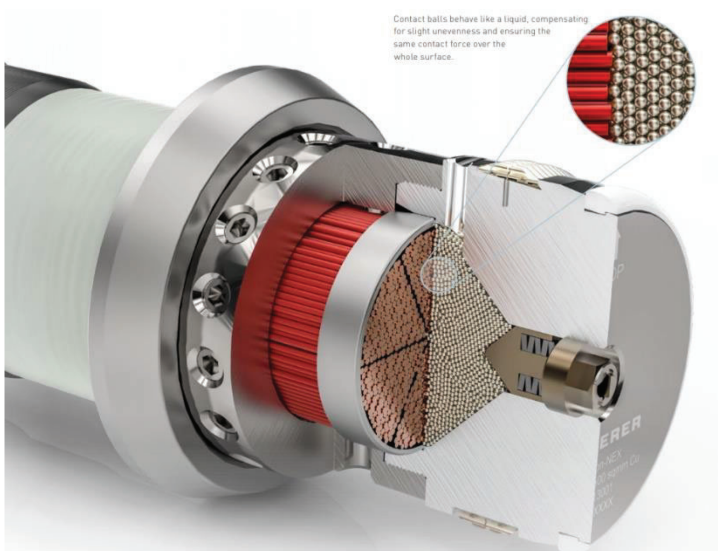

Figure 2-9: Contact balls system [36]

- Contact needles (Figure 2-10): A set of spring mounted needles is arranged to ensure contact with each individual wire. Each needle is connected either through the support plate or individually to the current source. It must be noted that to exert homogeneous pressure on the wires, the device must be aligned carefully with the conductor end.

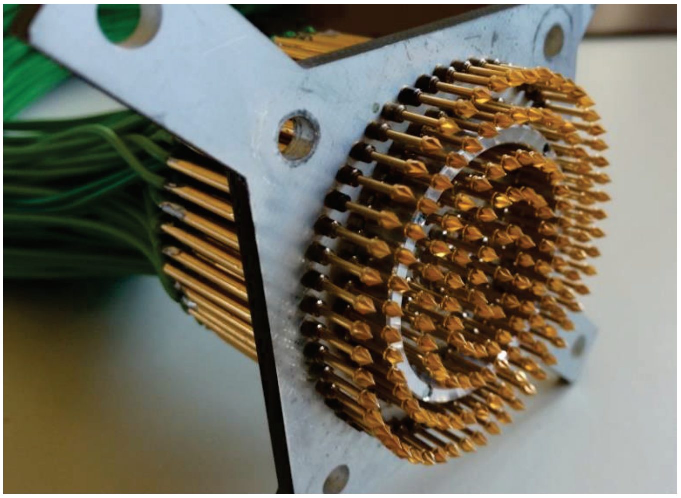

Figure 2-10: Contact system with needles

2.5.3.3 Intermediate/Combined Solutions

In the case of the round robin samples, the cable ends were welded over the whole surface on a very short length (Figure 2-11) and pressure clamps were used.

Figure 2-11: Welded terminals of round robin test

This allows improving the current distribution as compared with a bare pressure clamp with a relatively limited effort of welding. The current should be inserted into the cross section and also around the circumference of the conductor.

2.5.3.4 Special Considerations on Connections

The purpose of the connections is to inject the measuring current as homogeneously as possible in the conductor to guarantee an accurate measurement.

It is important to understand that the effect of poor current distribution can affect the result of the measurement as detailed in section 1.3.4.

As injected current may be relatively high to improve accuracy, the electrical contact must be sufficient to avoid heating of the connection that could perturbate the measurement, but also to avoid mechanical deformation that might disturb current distribution, or completely destroy the connection due to over-heating.

A representative current distribution through the cross-section and stable along the CUT, is one of the most critical parameters. Providing a low resistance current path from the current lead into every single wire of the CUT's cross section is the main goal of a current connection system (see section 1.3.4). Nevertheless, it is difficult to identify deviations because:

- It is not possible to measure the current in each wire without disassembling the conductor and hence perturb the system.
- Voltage drop measurement (which is an image of the circulating current) is possible only on wires placed on the outer layer of the conductor.
- The required measurement accuracy (below 1 %) means an even better accuracy in the determination of the single wire current.

Recommended practices are given below. Although they cannot guarantee that the current can reach each strand over a low resistance path, they give good hints and feelings about the steadiness and stability of the system

1. Measuring the DC resistance and comparing it to the expected value will give a first estimation of the DC current distribution.
2. DC measurements, that are less sensitive to environment and return leads configurations, and accurate enough for evaluation of current steadiness can be used in the following manners:
    a. The homogeneity of the current in the outer layer can be assessed by measuring the voltage drop over a well-defined distance (using for example two voltage taps placed on a rigid bar) at different angular positions around the conductor
    b. The homogeneity of the current over the conductor length (if a redistribution of the current takes place from the connection along the conductor through inter-wire contacts) can be similarly assessed by measuring the voltage drop over a well-defined distance (using for example two voltage taps placed on a rigid bar) at different longitudinal positions along the conductor. This is shown in Figure 2-12 where the DC resistance of a 240 mm^2 greased aluminum conductor is determined for different longitudinal positions of the voltage taps between both current injection systems (clamping jaws).
        i. The green curve shows a poor axial connection. The wavelength of the sinusoidal shape of the curve corresponds to the lay length of the outer layer. This reflects the fact that some wires on the external layer transports more current than some others. According to the symmetric design of stranded conductors this should not be the case at DC and also at AC (if proximity effect is absent). The reduction of amplitude in the middle of the curve correspond to a homogenization of the current in the outer layer when distancing from the current injection jaws (as described in section 1.3.4.2) . One can also notice that some wires transport less current than the mean value, giving to low measured resistance value. Finally, the means value of the curve (dashed line) is lower in the middle, showing that some current pass from the outer wires layer to the inner ones.
        ii. The blue curve corresponds to the same configuration but with higher pressure on the jaws (improved contacts between wires). The distribution is improved at current injection point, enhancing the accuracy of the measurement to a limited extend.
        iii. The red curve corresponds to an axial current injection. Even if the current is not perfectly distributed at the injection point, the homogenization of the current is quickly reached over the distance.
    c. These tests will however not give information on the distribution between the outer and inner layers on fully insulated wires.
3. Mechanical movement of the conductor that will affect inter-wire contact and hence current distribution (such as small displacement of the conductor on the bench, thermal cycles, …) may directly affect R_AC measurement and show that the system is not stabilized (see sections 1.3.6).

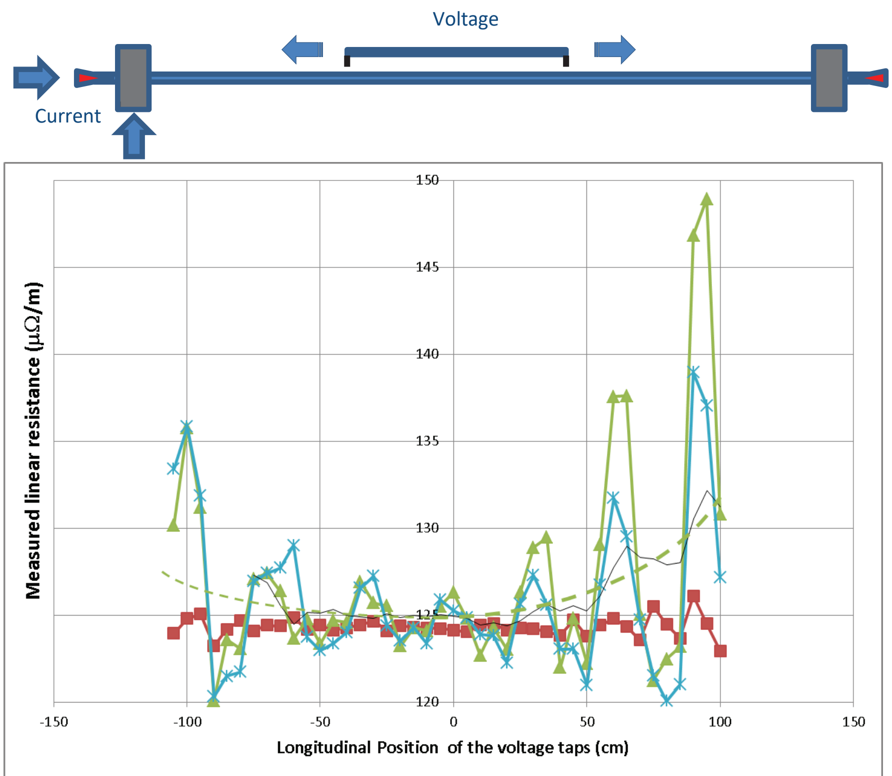

Figure 2-12: DC measurement with moving voltage taps
green curve: poor radial connection, blue curve: improved radial connection, red curve: axial connection

2.6 Conductors Under Test (CUT) in Round Robin Test

This section gives an overview of used conductors in the round robin test conducted in the group.

2.6.1 Copper Rod

Table 2-1 gives the material properties and geometrical parameters of the copper rod.

Table 2-1: Description of copper rod

Conductor Material	Cu-ETP (EN CW004A) Hard
cross sectional shape	circular diameter: 50.0 mm
total length	11.6 m

2.6.2 Copper Tube

Table 2-2 gives the material properties and geometrical parameters of the copper tube.

Table 2-2: Description of copper tube

Conductor Material	Cu-ETP (EN CW004A) Hard
cross sectional shape	tubular outer diameter: 50.0 mm inner diameter: 40.0 mm
total length	5.50 m

2.6.3 Milliken Conductor Cable (Copper)

Table 2-3 gives the material properties and geometrical parameters of the copper Milliken conductor.

Table 2-3: Description of copper Milliken conductor

Conductor Material	copper
cross sectional shape	Milliken conductor 6 sectors 2/3 insulated wires (enameled) watertight (swellable tapes) 2500 mm^2 outer diameter: 64.7 mm number of wires: >360 number of layers in segment: 5 pitch of layers: bidirectional
total length	12.50 m

2.6.4 Milliken Conductor Cable (Aluminum)

Table 2-4 gives the material properties and geometrical parameters of the aluminum Milliken conductor.

Table 2-4: Description of aluminum Milliken conductor

Conductor Material	aluminum
cross sectional shape	Milliken conductor 6 sectors watertight (swellable tapes) 2000 mm² outer diameter: 55.0 mm number of wires: >360 number of layers in segment: 5 pitch of layers: bidirectional
total length	12.50 m

2.7 Participants and Test Setups

Table 2-5: List of participants and measurement dates

Responsible for measurement	Copper Rod (section 2.6.1)	Copper Tube (section 2.6.2)	Copper Milliken (section 2.6.3)	Aluminum Milliken (section 2.6.4)
Technische Universität Berlin – High Voltage Engineering Department Contact: Ronald Plath Einsteinufer 11, 10587 Berlin, Germany	02/2017 measured by: René Suchantke Nick Wieczorek	03/2016 measured by: René Suchantke Nick Wieczorek	03/2017 measured by: René Suchantke Nick Wieczorek	03/2017 measured by: René Suchantke Nick Wieczorek
AESA SA Contact: Boris Dardel Rue de Neuchâtel 24 CH-2022 Bevaix Switzerland	DC only, 01/2020 measured by B. Curat	-	DC only, 01/2020 measured by B. Curat	DC only, 01/2020 measured by B. Curat
High Voltage Laboratory, Kinectrics Inc. Contact: Ivan Boev Kinectrics Inc. Toronto, Canada	12/2019 Measured by: Ziqin Li	12/2019 Measured by: Ziqin Li	12/2019 Measured by: Ziqin Li	12/2019 Measured by: Ziqin Li
Nexans SA Contact: Eric Beauguitte 536 Quai de la Loire 62225 Calais, France	2016/2020	2016/2020	2016/2020	2016/2020
Technische Universität Dresden Contact: Steffen Großmann 01062 Dresden Germany	08/2013	08/2013	08/2013	08/2013
Prysmian Group SE Contact: Abel Fustier ZI du port au Vin 89100 GRON France	11/2017-02/2018 Measured by: Abel Fustier	11/2017-02/2018 Measured by: Abel Fustier	11/2017-02/2018 Measured by: Abel Fustier	11/2017-02/2018 Measured by: Abel Fustier

NKT cables Contact Dag Willén Priorparken 560 DK-2605 Brøndby Denmark	08/2016 Measured by: Carsten Thidemann	07/2015 Measured by: Carsten Thidemann	08/2016 Measured by: Carsten Thidemann	08/2016 Measured by: Carsten Thidemann
ABB AB Contact Mats Sjöberg High Voltage Cables P.O.Box 546, Verkö SE-371 23 Karlskrona Sweden	11/2015 Measured by: Karl-Erik Rydler	11/2015 Measured by: Karl-Erik Rydler	11/2015 Measured by: Karl-Erik Rydler	11/2015 Measured by: Karl-Erik Rydler

2.8 Results

The results obtained from eight labs comprised a mix of AC and DC resistances. The results were frequency adjusted using the *Principle of Similitude* (described in more detail in section 1.2.5) to plot at 20 ºC and 90 ºC, as these are the most applicable for ambient temperature testing and maximum operational capability. For specific comparison at 50 Hz values were linearly interpolated. Although the change in resistance is not exactly linear with change in frequency this gave a good estimate since only slight adjustments were needed for measurements made at power frequency. The following table summarizes the testing frequencies and temperatures at participating labs:

Table 2-6: List of testing frequencies and temperatures per lab participant

Lab	AESA	TU Dresden	Nexans	Prysmian	Kinectrics	NKT	ABB	TU Berlin
Testing Frequency*	DC	DC & 50 Hz			DC & 60 Hz[6]	DC & Multiple AC frequencies		
Testing Temperature** (Copper Pipe)	n/a	20 °C	20 °C & 90 ºC	20 ºC	20 ºC	20 ºC	20 °C & 90 ºC	20 ºC
Testing Temperature** (other samples)	20 ºC	20 ºC	20 °C & 90 ºC	20 °C & 90 ºC	20 ºC	20 ºC	20 ºC	20 ºC
* Approximate testing frequency, minor variations due to power quality or testing equipment ** Approximate testing temperature, adjusted to 20 °C or 90 ºC for comparison using *Principle of Similitude*								

The values at 20 ºC are most relevant for measurement purposes, although the values at 90 ºC would be more desirable for use in ampacity calculations.

NKT, ABB and TU Berlin had equipment that allowed for measuring AC resistance across multiple frequencies and therefore provided results over a frequency range. TU Dresden, Nexans, Prysmian and ABB were able to make AC resistance measurements at temperatures above ambient temperature. Results later plotted at 90 ºC were obtained at or close to 90 °C. For the ones close but not directly at 90 °C, the *Temperature Scaling* (see section 3.1.2) was applied.

Of the four samples tested, the copper rod and copper pipe had closed-form solutions available. Therefore, measurements made across a frequency range on these samples would be expected to be in good agreement with the theoretically calculated values. When AC resistance is calculated for segmented conductors the k_s factor is applied. This would be expected to produce calculated AC resistances in good agreement with measured ones, based on previous theoretical work and historically measured lab results this may not always be the case. The following plots show the theoretical plots using Bessel equations (with the IEC 60287-1-1 k_s factors applied to the input argument for the segmented conductors) as solid-colored lines versus the results when calculating directly using equations from IEC 60287-1-1 (denoted using "X" marks):

[6] Kinetrics measurements at 60 Hz were scaled to 50 Hz to be comparable to other laboratory results, using the *Principle of Similitude*.

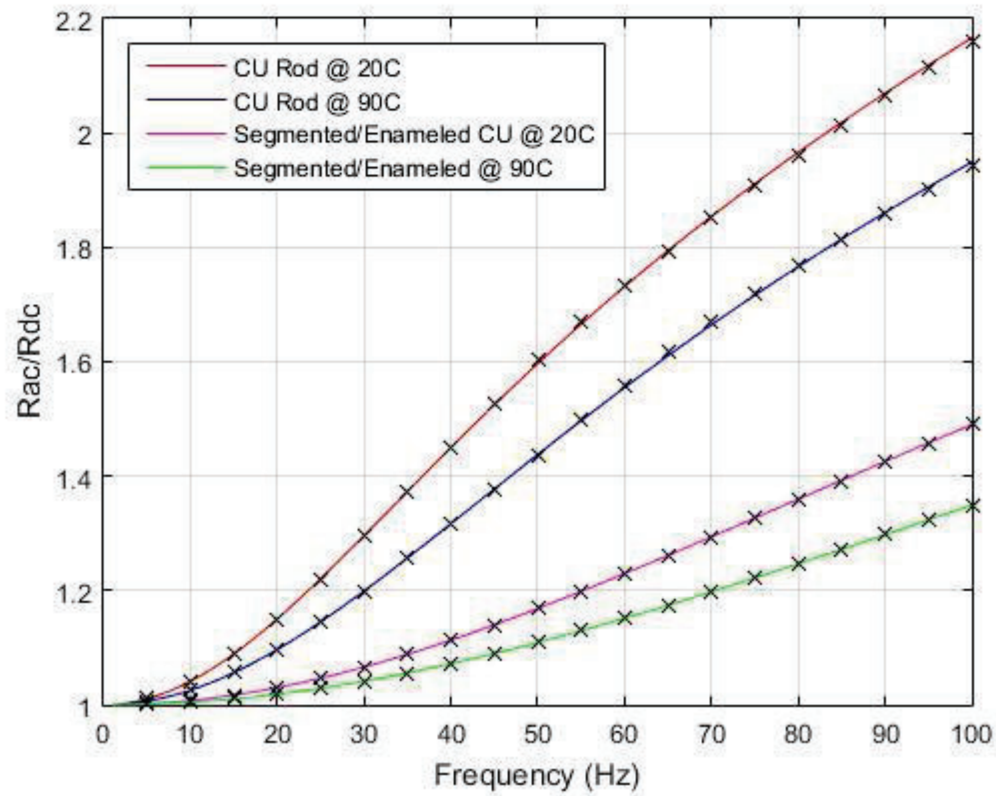

Figure 2-13: Theoretical (solid lines) vs. IEC (black markers) AC/DC resistance ratios (copper rod & segmented copper)

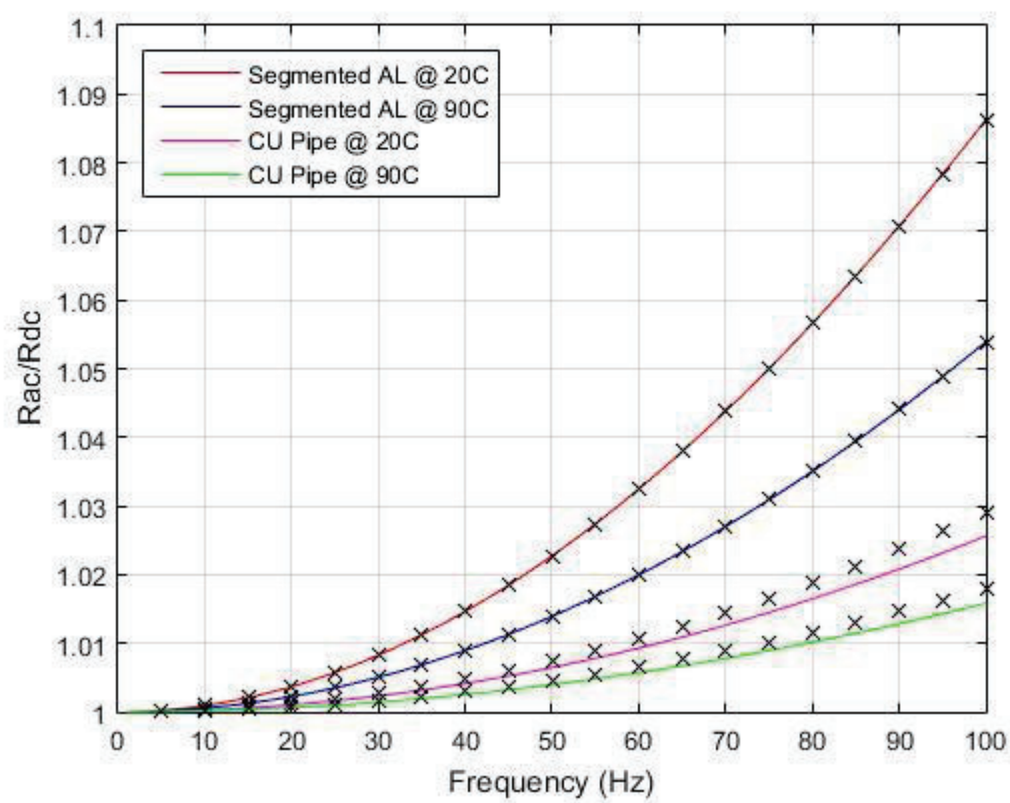

Figure 2-14: Theoretical (solid lines) vs. IEC (black markers) AC/DC resistance ratios (segmented aluminium & copper pipe)

Over the frequency range within the measurement results presented of 0-100 Hz there is good agreement between the Bessel function and IEC results. The copper pipe has a slight difference in AC resistance at 50 Hz between the theoretical solutions and IEC result (using the recommended k_s = 0.232 for hollow, helical stranded conductor) although less than 0.5 % (k_s = 0.217 found to be most accurate). At power frequencies k_s would vary for different segment designs due to the manufacturing variability and design parameters such as cross-sectional area of conductor, number and size of wires, number of segments, lay ratios, tapes used and compression obtained. Therefore, even when using k_s factors proposed in CIGRÉ TB 272 and later adopted in IEC 60287 the work presented herein and measurements presented in [2] have shown this factor for the segmented conductor designs tested to be different. Currently, IEC 60287 recommends k_s = 0.25 for segmented aluminum and k_s = 0.35 for segmented enameled copper. These values were used for the IEC plot, although not expected to match across a broad spectrum of testing frequencies.

There is also inherent variability in the true DC resistance of a manufactured conductor as compared to the IEC 60228 standardized DC resistances. This is because when conductors are manufactured standards specify a maximum DC resistance that cannot be exceeded, but each individual manufacturer or even each individual reel from a manufacture will not be uniformly beneath the maximum value. Additionally, the resistivity of the metal will not exactly match the theoretical value in IEC 60287 used for calculation purposes and the metal properties will change slightly through processing of the design (e.g., work hardening / compaction, line tension / elongation, extrusion tightness / compression).

For comparison of the lab measured results the AC and DC resistances will be taken as the standardized maximum DC resistance per IEC 60228 (for the segmented designs) or calculated using their dimensions and expected resistivity of copper per IEC 60287 (for the copper rod and pipe). Although the true values of DC resistances of the segmented conductor samples are assumed to be slightly lower, this gives consistent DC resistance values for all lab measurements to be compared against. Because the maximum DC resistances per IEC 60228 will also be used for calculating the IEC AC/DC resistance ratios, the calculated ratios would be expected to be slightly lower than the true ratios of the samples tested (i.e., as DC resistance increases the AC/DC resistance ratio decreases).

2.8.1 DC Measurements

The following table shows the conductor properties: inner/outer diameters were measured, DC resistance tabulated per IEC 60228 or calculated per IEC 60287, and the average value (Ave) of DC resistances measured by all labs. Note that the copper rod and copper pipe did not have tabulated maximum DC resistance in IEC 60228, so instead their DC resistances were calculated using their measured dimensions and the IEC 60287 recommended conductor metal resistivity ($1.7241 \cdot 10^{-8}$ Ωm for copper).

Table 2-7: Conductor dimensions and DC resistances

Description	AL-seg	CU-seg	Rod	Pipe
Inner Diameter in mm	0	0	0	40
Outer Diameter in mm	55	64.7	50	50
IEC DC Resistance @ 20 ^{o}C in µΩ/m	14.9	7.2	8.78	24.39
Lab Average DC Resistance @20 ^{o}C in µΩ/m	14.22	6.98	8.69	23.89
Average to IEC Measured DC Resistance in %	-4.5	-3.1	-1.1	-2.1

The specific change in values from IEC to that measured at each lab were as follows:

Table 2-8: DC resistance measurement deviations from the IEC value at 20 °C

Lab	AL-seg	CU-seg	Rod	Pipe
NKT	-4.8 %	-2.9 %	-0.9 %	-0.8 %
TU Berlin	-4.5 %	-3.7 %	-1.2 %	-0.7 %
Prysmian	-4.3 %	-3.0 %	-0.9 %	-3.9 %
AESA	-5.1 %	-3.7 %	-1.0 %	-
TU-Dresden	-4.7 %	-2.7 %	-2.8 %	-6.6 %
ABB	-5.0 %	-3.0 %	-0.8 %	-0.7 %
Kinectrics	-4.8 %	-2.6 %	-1.1 %	-0.8 %
Nexans	-3.3 %	-2.8 %	0.2 %	-0.8 %

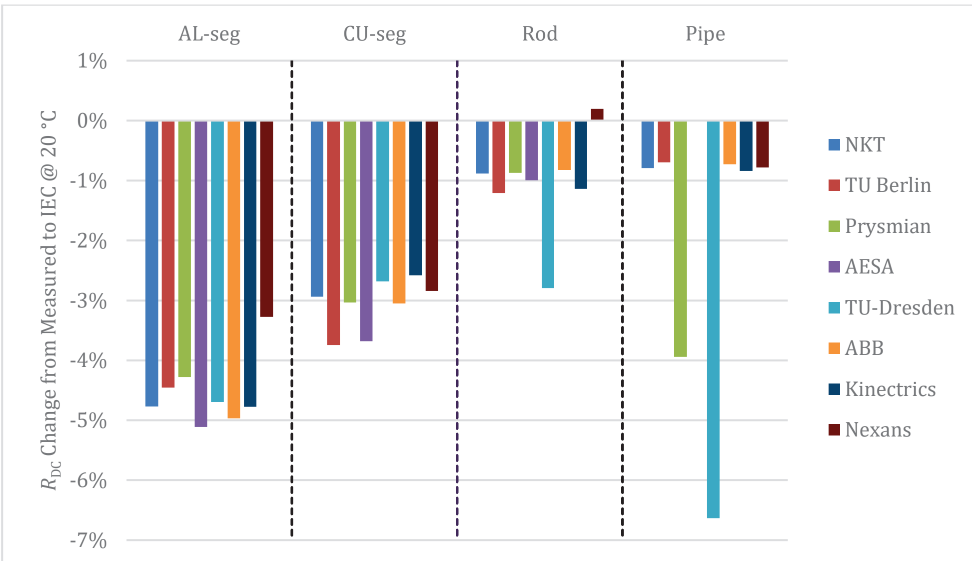

Figure 2-15: DC resistance measurement deviations from the IEC value @ 20 °C

Table 2-8 and Figure 2-15 show relatively good agreement across different labs for stranded conductors. Some "inconsistent" values appear however for rod and pipe measurements. Because the segmented conductors are being compared to IEC 60228 maximum DC resistance, its expected measured values would be lower. For previously mentioned reasons, the differences in % in Table 2-8 and Figure 2-15 and also in the following must not be interpreted as errors but only as deviations to the IEC.

2.8.2 50 Hz Measurements

The AC resistance at 50 Hz was calculated per IEC 60287. The average of the measurements from all labs are shown below for comparison to this standardized calculation method:

Table 2-9: AC-Resistance at 50 Hz measurement deviations from IEC calculation

Description	Unit	AL-seg	CU-seg	Rod	Pipe
k_s factor		0.25	0.35	1	0.232
AC Resistance at 20 °C (IEC)	µΩ/m	15.24	8.41	14.07	24.57
AC Resistance at 20 °C (Lab Average)		15.01	8.63	13.87	24.20
20 °C IEC vs Lab Average	%	-1.5	2.6	-1.5	-1.5
AC Resistance at 90 °C (IEC)	µΩ/m	19.37	10.18	16.08	31.24
AC Resistance at 90 °C (Lab Average)		18.95	10.10	15.94	30.09
90 °C IEC vs Lab Average	%	-4.0	-0.9	-0.9	-0.5

The copper rod and pipe show good agreement of the lab measured values vs the IEC calculated ones. The segmented conductors vary a little more, but this is to be expected due to the skin effect factor being assumed and design specifics. The lab measured AC resistance differences versus the IEC calculated values are shown here:

Table 2-10: AC-Resistance measurement at 50 Hz deviations from IEC calculation (detail for each lab measurement)

Conductor	AL-seg	CU-seg	Rod	Pipe	AL-seg	CU-seg	Rod	Pipe
Temperature	20 ºC				90 ºC			
NKT	-1.1 %	6.0 %	-1.2 %	-0.2 %	-	-	-	-
TU Berlin (Helix[7])	-1.5 %	-	-	-	-	-	-	-
TU Berlin (AVG[8])	0.0 %	3.6 %	-1.5 %	-1.2 %	-	-	-	-
Prysmian	-2.8 %	-1.4 %	-1.1 %	-2.6 %	-2.7 %	0.3 %	-0.6 %	-
TU-Dresden-1[9]	-3.9 %	-3.4 %	-2.8 %	-3.6 %	-	-	-	-
TU-Dresden-2[10]	-	-	-1.7 %	-3.1 %	-	-	-	-
ABB[11]	-1.5 %	5.9 %	-0.7 %	-0.7 %	-	-	-	-0.7 %
Kinectrics	2.7 %	9.7 %	0.3 %	-0.6 %	-	-	-	-
Nexans	-6.5 %	-3.8 %	-2.9 %	-0.4 %	-5.3 %	-2.0 %	-1.2 %	-0.3 %

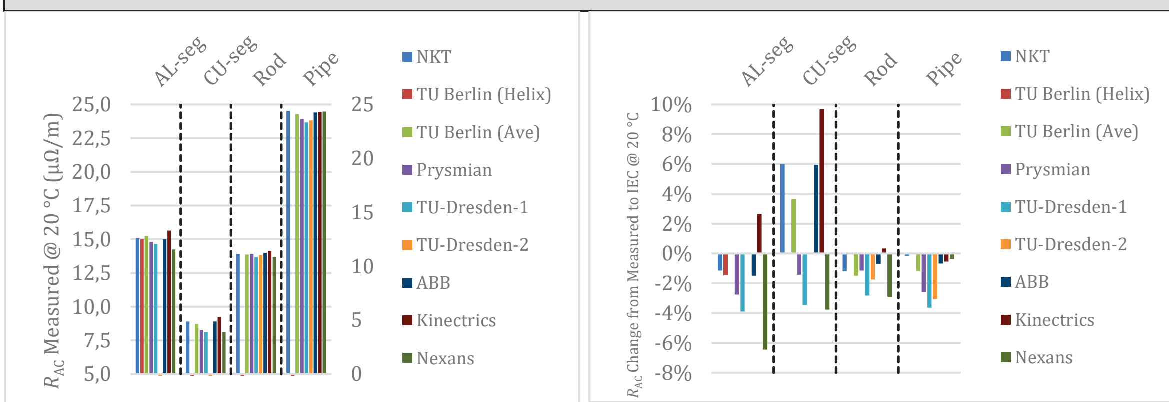

Figure 2-16: Lab measured AC resistances (left) and deviation from IEC calculation (right) @ 20 ºC

---

[7] Helix refers to a setup, where the voltage lead wire(s) perform a helical rotation along the cable axis around the circumference of the conductor. This is explained later in more detail in section 3.4.3.

[8] The AVG (average) setup uses 4 equally spaced voltage loops around the circumference of the CUT (see section 3.4.3).

[9] Multiple sets of measurements made on all samples using different setups. Segmented AL measurement 1 using AC pick up loop as small as possible & 2-4 using AC sheath return. Segmented CU measurement 1 using AC standard current clamps & 2-4 using AC sheet return. Copper rod test 1: measurement 1-2 using AC pick up loop as small as possible, 3 using AC pickup 10 cm & 4 using AC pickup 20cm. Copper rod test 2: measurement 1 using AC pick up loop as small as possible, 2 using AC pickup 10 cm & 3 using AC pickup 20 cm. CU pipe measurement 1 rms values and 2 using first harmonics. using RMS values in case of AC Measurements made using first harmonics in case of AC

[10] Same as footnote above.

[11] Two separate measurements made on the copper pipe using the same technique.

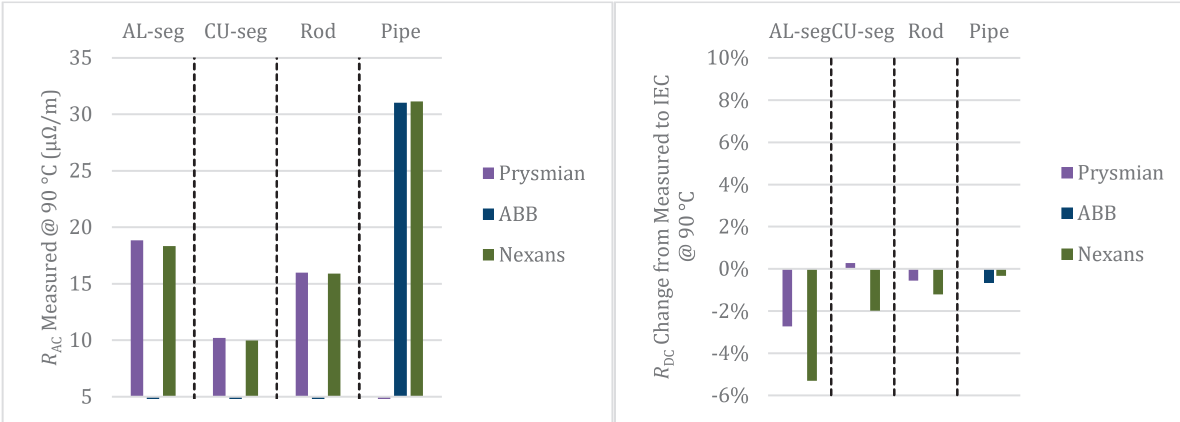

Figure 2-17: Lab measured AC resistances (left) and deviation from IEC calculation (right) @ 90 °C

Using both the AC and DC resistances measured at each lab, the skin effect factor k_s corresponding their measurements is as follows:

Table 2-11: Implied k_s factor at each lab per their measured AC and DC resistance values

Conductor	AL-seg	CU-seg	Rod	Pipe	AL-seg	CU-seg	Rod	Pipe
Temperature	20 °C				90 °C			
NKT	0.40	0.46	0.98	0.31	-	-	-	-
TU Berlin (Helix)	0.38	-	-	-	-	-	-	-
TU Berlin (Ave)	0.43	0.43	0.98	0.14	-	-	-	-
Prysmian	-	0.36	0.99	0.38	0.36	0.40	1.00	-
TU-Dresden-1	0.28	0.33	0.97	0.51	-	-	-	-
TU-Dresden-2	-	-	0.99	0.55	-	-	-	-
ABB	0.39	0.46	0.99	0.24	-	-	-	0.25
Kinectrics	0.52	0.50	1.02	0.27	-	-	-	-
Nexans	n/a*	0.33	0.94	0.29	n/a*	0.36	0.97	0.33
Average	**0.40**	**0.41**	**0.98**	**0.34**	**0.36**	**0.38**	**0.99**	**0.29**
* Measured $R_{AC} < R_{DC}$								

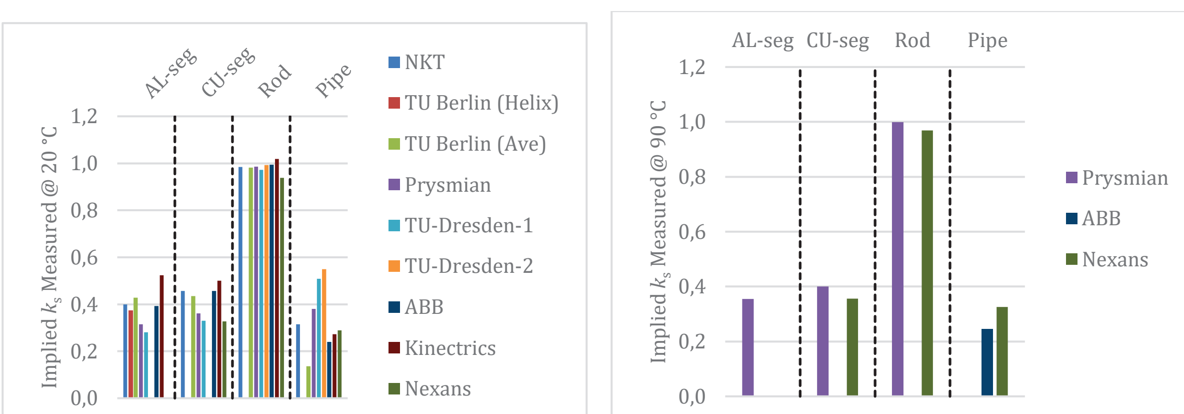

Figure 2-18: Implied k_s factor at each lab @ 20 °C (left) and @ 90 °C (right)

Note that small measurement error variability for a conductor with a low AC/DC resistance ratio can result in a large change in the skin effect factor, which is the effect seen on the segmented aluminum and (even more so) copper pipe samples (i.e., the difference between IEC AC and DC resistance is 1-2 % and < 1 %, respectively). For the segmented conductors, the k_s factor appears higher than those given in IEC 60287. IEC 60287 uses a uniform k_s per the design regardless of operating temperature.

2.8.3 AC to DC Resistance Ratio

All AC resistance values discussed in the following tables are at 50 Hz. The AC/DC resistance ratios obtained by each lab are as follows (note both the AC resistances at 50 Hz and DC resistances used were the values measured at the lab and the IEC value was calculated per IEC 60287):

Table 2-12: R_{AC}/R_{DC} measured at each lab at 50 Hz

Conductor	AL-seg	CU-seg	Rod	Pipe	AL-seg	CU-seg	Rod	Pipe
Temperature	20 °C				90 °C			
NKT	1.06	1.28	1.60	1.01				
TU Berlin (Helix)	1.05	-	-	-				
TU Berlin (AVG)	1.07	1.26	1.60	1.00				
Prysmian	1.04	1.19	1.60	1.02	1.03	1.15	1.44	
TU-Dresden-1	1.03	1.16	1.60	1.04				
TU-Dresden-2	-	-	1.62	1.05				
ABB	1.06	1.28	1.60	1.01				1.01
Kinectrics	1.10	1.32	1.63	1.01				
Nexans	0.99	1.16	1.55	1.01	0.99	1.12	1.42	1.01
IEC	1.02	1.17	1.60	1.01	1.01	1.11	1.44	1.00

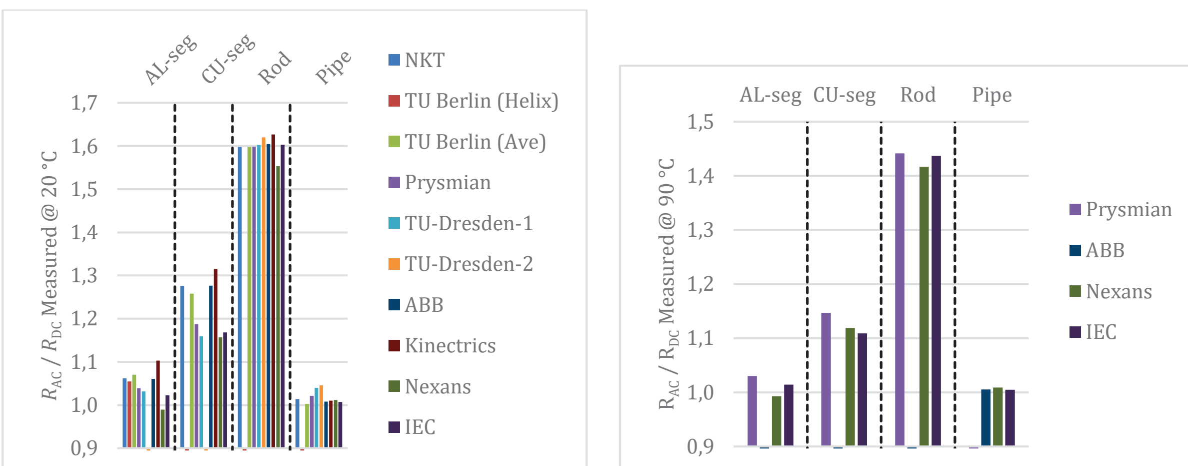

Figure 2-19: R_{AC}/R_{DC} measured at each lab at 20 °C (left) and 90 °C (right)

The changes of each labs reported AC/DC resistance ratios compared to those calculated per IEC 60287 at 50 Hz are:

Table 2-13: Deviation in R_{AC}/R_{DC} from IEC to lab measurements

Conductor	AL-seg	CU-seg	Rod	Pipe	AL-seg	CU-seg	Rod	Pipe
Temperature	20 °C				90 °C			
NKT	3.8 %	9.2 %	-0.3 %	0.6 %				
TU Berlin (Helix)	3.1 %	-	-	-				
TU Berlin (Ave)	4.6 %	7.7 %	-0.3 %	-0.5 %				
Prysmian			-0.3 %	1.4 %	1.6 %	3.4 %	0.3 %	
TU-Dresden-1	0.8 %	-0.8 %	0.0 %	3.2 %				
TU-Dresden-2	-	-	1.1 %	3.8 %				
ABB	3.7 %	9.3 %	0.1 %	0.1 %				0.1 %
Kinectrics	7.8 %	12.6 %	1.5 %	0.3 %				
Nexans	-3.3 %	-1.0 %	-3.1 %	0.4 %	-2.1 %	0.9 %	-1.4 %	0.5 %

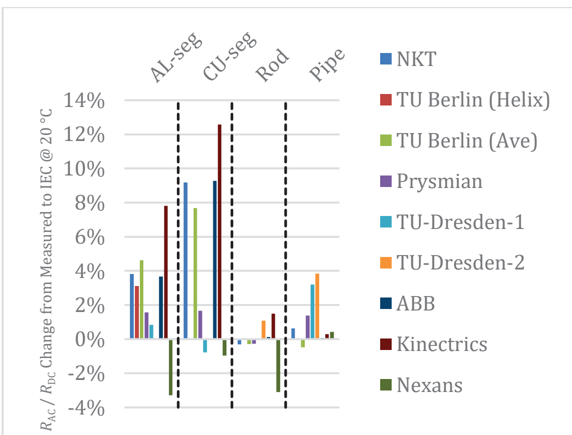

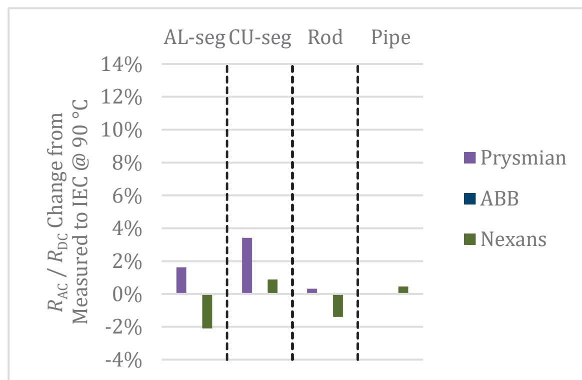

Figure 2-20: Deviation in R_{AC}/R_{DC} from IEC to lab measurements at 20 °C (left) and 90 °C (right)

As stated before, the given values only give the deviation to the recent IEC values and do not state the accuracy/error of a lab as IEC has some inherent assumptions and also cannot predict the performance of complex conductors.

2.8.4 Behavior with Frequency

The lab measured values for each individual conductor sample are plotted next. For each there are four plots:

1. DC & AC resistance at 20 ºC
2. AC/DC resistance ratio at 20 ºC
3. DC & AC resistance at 90 ºC
4. AC/DC resistance ratio at 90 ºC

The segmented aluminum conductor results are as follows:

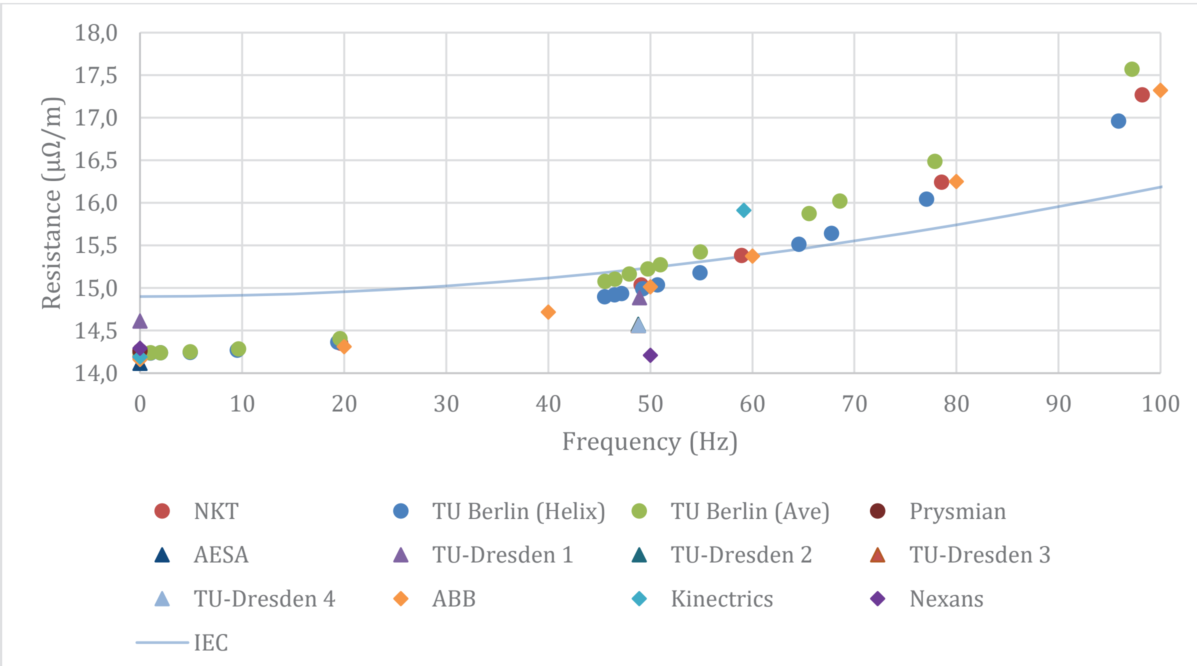

Figure 2-21: Segmented aluminium AC & DC resistance at 20 °C

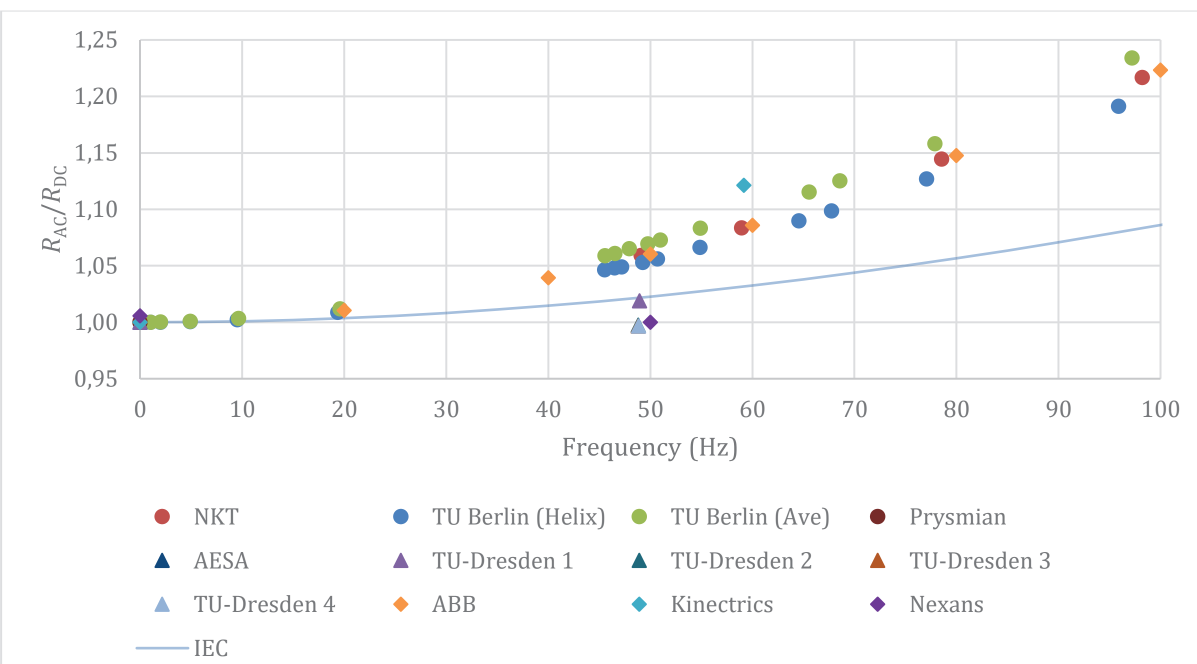

Figure 2-22: Segmented aluminium AC/DC resistance ratio at 20 °C

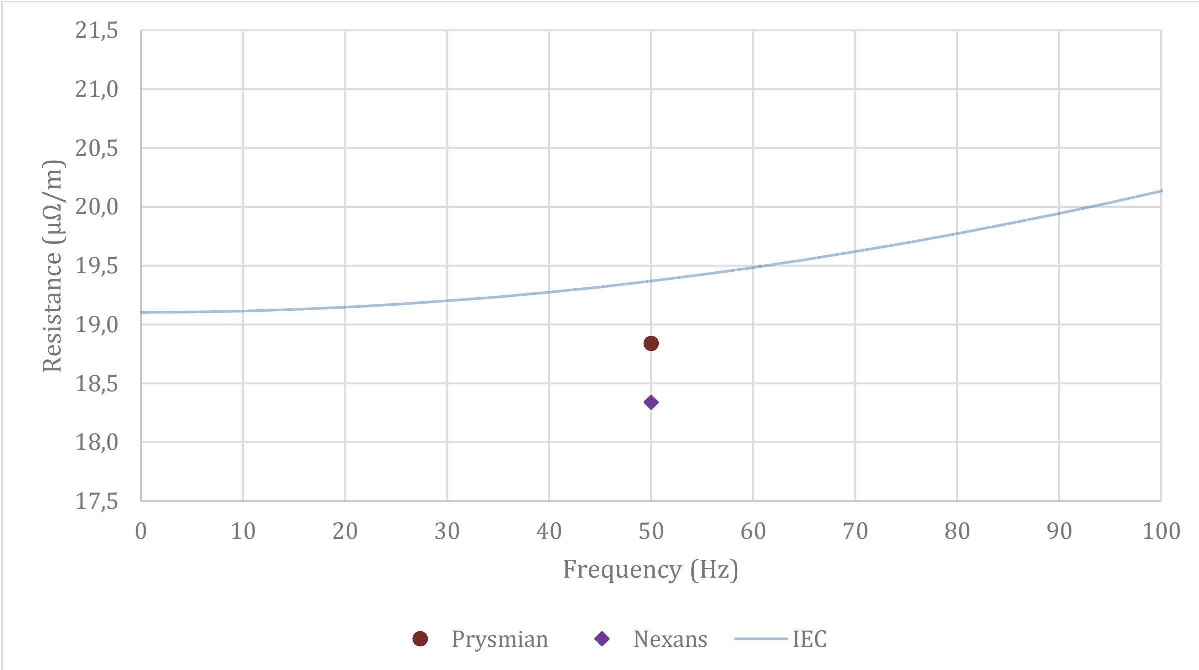

Figure 2-23: Segmented aluminium AC & DC resistance at 90 °C

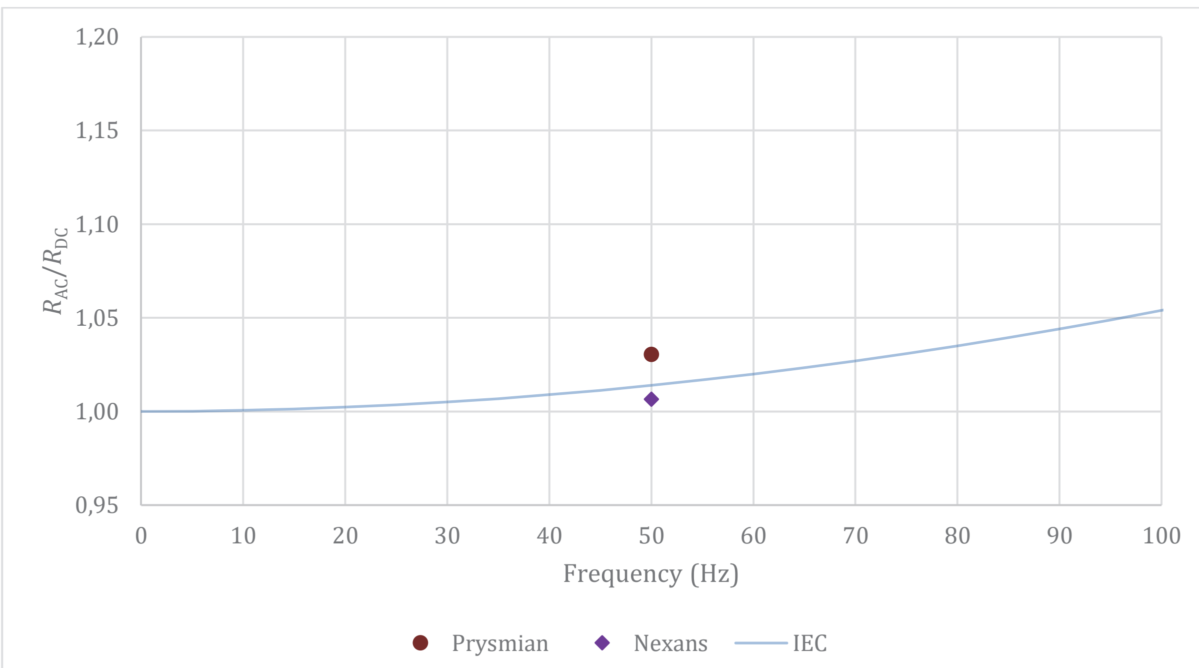

Figure 2-24: Segmented aluminium AC/DC resistance ratio at 90 °C

The segmented enameled copper conductor results are as follows:

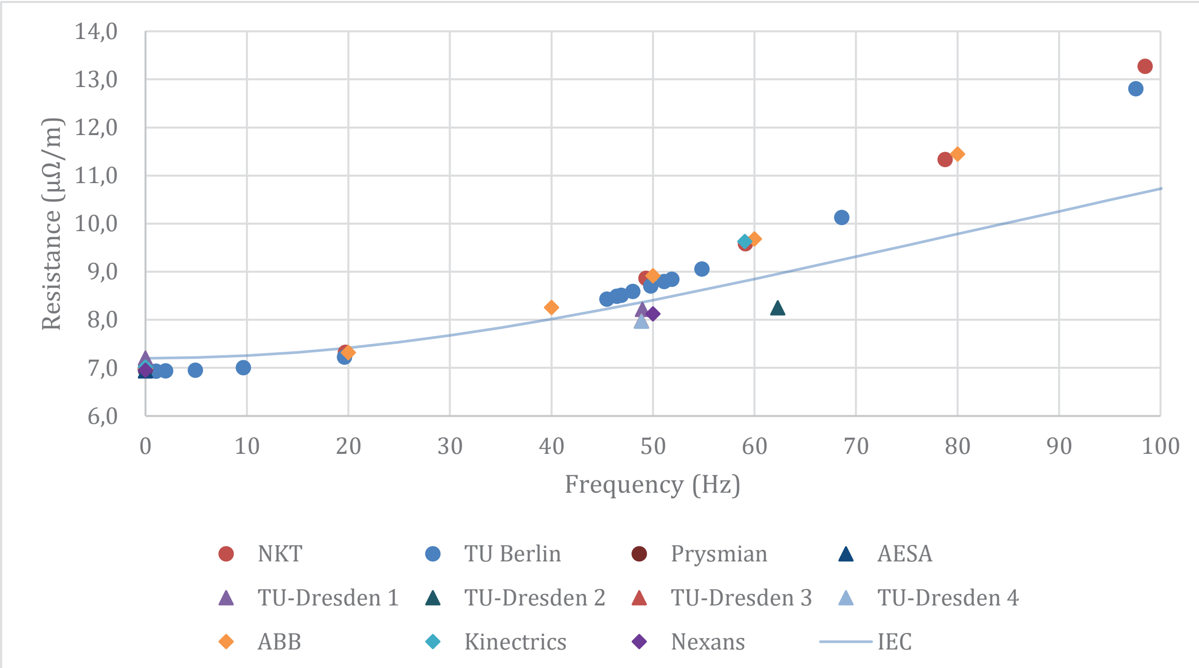

Figure 2-25: Segmented enameled copper AC & DC resistance at 20 °C

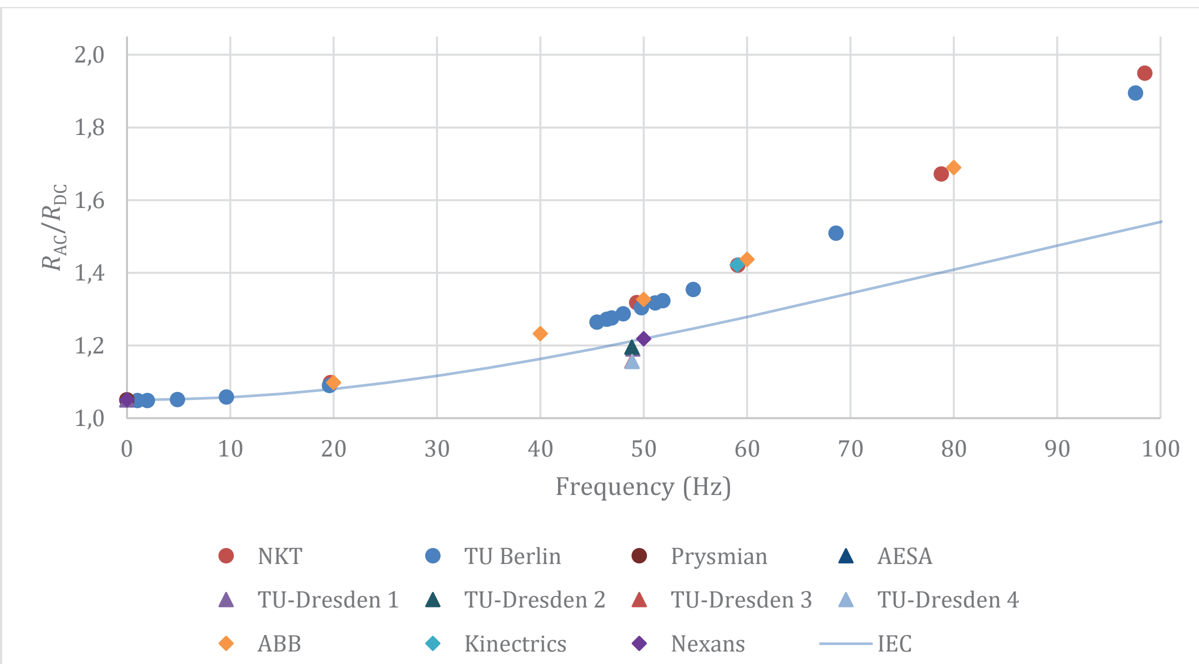

Figure 2-26: Segmented enameled copper AC/DC resistance ratio at 20°C

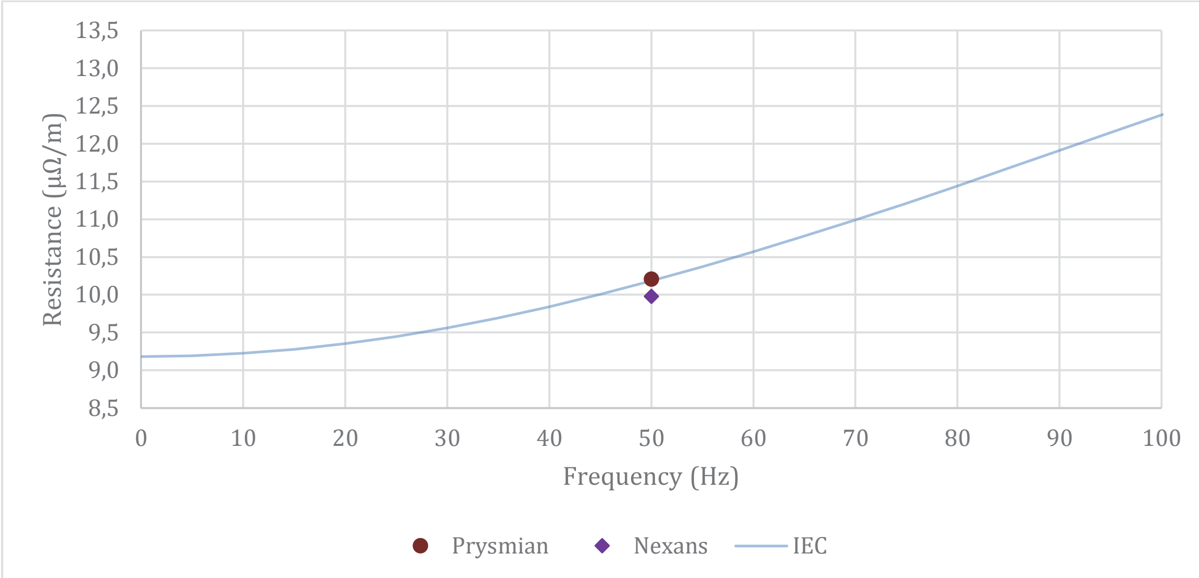

Figure 2-27: Segmented enameled copper AC & DC resistance at 90 °C

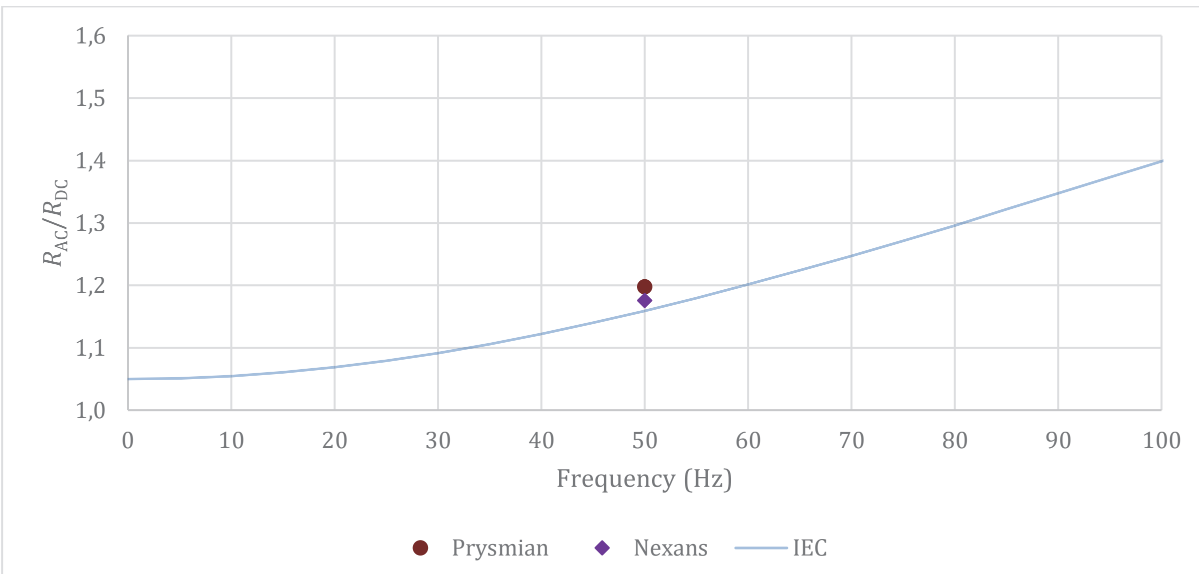

Figure 2-28: Segmented enameled copper AC/DC resistance ratio at 90 °C

The copper rod conductor results are shown in the following. For TU-Dresden different configuration were tested, showing some variance in the results.

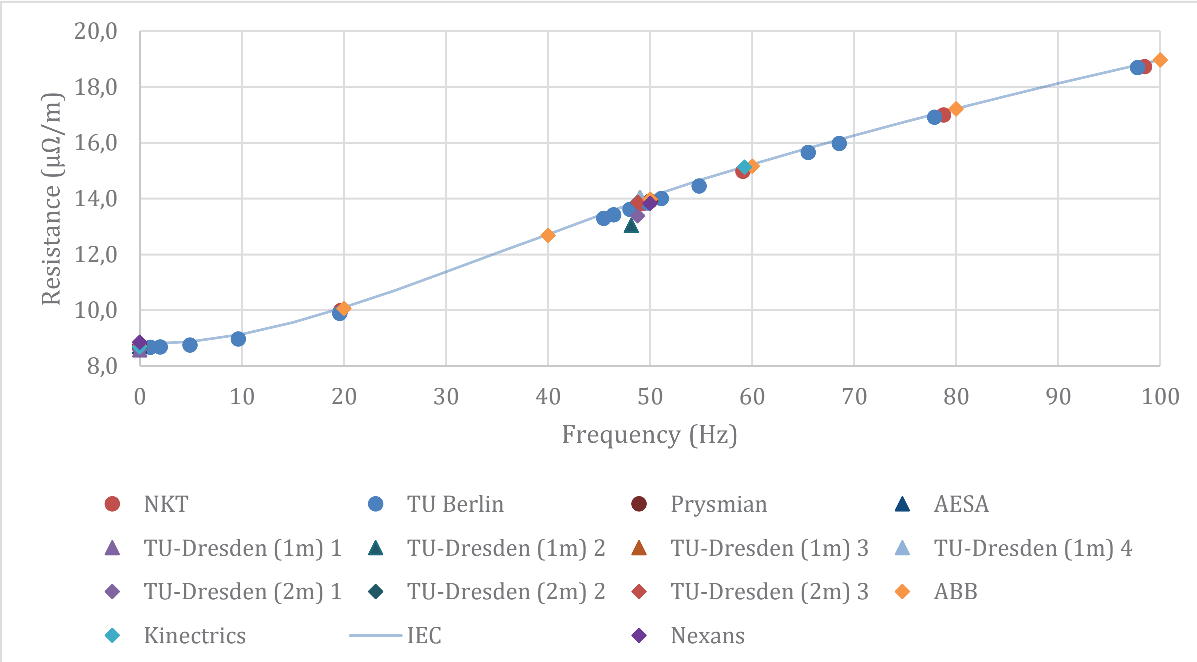

Figure 2-29: Copper Rod AC & DC resistance at 20 °C

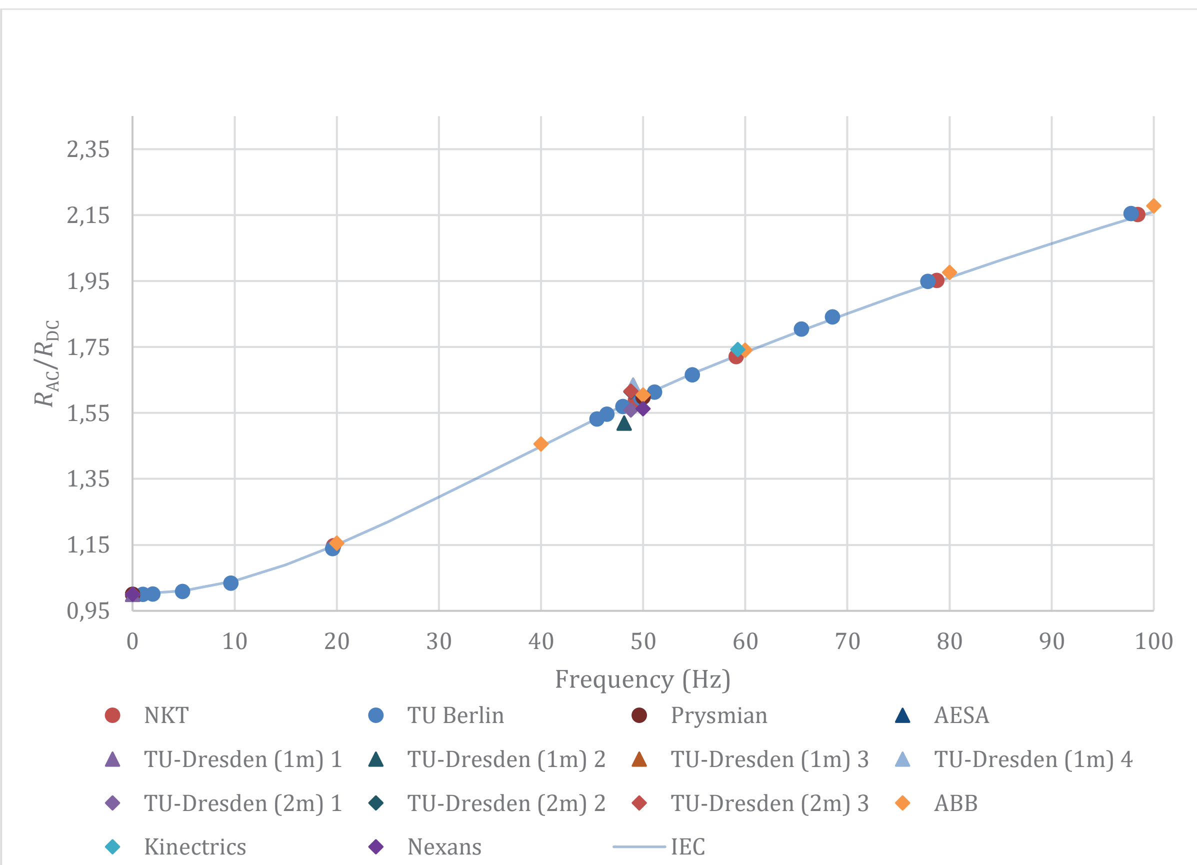

Figure 2-30: Copper Rod AC/DC resistance ratio at 20 °C

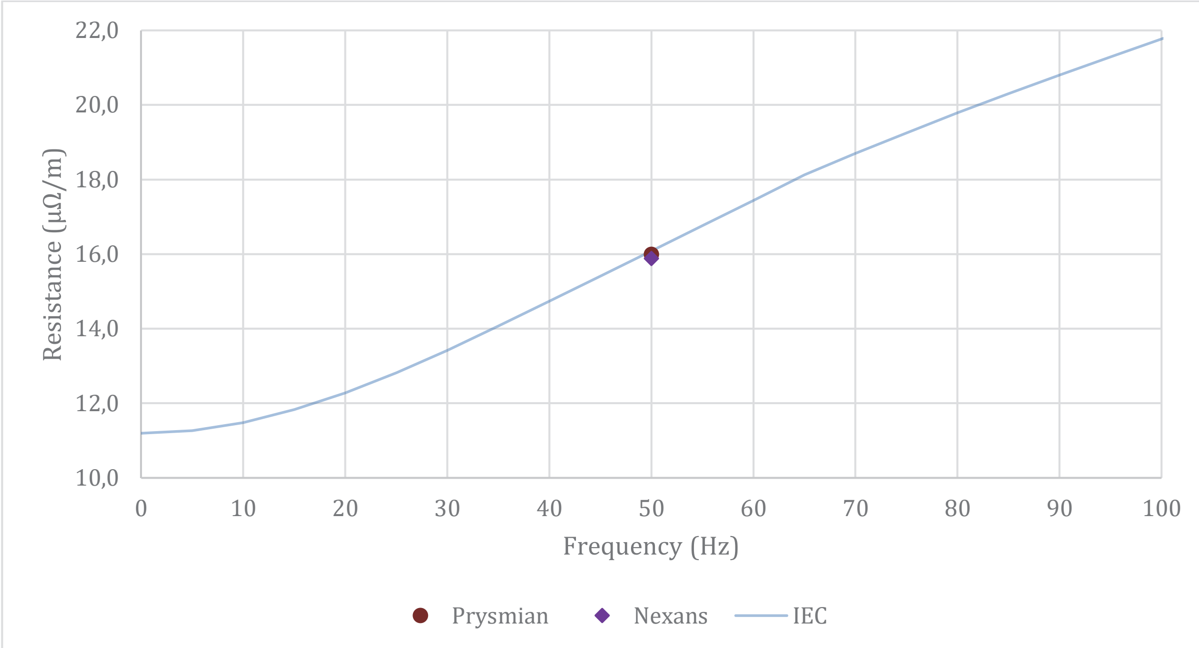

Figure 2-31: Copper Rod AC & DC resistance at 90 °C

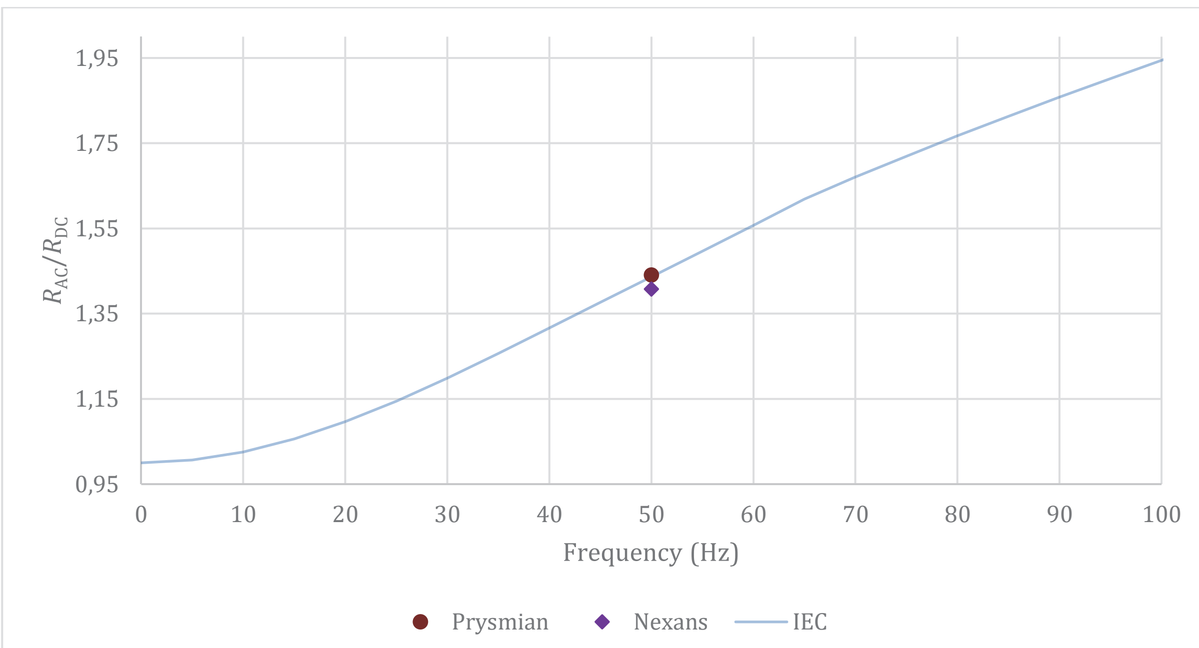

Figure 2-32: Copper Rod AC/DC resistance ratio at 90 °C

The copper pipe conductor results are shown in the following. ABB presents 2 measurements in the same configuration (repeated), but with renewed connections to check stability of the setup.

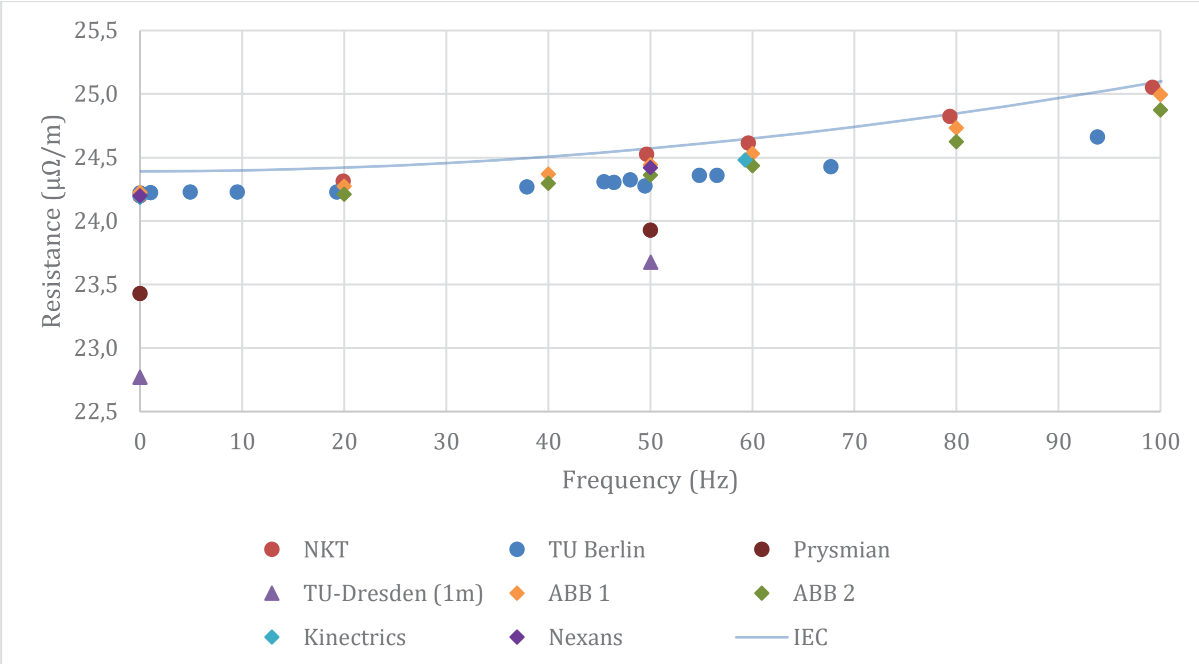

Figure 2-33: Copper Pipe AC & DC resistance at 20 °C

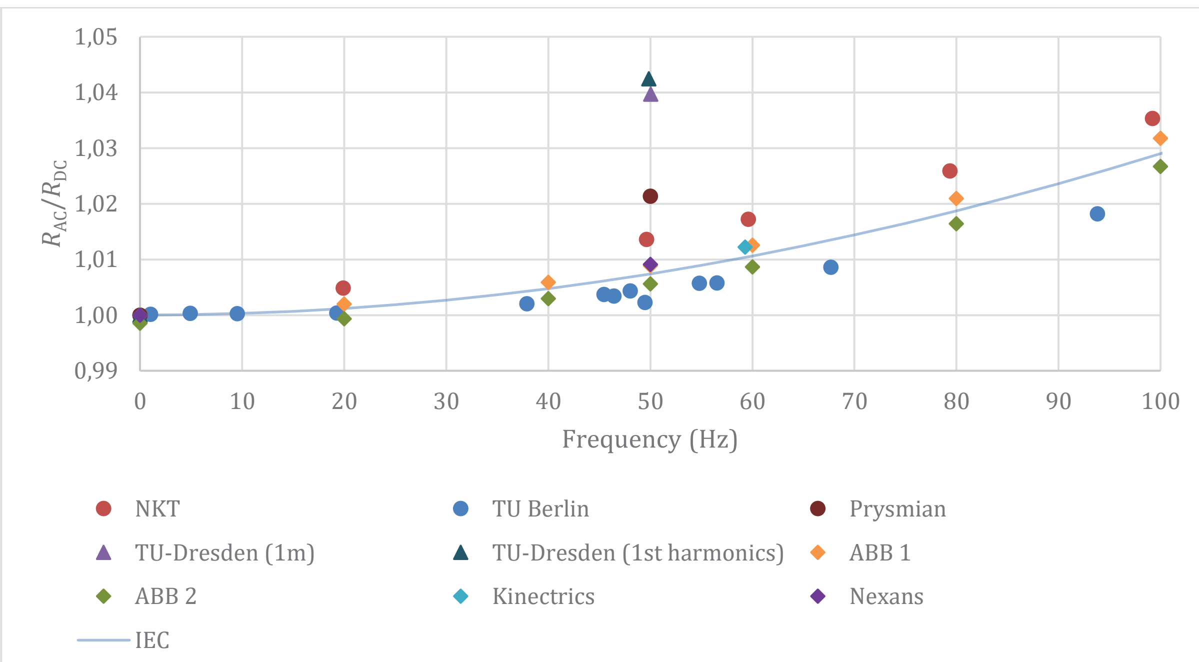

Figure 2-34: Copper Pipe AC/DC resistance ratio at 20 °C

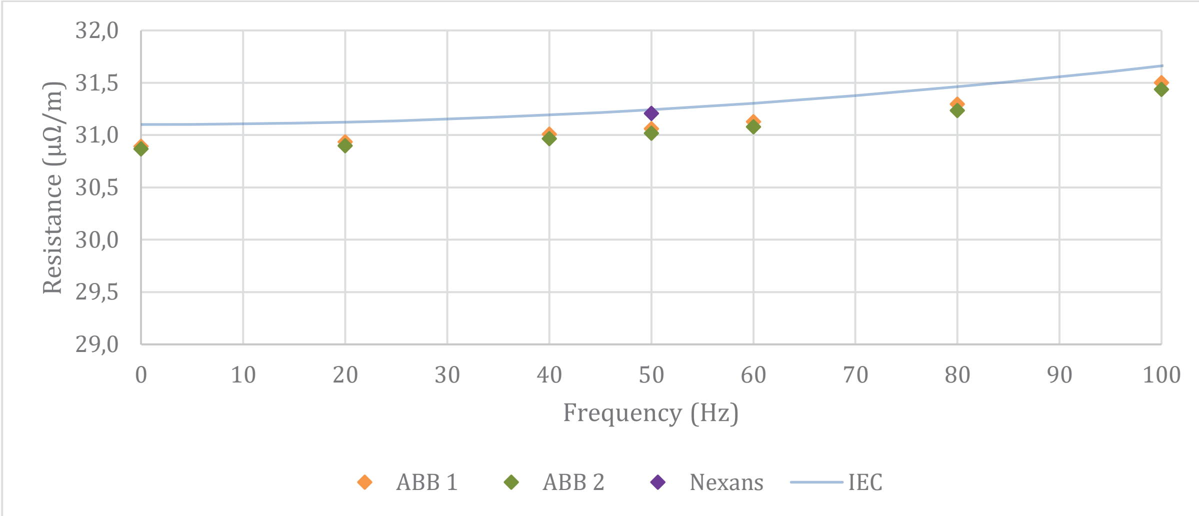

Figure 2-35: Copper Pipe AC & DC resistance at 90 °C

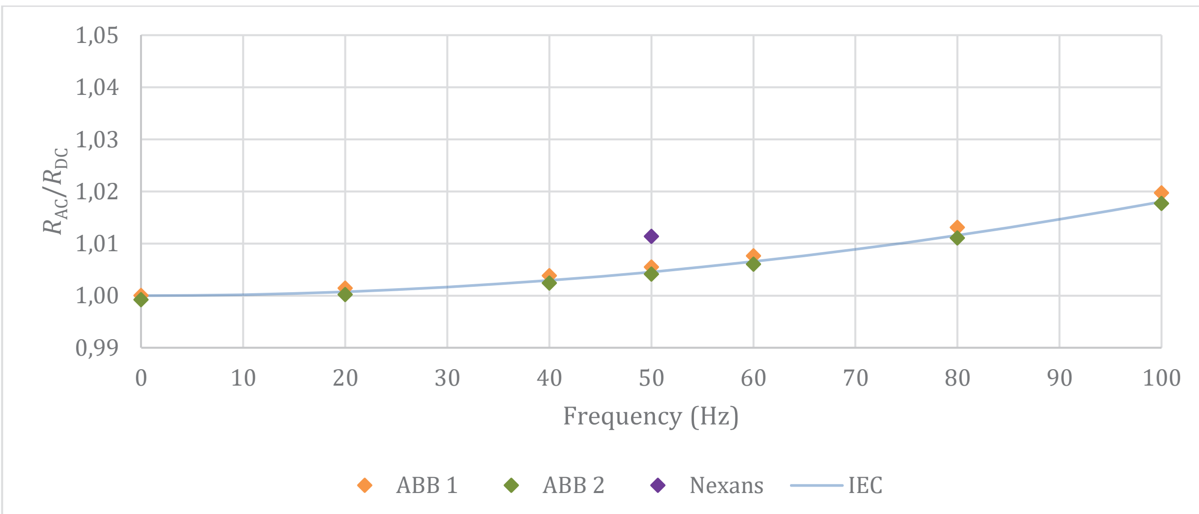

Figure 2-36: Copper Pipe AC/DC resistance ratio at 90 °C

2.9 Interpretations of Round Robin Test Results

The discrepancies between the measurement in the different labs are larger than the reproducibility one would hope for, and probably expect on a single system. This can be explained by the fact that the measurements were performed from the beginning on, throughout this investigation, using different configurations. Therefore, most of them did not follow the recommendations presented in the next chapter. They were mainly used to investigate different effects and therefore served as a basis for their discussion.

Nevertheless, measurement on well-defined and rotationally symmetric samples (rod + pipe) show less variation. This reflects the difficulty of the measurement linked with complex cable conductors and how important it is to follow specific guideline and recommendations to have comparable results, when performing AC resistance measurements. Therefore, users are strongly advised to follow the recommendations presented in chapter 3.

Moreover, the behavior over frequency measured in different labs confirms that for simple conductors (rod and pipe) measurements reflect adequately the exact mathematical models. For complex conductors, models using scaling effects (such as k_s description of the AC resistivity) cannot generally be used. Hence, it is necessary to measure each conductor design, independently of its design, size, … to get accurate results.

3. Recommendations For AC Resistance Measurements

3.1 Equipment and Environment

Different measurement techniques/equipment are adapted for AC resistance measurements as shown in 2.2.3. The choice of the equipment may depend on the conductor characteristics, size and length, the purpose of testing (qualification, routine, type test), the test parameters (temperature) and on the required accuracy.

3.1.1 Thermal Stability Management

In order to reach a high precision, the homogeneity of the temperature in the sample is of fundamental importance. Depending on the configuration, one or more temperature sensors must be installed in direct contact with the conductor surface. Common practices were displayed in section 2.1.

At least one temperature sensors must be placed between the voltage taps. Other temperature sensors placed along the conductor must be used (depending on configuration) to assess the longitudinal gradient due to variations in the thermal insulation system, connector effects, cable ends effects etc. To obtain a good thermal contact, thermally conductive grease may be used.

If multiple temperature sensors between the voltage tap-offs are used, the mean value of the reading of these sensors is to be used as measured temperature for evaluation of AC resistance.

3.1.1.1 Measurement at Room Temperature

The requirements for thermal stabilization at room temperature are depicted in Figure 3-1.

In step 1, the CUT must be placed in the laboratory, where it shall be measured. Close by heating or cooling sources (e.g., direct sunshine onto the setup or nearby heaters/coolers) shall be avoided. Optionally, if the CUT was previously stored at significantly different temperatures (e.g., outside in winter), it is good to include a waiting time of 12 hours before proceeding with step 2.

In step 2, the temperature then needs to be tracked for 10 min to check if it is stable in the laboratory environment and does not vary more than ±0.5 °C around the measurement temperature T. Optionally, if the test current is large and expected to cause significant heating of the CUT during testing (increase its temperature by more than 0.5 °C), one can stabilize the temperature already driving the test current, before the actual measurement and observe if the deviation of the temperature T is less than ±0.5 °C for at least 10 min.

Step 3 is the first bipolar DC resistance measurement where one can obtain $R_{\mathrm{DC},1}$ from two measurements of opposite test current polarity as explained in section 2.2.3.

Directly after that, in Step 4, the AC resistance measurements are conducted. Here, the average of at least 10 consecutive measurements will deliver the AC resistance. As discussed before, in case the resistance at the desired frequency (e.g., 50 Hz or 60 Hz) is interpolated by multiple measurements at frequencies close to this frequency, all measurements at those frequencies need to be performed at least 10 times (the curve of all averaged values is then used as the final resistance over frequency curve).

Directly after step 4, one will perform the second bipolar DC resistance measurement to obtain $R_{\mathrm{DC},2}$ in step 5. The difference between $R_{\mathrm{DC},1}$ and $R_{\mathrm{DC},2}$ should be less than 0.5 %. The average of both DC values, $R_{\mathrm{DC},1}$ and $R_{\mathrm{DC},2}$, is taken to calculate the final DC resistance R_{DC}.

During the measurements, step 3, step 4 and step 5, the conductor temperature shall be monitored.

Temperature sensors are ideally placed at both voltage tap-off positions and at the center of the measurement length (at the surface of the CUT), see sensor positions (1), (2) and (3) in Figure 3-1. The difference between all readings should not be larger than ±0.5 °C. The average of all readings is taken as the conductor temperature.

Any uncertainty or deviations from the best practice shown above, needs to be included in the uncertainty calculation of the measurement.

3.1.1.2 Measurement at High Temperature

The requirements for thermal stabilization at room temperature are depicted in Figure 3-2.

To bring the CUT to the desired high temperature in step 1, the CUT can be driven by a large heating current (Step 1-A) or can be placed in an oven (Step 1-B). The complete conductor can be placed in an oven or only the part of the cable between the voltage taps. If only part of the cable is placed in the oven, additional thermal insulation systems may be necessary and placed over the conductor outside the oven.

In both cases, in step 2, the temperature then needs to be tracked for 10 min to check, if it is stabilized and does not vary more than ±2.5 °C around the measurement temperature T.

Step 3 is the first bipolar DC resistance measurement where one can obtain $R_{\mathrm{DC},1}$ from two measurements of opposite test current polarity as explained in section 2.2.3.

Directly after that in step 4, the AC resistance measurements are conducted. Here, the average of at least 10 consecutive measurements will deliver the AC resistance. As discussed before, in case the resistance at the desired frequency (e.g., 50 Hz or 60 Hz) is interpolated by multiple measurements at frequencies close to this frequency, all measurements at those frequencies need to be performed at least 10 times (the curve of all averaged values is then used as the final resistance over frequency curve).

Directly after step 4, one will perform the second bipolar DC resistance measurement to obtain $R_{\mathrm{DC},2}$ in step 5. The difference between $R_{\mathrm{DC},1}$ and $R_{\mathrm{DC},2}$, at the reference temperature, should be less than 1.0 %. The average of both DC values, $R_{\mathrm{DC},1}$ and $R_{\mathrm{DC},2}$, is taken to calculate the final DC resistance R_{DC}.

During the measurements, step 3, step 4 and step 5, the conductor temperature shall be monitored.

Temperature sensors are ideally placed at both voltage tap-off positions, at the center of the measurement length (at the surface of the CUT) and close to both terminals (see sensor positions (1), (2), (3), (4) and (5) in Figure 3-2). The latter is necessary to observe any significant temperature drift along the cable axis. The difference between sensors (2), (3) and (4) should not be larger than ±2.5 °C. The average of the readings of those three sensors (sensors (2), (3) and (4)) is taken as the conductor temperature.

Any uncertainty or deviations from the best practice shown above, needs to be included in the uncertainty calculation of the measurement.

3.1.2 Measurement Temperature & Temperature Scaling

The measurement temperature T should be as close as possible to the desired/reference temperature T_0 (usually T_0 is 20 °C or 90 °C). Deviations of T in the range of T_0±5 °C are allowed, resulting in typical values of 15 … 25 °C and 85 … 95 °C. Even though an offset is allowed, as explained before, the temperature needs to be stable/constant. If the temperature deviates from its reference temperature ($T \neq T_0$) the user has 2 options:

1. Adapt the measuring frequency f in advance (if technically possible) according to the *Principle of Similitude* and as shown in detail in section 1.3.8 and only perform one measurement. Or
2. perform multiple measurements close to the desired frequency f_0 (usually f_0 is 50 Hz or 60 Hz) and then perform *Temperature Scaling* as described in detail in section 1.2.6 on the whole resistance over frequency curve after the measurements.

Only for conductors, for which all electrical and geometrical interdependencies are exactly known, *Temperature Scaling* is not limited to a temperature range of ±5 °C, as it is for complex conductors (see section 1.2.5 and [2, p. 48]).

3.1.3 Measurement Frequency & Noise

The mean value of at least 10 AC measurements must be taken. The standard deviation, reflecting the effect of external electromagnetic perturbations, is to be used in the error calculation. With larger measuring currents (>100 A) the effect of external noise may be reduced.

Also, it is recommended that each measurement consists of an evaluation of a signal over multiple cycles (e.g. 10 to 100 cycles) of the measurement frequency (e.g. at 50 Hz: 200 ms to 2 s).

In very noisy environments, when the noise level of the environment is high relative to the measured signal, it is recommended to not measure directly at power frequency, if the measurement device allows it. Also, even if the measurement temperature T is exactly the desired temperature T_0 ($T = T_0$), it is recommended to perform multiple measurements of the AC resistance close to the desired power frequency value f_0 but not directly at that frequency to avoid electromagnetic interferences as stated above. By interpolating two or more measurements taken symmetrically around the power frequency and distant by 1 to 5 Hz to f_0 (e.g., 45 Hz and 55 Hz). A linear interpolation between both values is sufficient for the accuracy. See section 1.3.8 for more details.

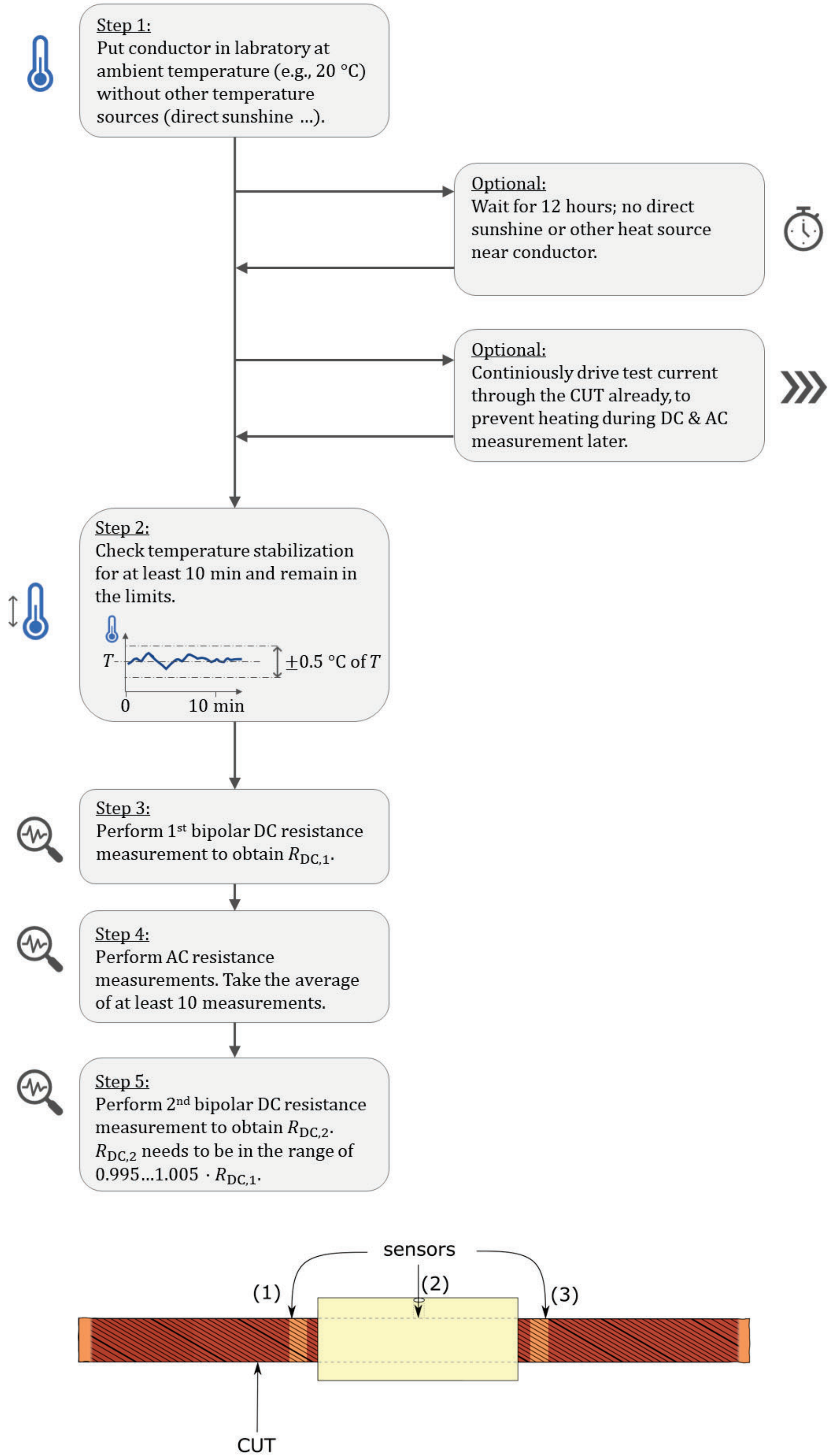

Figure 3-1: Temperature stability requirements at room temperature

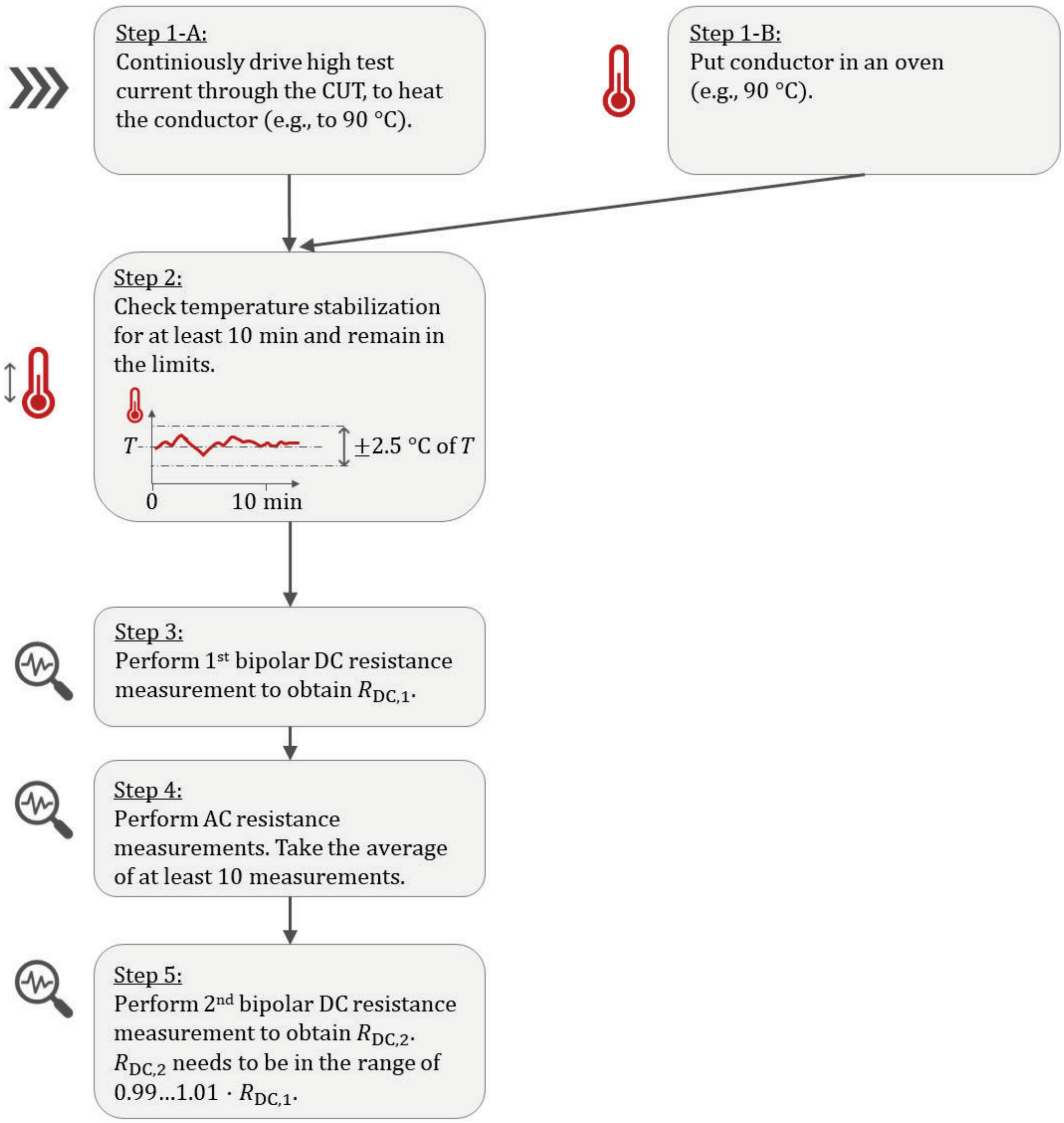

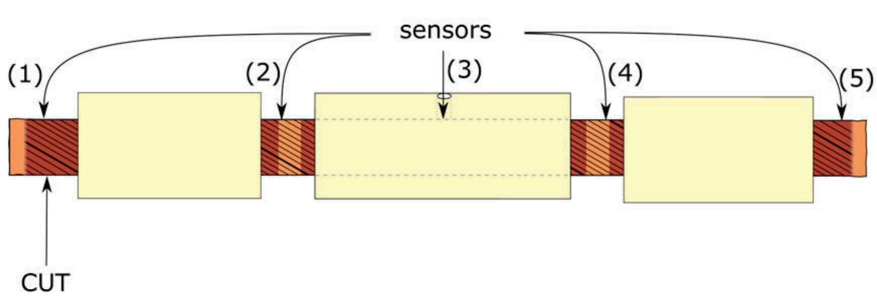

Figure 3-2: Temperature stability requirements at high temperature

3.2 Performance Check Of Measurement System

3.2.1 Measuring System

The measuring device must be calibrated using a calibrated resistor. For example, a calibrated impulse shunt, whose resistance is usually frequency-independent up to very high frequencies or a well-defined large conductor (solid or tubular), whose frequency dependent resistance can be calculated analytically.

To gather additional experience about the measurement system and sensitivities, it is recommended to test the measurement system on a complex conductor first, whose exact resistance can still be obtained. For example, a rectangular solid copper conductor with a cross section of 2 cm x 12 cm has a significant amount of complex magnetic fields in its surrounding at 50 Hz and already an AC to DC resistance ratio of approximately 1.5 at 20 °C and 50 Hz. Its true losses can be easily computed by an FEA for example and benchmarked against the measurement system at different loop sizes. For a single[12] rectangular copper conductor of above-mentioned dimension, the resistances are given in the following table, Table 3-1.

Table 3-1: DC and AC resistances per unit length and resistance ratio at different frequencies for a rectangular copper conductor with a cross section of 2 cm height and 12 cm width at 20 °C obtained by FEA simulations (proximity effect losses of the return conductor not included)

Frequency in Hz	Resistance in μΩ/m	R_{AC}/R_{DC}
0	7.18	1.00
10	7.74	1.08
20	8.64	1.20
30	9.43	1.31
40	10.14	1.41
50	10.81	1.50
60	11.44	1.59
70	12.07	1.68
80	12.68	1.76
90	13.28	1.85
100	13.88	1.93

For other conductor shapes and sizes, the AC resistances can also be obtained from the following plot (Figure 3-3) using the *Principle of Similitude* (see section 1.2.5).

[12] The return conductor is sufficiently far away to not introduce additional/proximity effect losses.

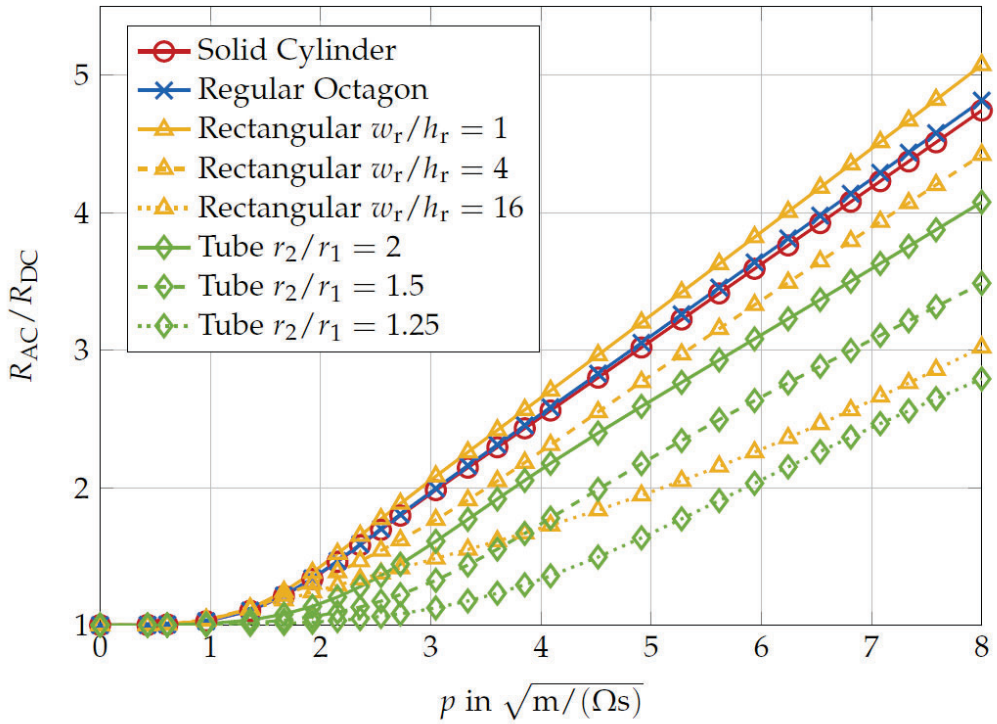

Figure 3-3: AC resistance ratio plotted over p; w_r and h_r respectively are the width and height of a rectangular conductor; r_1 and r_2 are inner and outer radius of tubular conductors [2, p. 65]

The error of the performance test must not be larger than declared error of the system.

3.2.2 Mechanical

The distance between the voltage taps must be measured mechanically or electrically. The precision of the measurement is recommended to be below 0.1 %. Special considerations may be applied when measuring the length of bent samples, to get an accurate length. The length (reference length) should be measured at 20 °C.

3.2.3 Thermal

Temperature sensors must be calibrated using a reference thermometer. The uncertainty of the temperature measurement is recommended to be lower than 0.2 °C. Precautions must be taken to protect the temperature sensors from external influences (e.g., air flow …).

3.3 Sample Preparation

Sample preparation is an integral part of the connection and must be taken into consideration in the design/description of the connection.

3.3.1 Conductor Length

The minimum conductor length (between the current injection systems) must be 100 times the diameter of the conductor. This shall guarantee a sufficient length so that the impedance of single wire paths is the dominant factor influencing current distribution in the cross section and hence delivers a representative behavior of the CUT [11].

3.3.2 Treatment of Terminals

The best way to achieve a representative current distribution is to inject the current from the end of the conductor through a solid conductive part contacting directly each individual wire and having a sufficient sample length [11]. This can be best achieved by soldering/welding all the wire together. This method must be considered first, in any case.

The main practices are given here and were discussed in section 1.3.4:

- The surface of the connector may be cleaned to remove dust and dirt and possibly wiped with solvent to eliminate grease.
- Aluminum conductor may be scratched with sandpaper (or similar materials) to remove thick oxide layer at contact position. Note however that the oxide is formed again very quickly so that the connection must be installed right after cleaning operation for best results.
- In the case of Milliken or watertight conductor, the insulating tape may be removed over a predefined distance to improve current homogenization. Careful reassembling of the conductor after this operation is necessary to fit properly to the connectors.
- Burning or scratching the surface of enameled wire can be necessary to establish an inter-wire contact in the case a homogeneous current distribution cannot be guaranteed directly by the axial connection. Similarly, the surface of oxidized wires must be scratched.
- Semiconducting tapes placed above the conductor are usually removed directly under the connector to improve electrical contact and avoid overheating.

If soldering and/or axial connection cannot be used, other techniques as described in section 2.5.3 might be considered. The choice will depend on the conductor design and cross-section.

Usually, in bare copper conductors, the contact resistance between the individual wires is low and all the contacting techniques described in section 2.5.3 are suitable.

A peculiarity of aluminum conductors is that the contact resistance between the individual wires is high because of the presence of an oxide layer on the surface of each wire. It is then recommended to inject the current from the cable end surface in a homogeneous way through all the wires (soldering or similar). If the current is injected from the outer wire layers, to get a reasonable contact, it is necessary to break or remove the oxide layer between inner strands. Although scraping the surface of the conductor will help, inter-wire contact in the inner layers is more difficult to achieve. High compression forces leading to conductor deformation (for example: screws going through the conductor) are preferred solutions.

Material used to make the cable watertight might be an issue when inter-wire contact resistance is considered.

- Swellable material: Usually, swellable powder and yarns only introduce localized insulation between wires that barely affects the current homogenization. Swellable tapes, on the contrary, are good insulators (when not conductive) and may strongly hinder the current homogenization. These must then be removed over at least the length of the connector or weld to allow for inter-wire contacts.
- Extruded Material: Extruded plastic or grease may hinder the current homogenization, depending on its nature. Removal of this material may then be necessary to achieve an accurate measurement results.

Milliken conductors most often are built from sector segments insulated from each other by tapes. Removal of these tape might be necessary, depending on the connection technique used. In conductors using enameled or oxidized wires, the current cannot circulate between the individual wires. The end connection is then of utmost importance. Welding all the wires together (if necessary, after removal of the insulated layer over the length of the wires to be welded) is compulsory. The use of other similar techniques using axial contact (such as metallic deposition) might also be considered with care. Different methods were proposed in section 2.5.3.

3.3.3 Treatment of the Cable

The conductive screen and, if available, armor of the cable needs to be removed for an accurate measurement of the resistance of the inner conductor, which is the CUT. Ideally, only the inner conductor and the insulation system (semiconductors & high voltage insulation) on top of the conductor are present. The insulation system may be an important part of the design as it can influence the CUT performance due to its compression forces. Hence, if present, the insulation system needs to remain on the CUT.

Measurement of screened cables will show additional losses that will depend on screen design, and care should be taken on the interpretation of the results. Additional true skin effect losses can affect the inner conductor and, when extending the voltage loop over the screen, additional apparent losses will be included in the measurement [2, p. 105].

Mechanical constraints may be applied to reflect the laying conditions of the conductor. These measurements conditions must be included in the report (see section 1.3.6).

Appropriate cleaning of the surface of enameled/oxidized wires, as explained above in section 3.3.2, is also relevant for the contacting of voltage tap-offs (see Figure 3-5).

3.4 Setup

The following recommendations are given for the AC Resistance measurement of round conductors (this includes solid, tubular, stranded and Milliken conductors of all kinds). As described in detail before, additional considerations need to be considered for conductor cross sections with larger asymmetries (rectangular conductors, three phase arrangements etc.).

3.4.1 Surrounding

Recommendation: Along the complete sample length, any other conductive/metallic objects or other conductor should be placed further than 1 m away from the sample. This includes walls and the laboratory floor, which may have conductive elements.

Background: It has been shown in Figure 1-10 and Figure 1-11 that at a distance of more than 1 m, additional true losses due to proximity effect are negligible (<0.1 %) in typical arrangements.

3.4.2 Return Conductor

Various return conductor arrangements are possible and reasonable. Except for recommendation 4, the return conductor(s) need(s) to run in parallel to the CUT.

Recommendation:

1. One separate conductor placed at least 1 m apart from the CUT. This can be an identical cable/conductor as the CUT for example or a much smaller conductor having negligible AC losses itself.
2. Two separate identical conductors placed in the same plane as the CUT and at least 0.5 m apart from the CUT, both at the same distance to the CUT.[13]
3. A tubular return conductor around the CUT can also be used. It needs to be concentric with the CUT. Perfect concentricity does not introduce additional losses. Small deviations from concentricity as observed in practice, can introduce small additional losses in the CUT. These losses are usually negligible if the tubular return conductor is of similar dimension[14] and spacing as typical cable screens. This should also be checked with Figure 1-10.[15]
4. The CUT can also be bend into a single large loop. Bending along the measurement length should be low, as mechanical stress may alter conductor performance.

Background: In addition to not introducing additional true losses in the CUT itself, also symmetries in return conductor placement can be used to simplify the voltage lead positioning (see section 3.4.3).

3.4.3 Voltage Loop

Various voltage loop setups are possible and reasonable depending on the return conductor placement put forward in section 3.4.2. In any case, the radial extension of the loop should be placed at a larger distance than the wire diameter used in the conductor design (d_{Wire}) and not directly on

---

[13] The distance can also be smaller than 0.5 m according to Figure 1-10. The lower limit to not introduce more than 0.1 % of additional losses in the CUT, should be checked with FEM simulations or Figure 1-10 if below 0.5 m. Asymmetries may be considered.

[14] Similar or thinner thickness and similar or larger radius.

[15] The cable screen can be used directly as a return conductor. However, the voltage loop (section 3.4.3) should not include other conductors in theory, as it captures their additional AC losses. For typical screen configuration additional AC losses are usually low, as they are essentially a thin tube with large inner diameter having little AC losses. Still additional losses will be measured at AC [2, p. 105]. Hence, it is recommended to use a tubular return conductor and place the voltage loop between CUT and return conductor. For cables, this can only be done, if the screen is removed and the cable is put into a new/separate large tubular return conductor (see Figure 3-10).

the surface of the CUT, if the CUT is a complex conductor or has non-rotationally symmetric cross section. If the CUT has an insulation system, the loop should be attached to the surface of the insulation (see Figure 3-6 to Figure 3-12), in other words at $d_{\mathrm{Insulation}}$, which is the thickness of the dielectric. For every setup it is required that the wires of both voltage taps are tightly twisted from the place they meet first (at least close to the setup) and are then brought to the measurement system, to avoid any further induction of spurious voltages (magnetic coupling) on the way to the measurement system. Depending on the measurement system, an additional screen on the twisted pair voltage lead wires may be applied to reduce electric interference (electric coupling).

Recommendation:

A. One rectangular[16] voltage loop can be sufficient, if electromagnetic field asymmetries are well-known (position of all other nearby conductors/conductive objects (walls, floor, …)). For example, one could use two symmetrical return conductors (recommendation 2; section 3.4.2) and put the voltage loop on top of the insulation (if present). This recommended setup is shown in Figure 3-6. This solution is not recommended for large a CUT loop (option 4 of 3.4.2) because of the unsymmetric field distribution.

B. Four or more rectangular voltage loops distributed homogenously[17] around the conductor circumference placed at a distance greater than d_{Wire} (e.g., on top of the insulation if the CUT has an insulation system). The measurement loops should all be set up before the first measurement. Then each loop is measured. The average of all four measurement loops gives the final value. This is depicted with one return conductor in Figure 3-7.

C. A helical voltage loop can be placed at any distance above the surface of the CUT. In a cross sectional view it must follow a circular path (not elliptical). The center of this circle (path) does not need to coincide with the center of the CUT. The helix also needs to have a constant pitch and an integer number of turns along the measurement length [9], [10]. It should be checked, that the pitch of the helical voltage loop does not coincide with the pitch (direction and lay length) of Milliken conductor segments for example. If this would be the case, the effect of the helical loop would be compromised, as its relative position to the conductor elements (e.g., segments in Milliken conductor or stranded wires) remains the same and does not capture the complete conductor properties. Ideally two counter-helices[18] are used and the average of both measurements is taken. As the losses measured by the helix are affected by the losses transferred from the CUT to the surrounding (e.g. return conductor), here the return conductor should ideally be identical to the CUT or very thin (having very little AC losses) [9], [10]. Figure 3-4 shows a setup using two counter-helices on a rectangular copper conductor.

In case of doubt, the helical voltage loop (C) is the reference method. It is also the recommended method for non-circular conductors.

Note: A tube or the screen of the cable can be used as a voltage loop, but it will capture part of the screen losses, depending on concentricity. Therefore, further study is required before introducing this method.

---

[16] Rectangular, when viewed from the side as in Figure 1-8 for example.

[17] Homogenously refers to being at the same distance from a central point (in other words on a certain radius or annulus). This central point should be the center of the conductor. On this imaginary circle (same distance from the center point) the taps shall be equally distributed. For example, in case of four loops every 90° (12, 3, 6 and 9 o'clock). This can be easily realized for circular conductors, but a support structure may be needed for rectangular conductors for example.

[18] Clockwise and counterclockwise along the CUT.

Background: All complex magnetic fields originating from the CUT need to be captured to account for the true losses of the conductor. Therefore, space (a certain radial voltage loop extension d_{VL}) is needed between conductor surface and voltage lead to capture sufficient field if the CUT is not a perfectly round conductor (which would not have outer complex magnetic fields). As only little asymmetry is expected from real round (solid, stranded, hollow and Milliken) conductors, a spacing of at least one time the wire diameter d_{Wire} of the CUT is sufficient. For insulated conductors, this requirement is always satisfied as the insulation system needs to stay on the CUT and hence the voltage loop cannot be placed beneath it but only on top of the insulation. The radial extension of the loop should also not be too large to not measure complex fields (AC losses) of other nearby conducting materials and keep the inductive component of the measured voltage $\underline{u}_{\mathrm{meas}}$ low (see also examples in [2, p. 98]). Important to note is that the necessary radial voltage loop extension d_{VL} for other asymmetric conductor shapes (e.g. rectangular bus bars etc.) can be much larger [2, p. 83], when a helical loop is not used.

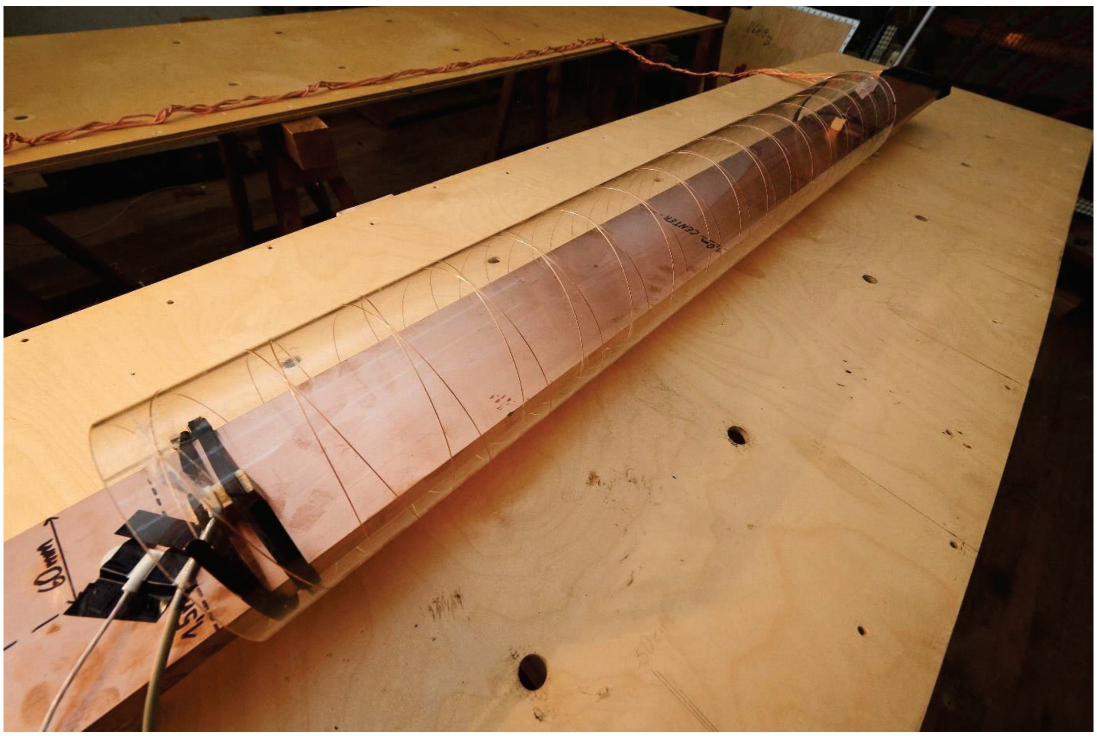

Figure 3-4: Two counter-helices on a transparent plastic tube used as voltage loops for measuring the AC resistance of a rectangular copper conductor with a large asymmetry (cross section of 2 cm x 12 cm)

3.4.4 Connections for Current Injection

In order to mitigate the effect of the field generated by the connection, the distance between the connectors and the voltage drop measurement points (voltage tap-offs) must be at least 15 times the conductor diameter as seen in Figure 3-5 and following.

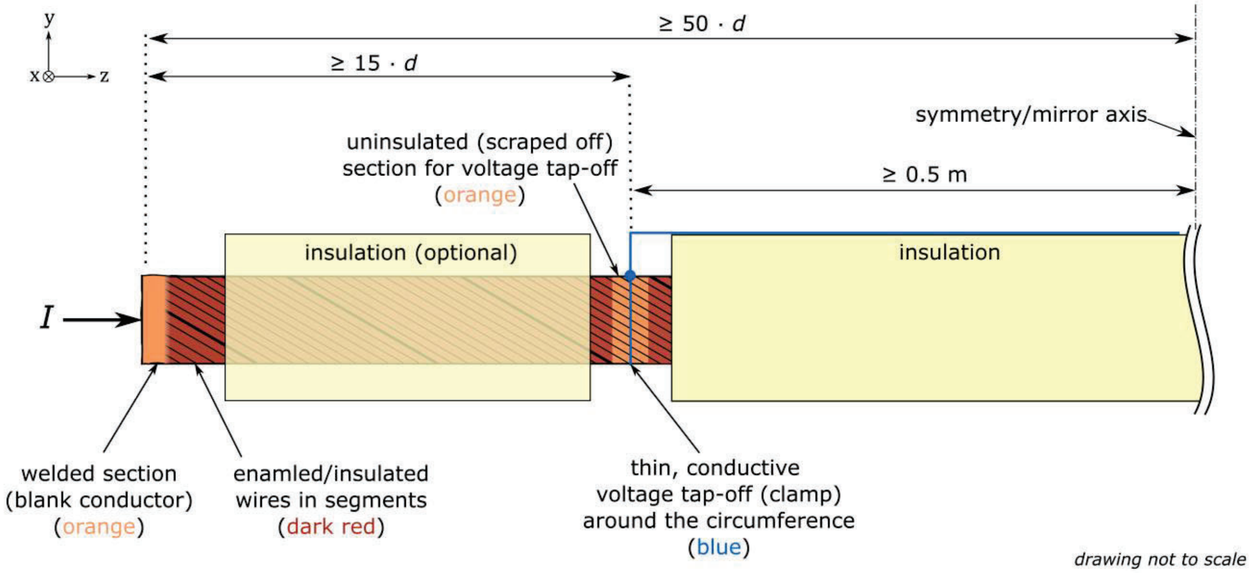

Figure 3-5: Recommend current injection (side-view of one side)

The current injection system must be adapted to the conductor design to allow for steady current distribution through the cross-section of the conductor over the measured length.

In order to check the current homogeneity over the outer layer, 2 measurements done with different contact positions of the voltage taps (either longitudinally or radially – the goal being to contact different wires on the outer layer), but without moving the current connector, must be compared. Note that this procedure only gives an overview of the current distribution in the outer layer (except for Milliken where the wires are alternatively in different layers).

Comparing the measured and expected DC value (if known) is another method to check the current distribution homogeneity. The difference must not be larger than the declared error resulting from the uncertainty calculation. Whenever possible, the current leads to and from the measurement system should be coaxial connections to prevent stray fields as much as possible.

3.4.5 Voltage Tap-Offs

Distance between voltage taps must be at least 1 m but are preferably larger as this increases the measured voltage drop and therefore sensitivity of the measurement equipment. Voltage taps may consist of (non-magnetic) knives or wires wrapped around the conductor. When the current injection (short-circuit of all single wires) is sufficiently good at both terminals, it should also be possible to attach the voltage tap-offs to a single wire at both connection points (see section 1.3.5 and [2, p. 79]).

If wires are used as voltage tap-offs and wrapped around the circumference of the conductor, it should be of very small diameter (smaller than d_{Wire}) to allow for an accurate length measurement between the voltage taps and also to prevent currents jumping from one segment outer layer to another via this short-circuit formed by the voltage tap-off. The latter would only be relevant, when the outer layers of different segments do not have the same design (different pitch lengths, …).

Distance between taps may be measured electrically (by DC measurement of a cylindrical solid calibrated reference conductor - with a known resistance), mechanically with a tape measure, laser rangefinder or similar device. Measurement error must be declared and considered in the error calculation.

3.4.6 Recommended Setups: Examples

The recommendation combination numbers used below, e.g. 2A, relate to the different recommendations for return conductor placements (1, 2, 3 and 4) in section 3.4.2 and different voltage loop configurations (A, B and C) in section 3.4.3. The recommended setups shown in this section (including all geometrical constraints) can be used directly out-of-the-box and will deliver accurate measurement results (concerning voltage and current loop considerations). Some required features as thermal sensors are not shown in the pictures to limit their complexity but are necessary as described earlier. Accurate results can of course also be obtained with other combinations as for example: 3C, which is a tubular return conductor with a helical loop (beneath the return conductor).

From the point the voltage lead pairs first meet, they need to be tightly twisted and can be led directly to the measurement system (they do not have to leave the CUT perpendicular from this point on as shown in the pictures). The position, where the voltage lead wires come together does not need to be halfway in between the voltage tap-offs necessarily.

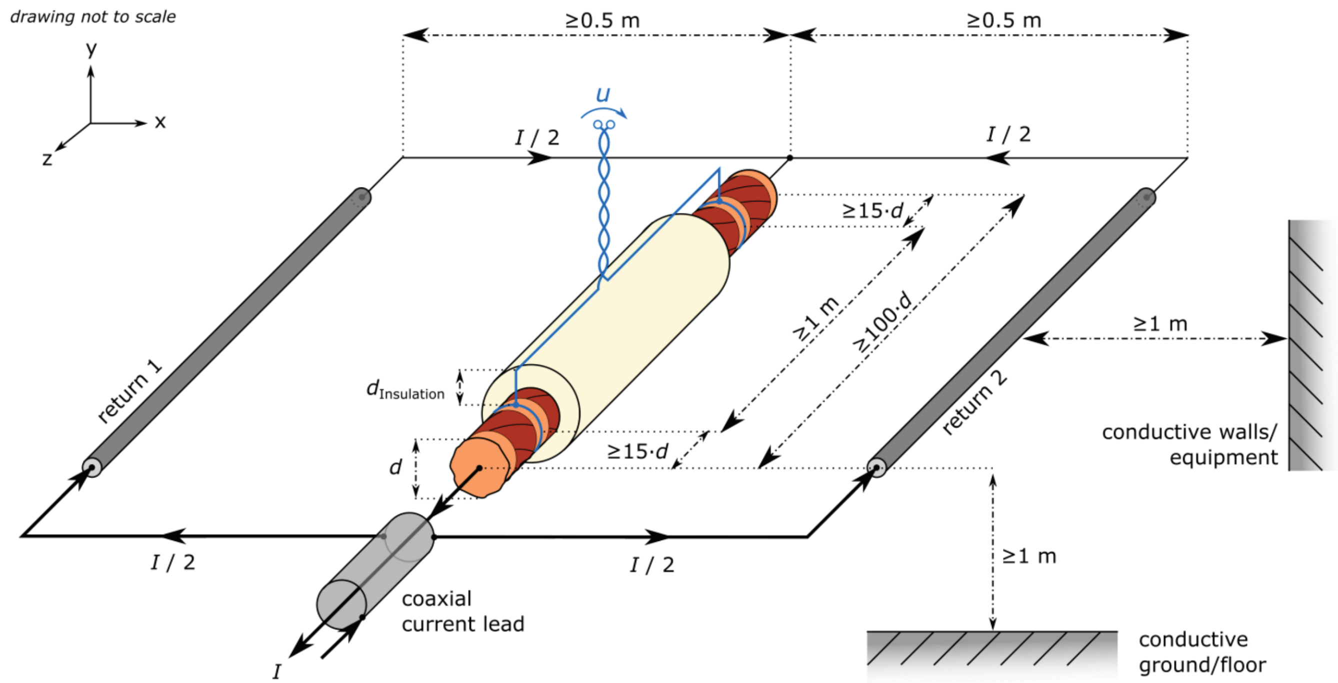

Figure 3-6: Dual return, single voltage loop configuration (recommendation combination 2A)

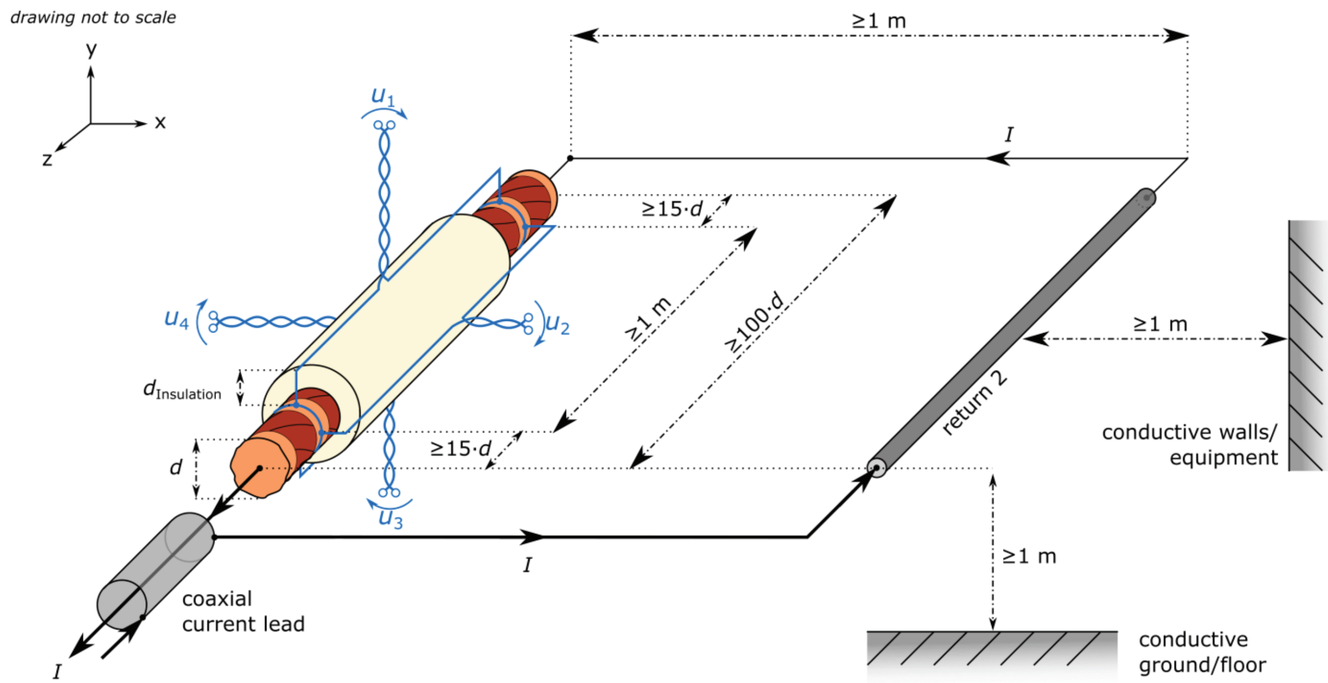

Figure 3-7: Single return, average (AVG) voltage loop configuration (recommendation combination 1B)

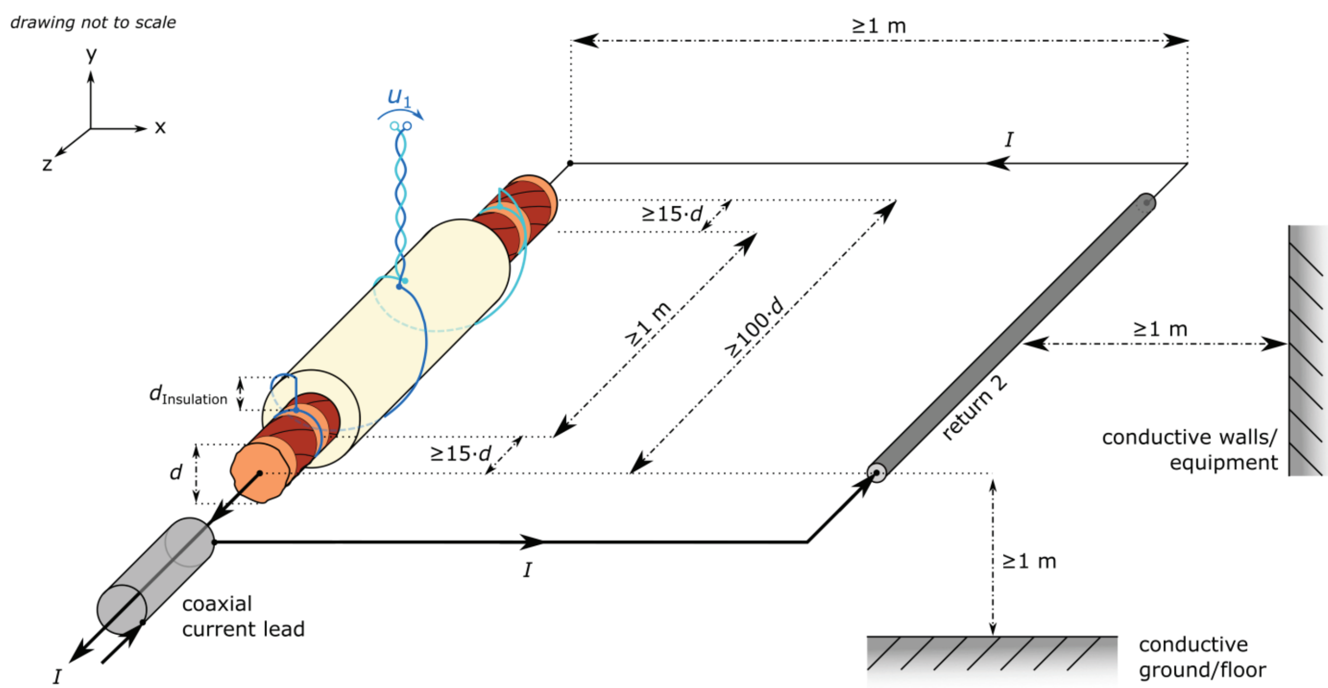

Figure 3-8: Single helix configuration (recommendation combination 1C)

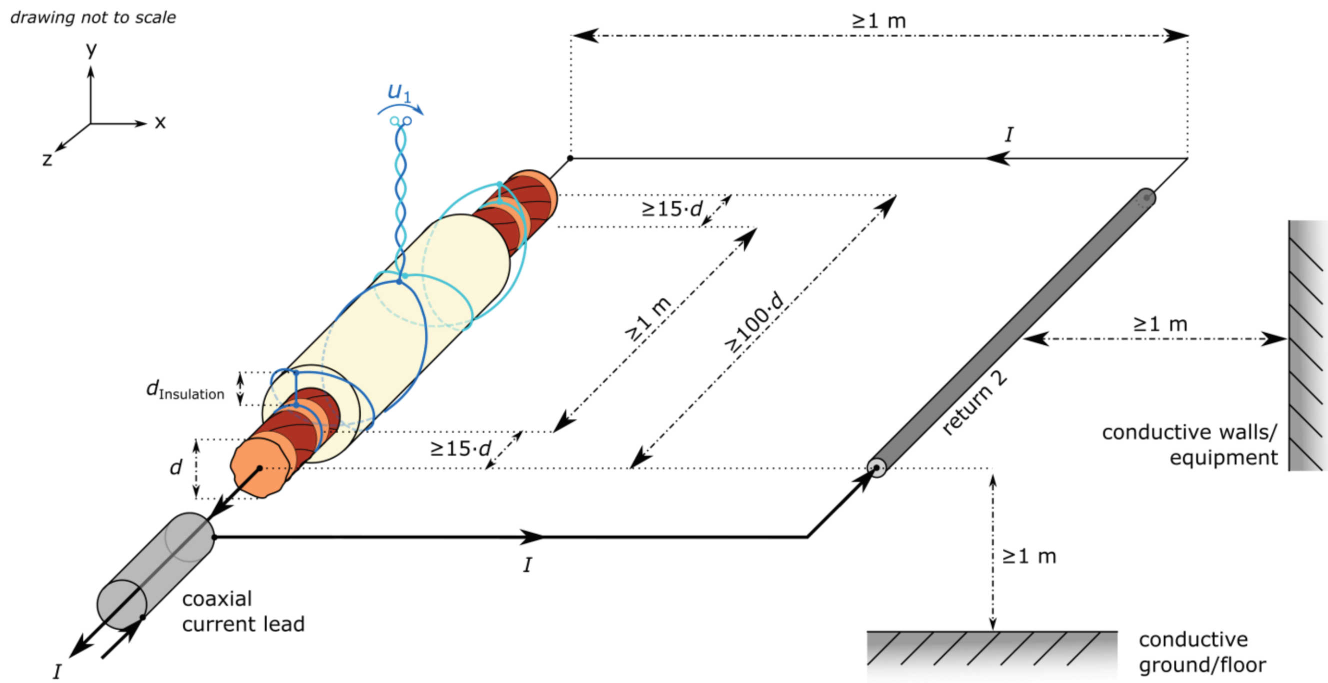

Figure 3-9: Single return, double helix configuration (recommendation combination 1C)

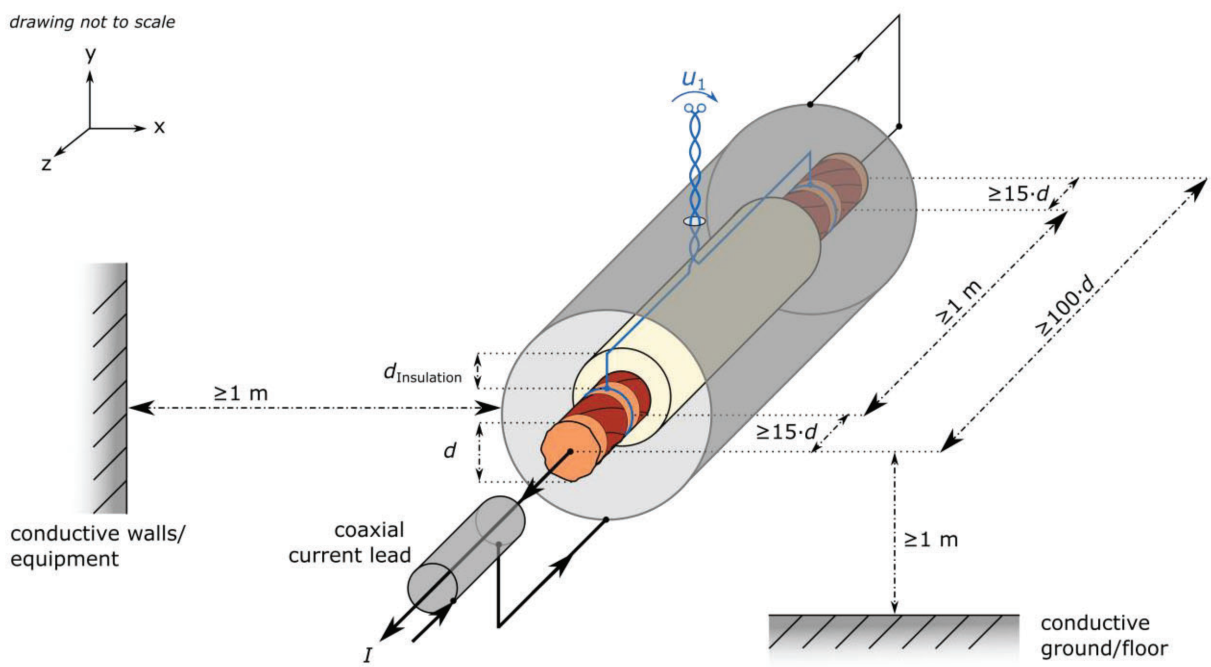

Figure 3-10: Screen return, single voltage loop configuration (recommendation combination 3A)

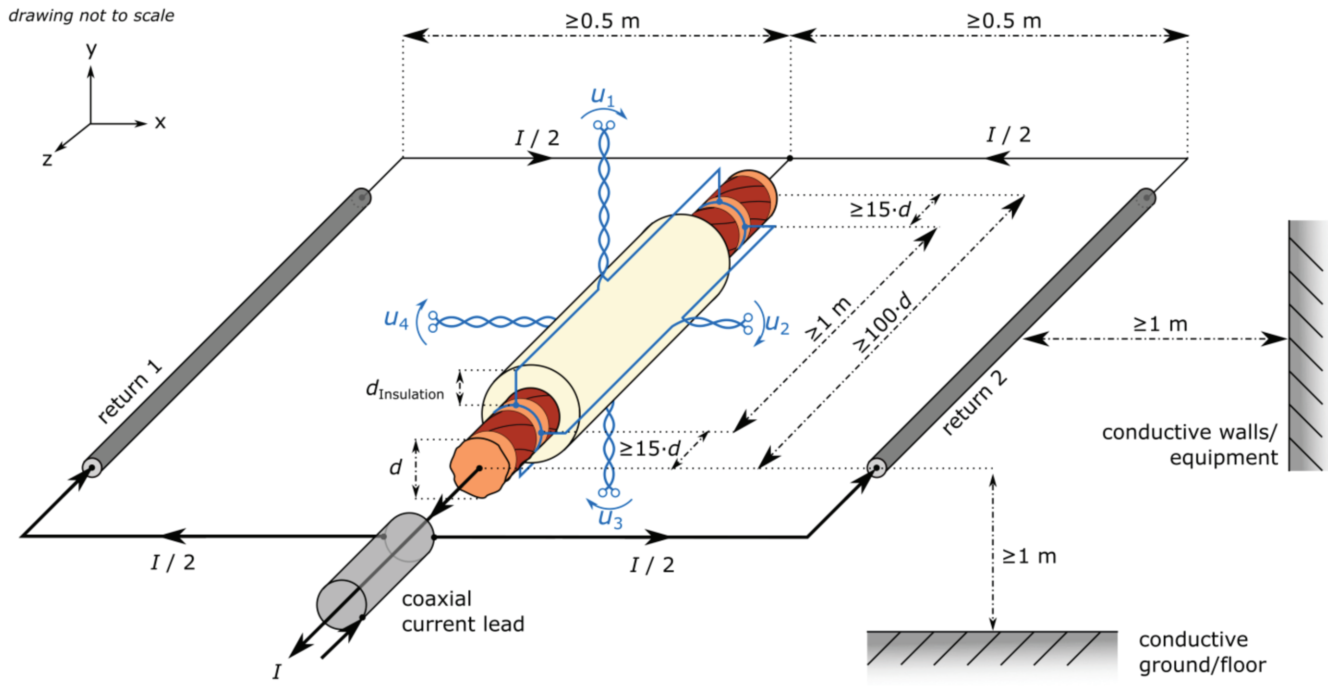

Figure 3-11: Dual return, average voltage loop configuration (recommendation combination 2B)

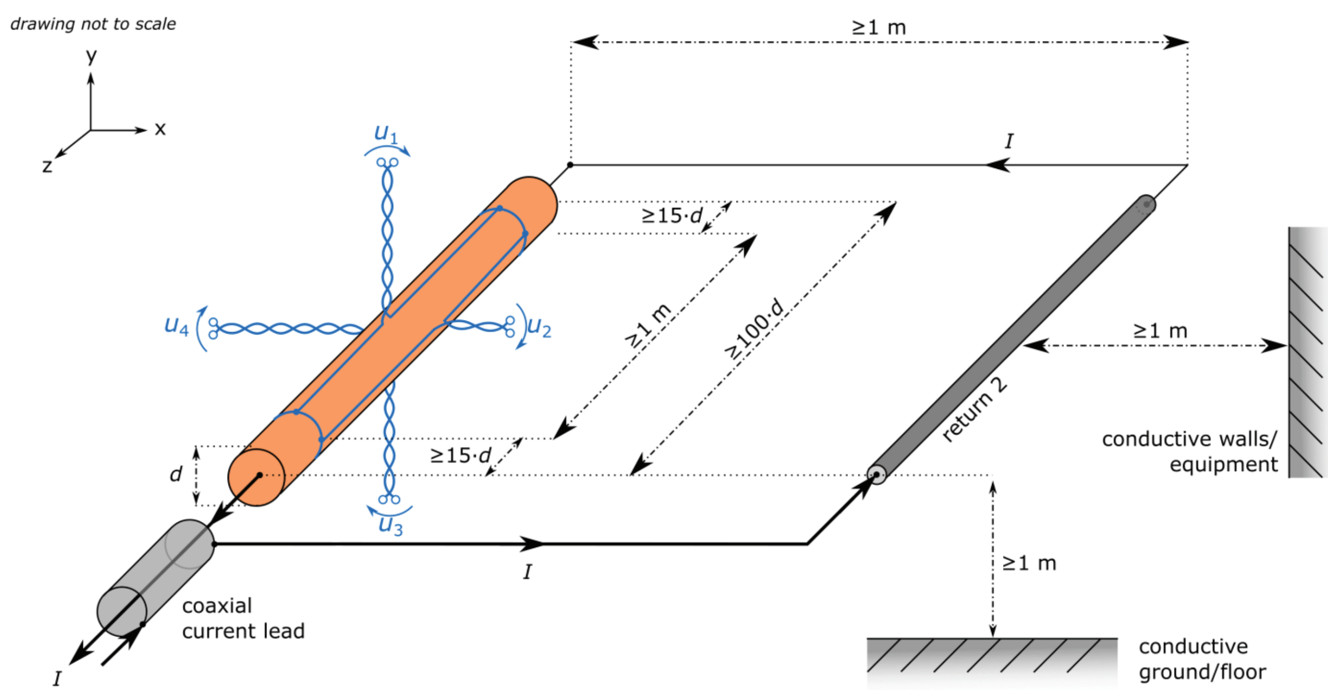

Figure 3-12: Single return, average (AVG) voltage loop configuration, where the CUT is a solid or will have no insulation system in its final state (recommendation combination 1B)

Figure 3-12 can be used when proximity effect losses are negligible. It reduces phase measurement uncertainty and noise due to its very small voltage loops (almost zero).

3.5 Measurement Procedure

After a measurement system and its components are benchmarked, as described in section 3.2, and mechanical preconditions are met (see section 3.3.3), the AC resistance measurement can be started. Arising from the recommendations put forward before, the following best practice procedure is recommended for the AC resistance measurement of complex conductors:

1. Prepare the CUT and its terminals
   (according to section 3.3)
2. Ensure temperature stability in the surrounding and prepare the surrounding
   (according to section 3.1.1 and section 3.4.1)
3. Put the CUT in place and set up the measurement circuit
   a. Set up the return conductors
      (according to section 3.4.6 or 3.4.2)
   b. Connect the current path
      (according to section 3.4.6 or 3.4.4)
   c. Check the DC resistance vs. expectations and also test the connection to different wires of the outer layer, if only one wire is contacted
      (according to section 2.5.3.4)
   d. Connect the voltage loop
      (according to section 3.4.6 or 3.4.5)
   e. Set up the thermal sensors
      (according to section 3.1.1)
   f. Check all electrical connections for good contact
4. Wait for temperature to stabilize
   (according to section 3.1.1)
5. Measure the length (if not calibrated by the setup) between taps
6. Perform a DC resistance measurement (bipolar)
7. Perform an AC resistance measurement (obtained by the average of at least 10 separate measurements):
   a. Either on one frequency value pre-adapted to the measured temperature
      (see section 1.3.8 and 3.1.3)
   b. Or of multiple frequencies close to the desired frequency
      (see section 1.3.8 and 3.1.3)
   c. Record average temperature between voltage tap-offs
8. Directly after step 7, perform a DC resistance measurement (bipolar) and take the average of both DC resistance measurements (step 6 and step 8)

Step 4 to step 8 according to section 3.1.1.

9. Optional if 7b. was performed: perform Temperature Scaling and then interpolate the measurement values with the Bessel function
   (according to section 3.1.2 and 3.1.3)
10. Calculate the uncertainty of the measurement
    (according to section 3.6)
11. Calculate the R_s value
    (according to section 3.7.2)

One could also only perform AC resistance measurement without DC resistance measurements and would then need to skip the steps above concerning DC resistance measurement.

3.6 Uncertainty Analysis

The evaluation of the uncertainty of the measurement is part of the measurement itself and must be performed either globally in the worst case, or individually for each measurement.

The GUM (Guide to the Expression of Uncertainty in Measurement) can be used as a reference for uncertainty evaluation [21].

In general, a measurement has imperfections that give rise to an error in the measured values. The uncertainty of the result of a measurement reflects the lack of exact knowledge on these values. Uncertainty gives a quantitative indication of the quality of the result so that those who use it can assess its reliability. Without such an indication, measurement results cannot be compared, either among themselves or with reference values.

When the result is obtained from the values of a number of other measured quantities, which is the case here, the standard uncertainty of the result of a measurement (termed combined standard uncertainty) is the estimated standard deviation associated with the result.

It is equal to the positive square root of the combined variance obtained from all variance and covariance components, using what is termed the law of propagation of uncertainty.

An expanded uncertainty is obtained by multiplying the combined standard uncertainty by a coverage factor k_{U} (this refers to k used in the GUM). If used, this factor must also be mentioned in the result.

For the purpose of our calculation, the following parameters may be considered in the uncertainty estimation.

Parameters directly linked to the measured quantities, whose uncertainty can be included in the calculation:

- Excitation current amplitude and phase;
- Voltage drop amplitude and phase;
- Harmonic content of the evaluated signals or quality of signal filtering;
- Frequency;
- Temperature;
- Length and
- Uncertainty on the device calibration.

Parameters indirectly linked to the measured quantities, whose effect can be evaluated using Figure 1-10, Figure 1-11 or other analogous assessments are:

- Return loop configuration;
- Symmetry (positioning of the conductor relative to voltage loop and return current loop);
- Measuring loop symmetry, for example in case of multiple measurements (4 rectangular loops) and
- Proximity effects (surrounding objects) and electro-smog “pollution”.

3.7 Interpretation of Results – The R_s Value

This chapter introduces a new method for evaluating the performance of a conductor, namely the R_s value. It may replace the k_s factor, as the R_s value uses actual measurement data. Moreover, it provides a more palpable representation of the conductor performance and hence allows better comparison between different conductor designs.

3.7.1 Shortcomings of the k_s Factor

The recent rating standard for power cables IEC 60287-1-1:2006/AMD1:2014 [37] provides a factor (namely the k_s factor), whose purpose is twofold:

1) without performing a measurement, the k_s factor allows an estimation of the expected conductor performance based on empirical data from previous cables with the same design and
2) it allows the manufacturer and customer to quickly rate and compare designs without elaborate measurements or calculations.

However, both the current standard from 2014 [37, p. 5] and the relevant CIGRÉ brochure B1.03 from 2005 [1, p. 52] recommend that a measurement should be performed for an accurate assessment of the AC losses of the conductor. The reason is that the performance of a conductor is not only affected by the design choices such as the treatment of wires (blank, oxidized or enameled wires) and other geometric features (strand diameter, pitch lengths of layers, influence of core conductor…) but also strongly depends on how well this design was realized (quality and constancy of manufacturing process). Moreover, the k_s factor does not account for the use of oxidized copper wires at the moment, cannot cover newer/upcoming designs and does not cover specific design choices as strand diameter, pitch lengths of layers, influence of core conductor and so forth.

Measurements showed that the same conductor design can vary strongly in performance and often designs do not perform as expected [2, p. 138], [38, p. 3]. These observations are consistent with extensive literature surveys for AC measurement results of different designs [2, p. 147]. Moreover, the k_s factor approach assumes that each conductor design behaves as a solid conductor and follows the low order (0 and 1) Bessel function of the first kind and measurements can be scaled for different frequencies and temperatures using the *Principle of Similitude*[19]. Both are not universally true. It is known that parallel conductors (as multiple parallel, insulated strands of a Milliken conductor) follow higher order Bessel functions [8] and not that of a solid circular conductor. Also, the *Principle of Similitude* can only be applied, when all conductor properties influencing the resistance ratio are scaled proportionally to different temperatures and frequencies. This can be easily done for simple and known geometries and interdependencies as for a solid round conductor, where the resistance ratio is only a function of the ratio of frequency to conductivity (synonymous with angular frequency to DC resistance as in the k_s factor): explained in detail in section 1.2.5. The problem with complex designs such as a Milliken conductor is that the geometry of each Milliken conductor design (quality of strand insulation, strand diameter, number of strands, number of layers, pitch of layers, …) is almost always unique. Not only between different manufacturers, but also for the same design depending on manufacturing quality and constancy. Additionally, the behavior of different strand insulations (enamel, oxidized, …) at different temperatures is usually unknown. Hence, it makes no sense to assume a common/general behavior for every Milliken conductor. A blank Milliken conductor could for example perform like a solid conductor (or very similar) and follow a low order Bessel function (which is assumed in the IEC standard), whereas an enameled conductor could follow a much different curve (higher order Bessel functions).

Hence, even though the k_s factor is recognized and widely used as a simple and practical approach, it does not represent the true behavior of a conductor well in general. Calculating an AC resistance using the k_s factor, which is too low or too high can result in a thermal over-, or even worse, under-dimensioning of the cable or complete cable system.

---

[19] This is done by including the $\sqrt{\omega/R_{\mathrm{DC}}}$ term in argument x_s. More on this topic can be found in chapter 1.2.5 or [2].

No analytical formula is available to calculate the AC resistance of a Milliken conductor. Some attempts are collected in [2, p. 70]. Even if it were, it could only be used for prior design optimizations and not for reliable evaluation of the manufactured conductor as the actual performance again strongly depends on the manufacturing features (e.g., quality of inter-wire resistances), which remains unknown in detail, as explained before.

3.7.2 The R_s Value

The R_s value was proposed in [38] and is introduced to stress the importance of performing a measurement, when aiming for an accurate performance assessment of a complex conductor. At the same time, it is an easy-to-interpret value also allowing the comparison of different designs of all cross-sectional sizes. It relates the losses (or performance) of a conductor design to its maximum possible AC losses.

The **r**esistance ratio to **s**olid value, hence R_s value is defined as the resistance ratio of the CUT to its solid, unoptimized counterpart.

$$R_s = \frac{R_{\mathrm{AC,meas}} - R_{\mathrm{DC,meas}}}{R_{\mathrm{AC,solid}} - R_{\mathrm{DC,meas}}} \cdot 100\,\% \qquad (13)$$

It is a direct measure of how close the CUT's losses are to the maximum theoretical AC losses of a comparable solid conductor. From the measured AC resistance $R_{\mathrm{AC,meas}}$ of the CUT and from the maximum possible AC resistance of this design $R_{\mathrm{AC,solid}}$ (a circular, unoptimized solid cross section), the measured DC resistance is subtracted $R_{\mathrm{DC,meas}}$. The ratio of both differences is multiplied by 100 %, so that the R_s value lies between 0 … 100 %.[20] Following the logic of the k_s factor, the R_s value of 0 % corresponds to a perfectly optimized conductor (the resistance does not increase with frequency, hence $R_{\mathrm{AC,meas}} = R_{\mathrm{DC,meas}}$) and an R_s value of 100 % corresponds to the CUT behaving like a round solid unoptimized conductor, which has the largest possible AC losses. Generally, the goal of a manufacturer and the client is to have a conductor design with an R_s value as low as possible or as agreed upon.

As it can be seen from equation (13), three values are necessary to calculate the R_s value. The R_s value shall be calculated as follows using these values. First, the DC resistance $R_{\mathrm{DC,meas}}$ of the conductor shall be measured, then at the same temperature the AC resistance $R_{\mathrm{AC,meas}}$ shall be measured. In the last step, the theoretical AC resistance of the comparable solid $R_{\mathrm{AC,solid}}$ shall be calculated as shown in APPENDIX B of this brochure. The script in APPENDIX B calculates the R_s value by using the user input and calculating the analytical AC resistance of a solid round conductor with the same DC resistance.

As put forward before, temperature- and frequency-dependencies cannot be removed from measurements on complex conductors, like Milliken conductors, as the behavior of the conductor is not known in advance at different frequencies and temperature regimes. Therefore, it is important to perform the measurement of AC and DC resistance at the desired temperature (usually 90 °C or 20 °C) and frequency (usually 50 Hz or 60 Hz)[21]. When providing the R_s value, one must provide the measurement frequency and temperature also for comparability.

Measurements at different temperatures or frequencies may result in different R_s values, except for solid conductor (always 100 %, if its round). Hence a cross comparison of R_s values is only reasonable at the same temperature and frequency.

[20] Theoretically, the R_s value could exceed 100 %, when measuring a conductor of a specific rectangular cross section as its AC losses can be greater than that of an unoptimized solid round conductor at certain p values [2, p. 65]. This special case is out of scope in this brochure as it is not relevant for cable ratings and can also be circumvented, when simply relating an optimized rectangular conductor design to that of an unoptimized rectangular design of the same cross section and side ratios.

[21] As explained in section 1.3.8, an electrical measurement should not be performed directly at 50 Hz or 60 Hz due to interferences, but rather be interpolated from measurements close to this frequency.

The following figure, Figure 3-13, shows some exemplary R_s value of actual measurements performed in [2, p. 131] on different cable designs. The given ranges for the measurements relate to different measurement setups being used and may be interpreted as uncertainties here.

Conductor Type	R_s in % (measurement)	k_s-factor (measurement)	k_s-factor (IEC[a] calculation)
2000 mm² Al (oxidized)	17.9...22.8	0.38...0.43	0.25
1773 mm² Cu (bare, bi)	44.5...44.7	0.58...0.58	0.80
1200 mm² Cu (oxidized)	44.9...58.7	0.68...0.71	-
2500 mm² Cu (oxidized)	13.4...13.5	0.26...0.27	-
2500 mm² Cu (oxidized)	58.4...62.5	0.63...0.65	-
2500 mm² Cu (enameled)	27.0	0.38	0.35

[a] IEC 60287-1-1:2006/AMD1:2014 (Table 2)

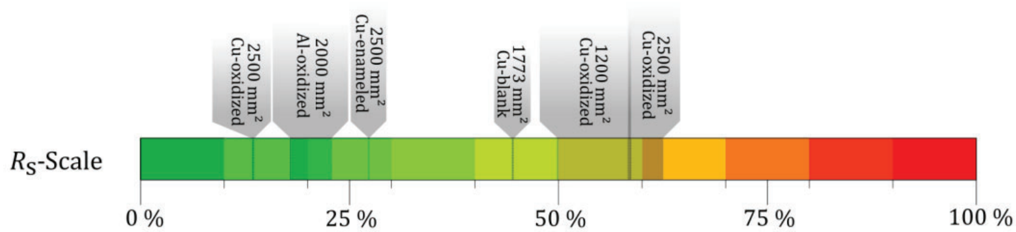

Figure 3-13: Table of measurement results and subsequently calculated R_s value and k_s factors at 50 Hz and approximately 20 °C, including the k_s given by the IEC standard ("bi" stands for bi-directional stranding, indicating opposing pitch direction between neighboring layers); the colored scale allows an intuitive ranking of the design's performances

Multiple important insights can be obtained by the table in Figure 3-13:

- two designs of the same type (2500 mm² Cu, oxidized) can perform drastically different, which the empirical IEC standard values would not have captured, if this type would have existed in the standard in the first place,
- a design (2500 mm² Cu, enameled) can perform worse than expected according to the IEC standard, which could result in a thermal under-dimensioning of a cable/cable system,
- some designs are very well optimized and some are not and
- every design "beats" the unoptimized round solid conductor (its reference).

A measurement may not be necessary, when constancy in the R_s value was demonstrated by a manufacturer for one cable design in multiple measurements on different manufactured cables.

To summarize the purpose and advantages of the R_s value:

- it is reliable as it is based on actual measurements and therefore represents the true performance of a conductor,
- it is easy to calculate,
- it is easy to interpret as it is referenced to the worst case,
- it is easy to compare different designs and different cross sections on a universal scale and
- new designs can directly be included and their performance can be compared (e.g., oxidized copper wires).

The R_s value can be calculated in free tools such as PYTHON and OCTAVE. A Python scripts for direct use can be found in APPENDIX B. An empty template of the scale to classify the performance of a CUT visually is given in the following.

3.8 Safety Considerations

The devices should be handled by qualified staff only. Please always refer to any devices' user manual safety requirements.

3.8.1 Electrical

AC resistance measurement usually implies large currents but low voltages. There are as such no general or specific precautions to be taken on this low voltage part of the device. Nevertheless, please refer to the user's manual of the device, especially at the mains side of any device. Grounding must be sound, stable and comply with wiring standards.

3.8.2 Mechanical

Measurement of AC resistance is usually done on large cross-section conductors/cables. The weight of the CUT can be some tens of kilograms per meter. Safety equipment (shoes, gloves, …) should be worn and necessary precaution taken during handling to avoid injuries of any kind. The mechanical stability of the measuring device must be sufficient to support such weights.

3.8.3 Temperature

If intended for high temperature measurements, the equipment (design, materials) must be adapted to thermal cycling. during the measurement at high temperature (usually 90 °C) some part of the instrument, connectors, as well as the CUT may reach high temperatures. some parts (connector for example) may also become hot due to measuring current even during room temperature measurement. it is necessary to wear gloves and other safety equipment to avoid burns.

4. References

[1] CIGRE, "Large cross-sections and composite screens design: Working Group B1.03," 2005.

[2] R. Suchantke, Alternating Current Loss Measurement of Power Cable Conductors with Large Cross Sections Using Electrical Methods: PhD Thesis, Berlin, Germany: TU Berlin, 2018.

[3] J. Zaborszky, "Skin and Spiraling Effect in Stranded Conductors [includes discussion]," *Transactions of the American Institute of Electrical Engineers. Part III: Power Apparatus and Systems (Volume: 72 , Issue: 4),* pp. 599-603, 08 1953.

[4] W. I. Middleton and E. W. Davis, "Skin effect in large stranded conductors at low frequencies," *Journal of the American Institute of Electrical Engineers (Volume: 40 , Issue: 9) ,* pp. 757-763, 09 1921.

[5] Z. Popovic and B. D. Popovic, Introductory Electromagnetics, NJ, Upper Saddle River: Prentice Hall, 1999.

[6] D. Lovric, V. Boras and S. Vujević, "Accuracy of approximate formulas for internal impedance of tubular cylindrical conductors for large parameters," *Progress In Electromagnetics Research M 16,* pp. 171-184, 2011.

[7] H. B. Dwight, "Skin effect in tubular and flat conductors," *J. Am. Inst. Electr. Eng., vol. 42, no. 8,* p. 977–998, 1918.

[8] H. B. Dwight, "A precise method of calculation of skin effect in isolated tubes," *J. Am. Inst. Electr. Eng., vol. 42, no. 8,* p. 827–831, 1923.

[9] O. Tsukamoto, Y. Yamato, S. Nakamura and J. Ogawa, "Measurements of AC Transport Current Losses in HTS Tapes in an Assembled Conductor," *IEEE Transactions on Applied Superconductivity (Volume: 15 , Issue: 2),* pp. 2895-2898, 06 2005.

[10] R. Suchantke, N. Wieczorek and R. Plath, "Ideal Measurement Setup for Short Cable Samples, ResearchGate," 14 03 2019. [Online]. Available: https://www.researchgate.net/publication/330703102_Using_Helical_Voltage_Loops_for_the_AC_Resistance_Measurement_of_Complex_Conductor_Designs_Milliken_conductors_Bus_Bars. [Accessed 08 12 2021].

[11] R. Suchantke, N. Wieczorek and R. Plath, "Numerical Investigation on Current Homogenization, ResearchGate," 26 08 2019. [Online]. Available: https://www.researchgate.net/publication/342521401_Investigation_of_Current_Homogenization_Numerical_Investigation_on_Current_Homogenization. [Accessed 08 12 2021].

[12] S. Großmann, "Current connections: Internal CIGRE WG D1.54 document," TU Dresden, 2013.

[13] R. Suchantke, R. Plath and R. Schuhmann, "Besonderheiten bei der Messung von Wechselstromwiderständen von kurzen Leitern und kurzen Kabelstücken mit großen Querschnitten: Difficulties with AC resistance measurements of short conductor- and cable samples with large cross-sections," in *VDE-Hochspannungstechnik 2016: Vorträge der ETG-Fachtagung 14.-16. November 2016*, Berlin, 2016.

[14] B. Dardel, P. De Bruyne and V. Arbet-Engles, "Electrical Linear Resistance Measurement of Large Cross-Section Conductors," *Conference Proceedings for the 87th Annual Convention of the Wire Association Intertnational,* 2017.

[15] J. Xia and e. al., "Study on AC Resistance Characteristics of Stranded Conductors by a High Precision Measuring System," *2019 IEEE 3rd International Electrical and Energy Conference (CIEEC),* 07 09 2019.

[16] K.-E. Rydler, M. Sjöberg and J. Svahn, "A measuring system of conductor AC and DC resistance," in *Jicable 2011 - 8th International Conference on Insulated Power Cables*, Versailles, France, 2011.

[17] P. De Bruyne and G. Mauron, "Effects of contact resistances in multistrand cables on linearresistance measurements," *Wire Journal International,* 2012.

[18] D. Milz, *Power Cables Under Inspection,* Wire & Cable Technology Internation, 2009.

[19] P. De Bruyne and B. Currat, "Temperature and frequency effects on cable resistance," 2015. [Online]. Available: https://www.aesa-cortaillod.com/fileadmin/documents/knowledge/AN_150617_E_Snapshots_multimaterials.pdf. [Accessed 20 06 2018].

[20] M. Sjöberg, Writer, *A measuring system of AC and DC conductor resistance.* [Performance]. 2013.

[21] JCGM, "Evaluation of measurement data - Guide to the expression of uncertainty in measurement: JCGM 100:2008 (GUM 1995 with minor corrections)," 2008. [Online]. Available: http://www.bipm.org/en/publications/guides/gum.html.

[22] S. K. Olsen, A. Kühle, C. Traeholt, O. Tonnesen and M. Däumling, "Alternating current losses of a 10 metre long low loss superconducting cable conductor determined from phase sensitive measurements," *Superconductor Science and Technology 12.6,* p. 360, 1999.

[23] E. Cereda, G. Coletta, G. Crotti, L. Gherardi, G. Ottoboni and S. Zannella, "Comparison between self-field AC losses of a single-phase Bi-2223 cable measured by electric and calorimetric methods," *Physica C: Superconductivity, vol. 310, no. 1-4,* p. 231–235, 1998.

[24] G. Schröder, V. Waschk, R. Plath, R. Schuhmann and R. Suchantke, "Measures to reduce skin-effect losses in power cables with optimized conductor design and their evaluation by measurement," in *Jicable 2015 - 9th International Conference on Insulated Power Cables*, Versailles, France, 2015.

[25] A. Kühle, C. Traeholt, S. K. Olsen, C. N. Rasmussen, O. Tonnesen and M. Däumling, "Measuring AC-loss in high temperature superconducting cable-conductors using four probe methods," *IEEE Trans. Appl. Supercond., vol. 9, no. 2,* pp. 1169-1172, 1999.

[26] S. Fleshler, L. C. G. E. Cronis, A. P. Malozemoff, T. Pe, J. McDonald, J. R. Clem, G. Vellego and P. Metra, "Measurement of the ac power loss of (Bi,Pb)2Sr2Ca2Cu3Ox composite tapes using the transport technique," *Applied Physics Letters 67, No. 21,* p. 3189, 20 11 1995.

[27] Z. Li, "Principle and Practice of AC Resistance Measurements Using External Field Cancellation Method: Internal CIGRE WG D1.54 document," Canada, 2013.

[28] Z. Li, "AC Resistance Measurements: Comparison of Shield Return Method and External Field Cancellation Method: Internal CIGRE WG D1.54 document," Canada, 2014.

[29] G. Schröder, D. Häring, A. Weinlein, A. Bossmann, R. Plath, M. Valtin and M., "AC resistance measurements on skin-effect reduced large conductor power cables with standard equipment," in *Jicable 2015 - 9th International Conference on Insulated Power Cables*, Versailles, France, 2015.

[30] G. Coletta, L. Gherardi, F. Gömöry, E. Cereda, V. Ottoboni, D. Daney, M. Maley and S. Zannella, "Application of electrical and calorimetric methods to the AC loss characterization of cable conductors," *IEEE Trans. Appl. Supercond., vol. 9, no. 2,* p. 1053–1056, 1999.

[31] P. Dolez, J. Cave, D. Willén, W. Zhu and M. Aubin, "Improvements and validation of the null calorimetric method for a.c. loss measurements in superconductors," *Cryogenics, vol. 38, no. 4,* p. 429–434, 1998.

[32] S. R. Systems, 2006. [Online]. Available: https://www.if.tugraz.at/bibliothek/handleitung/SR830m.pdf.

[33] M. Gatzsche, S. Großmann, H. Löbl, N. Lücke and R. Adam, "Particularities of AC resistance measurement at solid conductors with large cross sectional area: Internal CIGRE WG D1.54 document," TU Dresden, 2013.

[34] J. S. Juul, E. T. Molgaard, J. Jensen, N. H. Andersen, A. B. Abrahamsen, D. Willén, C. Traeholt, C. Thidemann and H. Lentge, "AC Losses in Bi2Sr2Ca2Cu3O10+x Tapes and a 3.15-m-Long Single-Phase Cable," *IEEE Trans. Appl. Supercond., vol. 21, no. 6,* p. 3599–3603, 2011.

[35] R. Suchantke, Investigations on AC losses of power cables with large cross sections and advanced conductor design: Master Thesis, Berlin: TU Berlin, 2015.

[36] Pfisterer, "Pfisterer - FrontCon," 11 2021. [Online]. Available: https://www.pfisterer.com/fileadmin/pfisterer/downloads/FrontCon-PI-DE.pdf. [Accessed 04 12 2021].

[37] IEC - International Electrotechnical Commission, *Electric Cables - Calculation of the current rating - Part 1-1: Current rating equations - IEC 60287-1-1:2006/AMD1:2014,* IEC, 2014.

[38] R. Suchantke, "A Proposal for a ks-Factor Replacement," Technische Universität Berlin, Berlin, 2019.

APPENDIX A. Definitions, Abbreviations & Symbols

A.1. Specific terms

Table A-1: Definition of technical terms used in this Technical Brochure

Acronym	Definition
AC	alternating current
ADC	analog-to-digital converter
CIGRÉ	Conseil International des Grands Réseaux Électriques
CUT	conductor under test
DC	direct current
DFT	discrete Fourier transform
EMF	electromotive force
End-effect	different influences from the terminals of the cable, which should not be included in the measurement, as they are not relevant for the CUT's performance in general.
IDE	integrated development environment
IEC	International Electrotechnical Commission
M-type conductors	synonym for Milliken conductor
measured losses/resistance	also called *apparent* losses are the losses or the resistance indicated by the measurement system; they should be as close as possible to the *true* losses, but can deviate strongly in electrical measurements due to spurious voltage signals captured in the voltage loop and hence don't always have a sensible physical meaning or relation to the CUT
R_S value	resistance to solid value; the new performance parameter of an optimized conductor design, which relates its losses it its unoptimized, equivalent counterpart
strands	same as wires in a stranded or Milliken conductor
TB	technical brochure
true losses/resistance	also called joule, ohmic, resistance are actual losses with a true physical meaning or relation to the CUT as they result in heating of the conductor
voltage loop or pick-up loop	a loop formed by voltage lead wires, the CUT and the measurement device susceptible to induction of spurious voltages
voltage tap-offs or voltage taps	two contact points of the voltage lead wires / the voltage loop to the CUT; usually at the surface of the CUT

A.2. Equation Symbols

Table A-2: Definition of equation symbols in formulas

Symbol	Definition	Unit
a and b	position (coordinate) of voltage tap-offs	m
A_L	voltage loop area	m²
B	magnetic flux density	T
ber_0, bei_0, ber_0', bei_0'	Kelvin functions (real and imaginary part of the Bessel function of the first kind J and order 0) and their derivatives (the derivatives are indicated by ')	-
d	axis- to-axis distance between CUT and one or more return conductors	m
$d_{\mathrm{Insulation}}$	the distance from the CUT's surface to the top of the insulation; in other words, the thickness of the insulation/dielectric	m
d_{VL}	radial voltage loop extension/perpendicular to the conductor	m
d_{wire}	diameter of a single wire in a stranded/Milliken conductor	m
E	electric field strength	V/m
f	electrical frequency ($\omega = 2\pi f$)	Hz or 1/s
I	total conductor test current	A
Im	takes the imaginary part of an expression	-
j	imaginary number	-
J	current density	A/m²
k	Bessel argument in resistance calculation of a tubular conductor	m
k_U	coverage factor; this refers to k used in the GUM	
k_s	k_s factor as given by the IEC standard	-
l_{meas}	measurement length between both voltage tap-offs	m
p	*Principle of Similitude* parameter	$\sqrt{\mathrm{m}/(\Omega\mathrm{s})}$
r_1	inner radius of tubular conductor	m
r_2	outer radius of tubular conductor	m
R	resistance (general)	Ω or Ω/m
R_{AC}	AC resistance	Ω or Ω/m
$R_{\mathrm{AC,meas}}$	measured AC resistance	Ω or Ω/m
$R_{\mathrm{AC,Solid}}$	equivalent AC resistance of a solid round conductor (unoptimized)	Ω or Ω/m
R_{DC}	DC resistance	Ω or Ω/m
$R_{\mathrm{DC,meas}}$	measured DC resistance	
Re	takes the real part of an expression	-
R_{meas}	measured resistance	Ω or Ω/m
R_S	R_S value (Resistance to Solid Value)	%
T	measured temperature (usually close to 20 °C or 90 °C)	°C
T_0	reference temperature (usually 20 °C or 90 °C)	°C
T_{SF}	*Temperature Scaling* factor	-
$\underline{u}_{\mathrm{meas}}$ or U	measured voltage drop between voltage taps (over measurement length l_{meas})	V
U_{res}	residual voltages like thermal voltages and offset voltages of the measuring electronics	V
x	Bessel function argument	-
y_s	skin effect factor from IEC standard	-
Greek Symbol	Definition	Unit
α_T	temperature coefficient	1/K
ρ	electrical resistivity	Ωm
σ	electrical conductivity	S/m or 1/(Ωm)
$\mu = \mu_0\mu_r$	magnetic permeability composed of vacuum μ_0 and material specific magnetic permeability μ_r	Vs/(Am)

APPENDIX B. R_s Value Calculation Script

B.1. Python Script

This appendix provides the calculation script for the R_s value. PYTHON (version 3 or above) is available free of charge. The code below can be copied and pasted into any PYTHON tool or online IDE.

This example script can be used in PYTHON 3. Line 9-12 need to be adapted after measurement by the user.

```
1   # -*- coding: utf-8 -*-
2   # Library Import:
3   ## These libraries (NumPy & SciPy) need to be installed
4   import numpy as np
5   import scipy.special as sc
6   
7   # User Input:
8   ## User inputs are only made here
9   RDC_meas    = 6.603E-6                # measured DC resistance in Ohm/m
10  RAC_meas    = 8.690E-6                # measured AC resistance in Ohm/m
11  f           = 50                      # measurement frequency in Hz
12  mur         = 1                       # magnetic permeability of conductor
13  
14  # Calculations:
15  ## R_AC,solid and R_s Calculation; DO NOT EDIT THIS PART
16  mu0         = 4*np.pi*1E-7            # magnetic vacuum permeability in Vs/(Am)
17  omega       = 2*np.pi*f               # angular frequency in 1/s
18  x           = np.sqrt(omega*mu0*mur/(np.pi*RDC_meas))
19  y_s         = x/2*((sc.ber(x)*sc.beip(x)-sc.bei(x)*sc.berp(x))/\
20                    (sc.berp(x)**2+sc.beip(x)**2))-1
21  RAC_solid   = RDC_meas*(1+y_s)        # AC resistance in Ohm/m
22  Rs          = ((RAC_meas-RDC_meas)/(RAC_solid-RDC_meas))*100 # R_s value in %
23  
24  # Print Output:
25  ## These 2 lines generate the console output and give R_AC,solid and R_s values
26  print('The AC resistance of the solid reference is: {:.3f}
    \u03BC\u03A9/m.'.format(RAC_solid*1E6))
27  print('The Rs value is: {:.1f} %.'.format(Rs))
```

ISBN : 978-2-85873-599-0